

# ***Modelling grass digestibility***

***on the basis of morphological and  
physiological plant characteristics***

Promotor: dr ir L. 't Mannetje  
hoogleraar in de Graslandkunde

Co-promotor: dr ir E.A. Lantinga  
universitair hoofddocent bij de leerstoelgroep  
Biologische Bedrijfssystemen

10031201, 2024

# ***Modelling grass digestibility***

***on the basis of morphological and  
physiological plant characteristics***

***Jeroen C.J. Groot***

Proefschrift  
ter verkrijging van de graad van doctor  
op gezag van de rector magnificus  
van Wageningen Universiteit,  
dr C.M. Karssen,  
in het openbaar te verdedigen  
op dinsdag 14 december 1999  
des namiddags te vier uur in de Aula

0 3 5 1

Cover design: Marije Groot.

CIP-GEGEVENS KONINKLIJKE BIBLIOTHEEK, DEN HAAG

Groot, J.C.J.

Modelling grass digestibility on the basis of morphological and physiological plant characteristics / J.C.J. Groot.

- [S.l : s.n. ]

Thesis Wageningen University, – With ref. – With summary in Dutch

ISBN 90-5808-140-0

Subject headings: grass.

The research described in this thesis was part of the research programme of the C.T. de Wit Graduate School Production Ecology.

BIBLIOTHEEK  
LANDBOUWUNIVERSITEIT  
WAGENINGEN

## STELLINGEN

1. In spruiten van *Lolium* spp. heeft temperatuur geen effect op de snelheid van afname van de celwandverteerbaarheid tijdens veroudering wanneer deze wordt uitgedrukt in blad-verschijningsintervallen.  
Dit proefschrift.
2. Variatie in celwandverteerbaarheid van *Lolium* spp. kan niet gerelateerd worden aan de morfologische kenmerken bladlengte en -breedte.  
Dit proefschrift.
3. In bladeren van spruiten van *Lolium* spp. die hergroeien na ontbladering wordt de specifieke massa van celinhoud sterker gereduceerd dan die van celwanden, zodat het celwandgehalte stijgt en de verteerbaarheid van de organische stof daalt.  
Dit proefschrift.
4. Wiskundige analyse van gedetailleerde gasproductiecurves die zijn gemeten tijdens de *in-vitro* vertering van veevoeders vereist een meerfasenmodel, dat in een twee-stappen benadering wordt gefit.  
Dit proefschrift.
5. Het gebruik van een object-georiënteerde benadering biedt grote mogelijkheden voor simulatie van morfologische en anatomische aspecten van de plantengroei.  
Bos H J 1999 *Plant morphology, environment, and leaf area growth in wheat and maize*.  
Dit proefschrift.
6. Bladscheden zijn cruciaal voor de stevigheid van stengelvormende grasspruiten.  
Niklas K J 1990 The mechanical significance of clasping leaf sheaths in grasses: evidence from two cultivars of *Avena sativa*. *Annals of Botany* 65 505-512.
7. Obsessies en theoriën zijn alleen nuttig wanneer ze aan een werkstuk dat al een formele structuur heeft een hartstochtelijke dimensie toevoegen.  
Harold Brodkey, *Stories in an almost classical manner*.
8. Het dilemma van de wetenschapper is de uitkomst voor de literator: de werkelijkheid is niet te beschrijven.
9. Ook in de software engineering is nieuwe technologie nooit een oplossing, maar slechts hulpmiddel bij het oplossen van veel voorkomende problemen, zoals het optreden van fouten, slechte onderhoudbaarheid en geringe herbruikbaarheid.
10. Wetenschappelijke activiteit leidt niet tot selectie uit een veelheid van hypothesen, maar tot het vergroten van die veelheid.  
Robert M. Pirsig, *Zen and the art of motorcycle maintenance*.
11. De opkomst van web-cams zal leiden tot een nieuwe vorm van sociale cohesie en controle, met als bindende factoren werk- en interessegebieden.
12. Kennis van structuren is voor een architect op z'n minst zeer wenselijk, omdat een goede structuur alleen maar kan bijdragen aan de schoonheid van de architectuur.  
Mario Salvadori, *Structure in architecture - the building of buildings*.

Stellingen bij het proefschrift: *Modelling grass digestibility on the basis of morphological and physiological plant characteristics*, Jeroen Groot, 14 december 1999.

## ABSTRACT

Grass digestibility is determined by the rate of plant development, mass of plant organs (leaf blades, leaf sheaths and stem internodes) and composition of organs. The development of an integrating model for grass digestibility necessitates the quantification of developmental characteristics of plants and their organs and the effects of environmental factors and management practices. The main objective of this study was a thorough analysis of changes in composition and digestibility of plant organs of two grass species (*Lolium perenne* and *L. multiflorum*). These characteristics were quantified in glasshouse experiments on vegetative and reproductive plants.

Detailed analyses were made of the specific cell wall ( $s_{cw}$ ) and cell contents ( $s_{cc}$ ) mass of the various organs ( $\text{mg OM cm}^{-2}$ ), which determine cell wall content (CWC), and of cell wall digestibility (CWD). During growth,  $s_{cw}$  and  $s_{cc}$  of all plant organs increased. After full organ expansion had been reached,  $s_{cw}$  remained unchanged, while  $s_{cc}$  declined, resulting in an increase of CWC. CWD of plant organs declined during ageing. The increase in the proportion of indigestible cell wall per leaf appearance interval could be described by a negative exponential curve, with a fractional rate that was the same for all plant organs, temperatures and populations. The decline in CWD of whole shoots was a linear function of shoot development stage, *i.e.* number of appeared leaves. Cutting had only a marginal effect on the digestibility of whole shoots.

The implementation of these trends in an object-oriented simulation model resulted in acceptable estimations of growth, development and digestibility of grass under contrasting environmental conditions in the field. Sensitivity analyses with the model demonstrated that the morphological plant characteristics leaf blade length and width, and leaf appearance rate have no systematic effect on composition and digestibility. The model using object-oriented principles offers large opportunities for simulation of collections of individual plants and plant organs in complex and varying environments.

The cumulative gas production technique is a potential addition to *in vitro* measurement of digestibility. It was demonstrated that a multiphasic equation is required for mathematical description of gas production curves. Curves from incubations with strongly contrasting types and concentrations of substrate, medium and inoculum could be fitted precisely with one flexible, multiphasic sigmoidal equation. Parameters in the equation were related to biological phenomena. These findings contribute to improved interpretation of *in vitro* fermentation studies and fine-tuning of the cumulative gas production technique.

## **PREFACE**

Van tienduizenden grasplanten zijn de individuele bladschijven, bladscheden en internodia gescheiden... duizenden monsters zijn verzameld en geanalyseerd... honderden plantorganen zijn gemeten. Veel personen hebben een enorme bijdrage geleverd aan de totstandkoming van dit proefschrift. Zonder anderen tekort te doen, wil ik een aantal mensen met name noemen.

Allereerst wil ik mijn begeleiders bedanken... Van mijn dagelijks begeleider Jan Neuteboom heb ik zeer veel geleerd in de vele discussies. Met zijn visie en zijn kritische en analyserende kijk op het onderwerp heeft hij een grote bijdrage geleverd aan het proefschrift. Egbert Lantinga heeft met opbouwende ideeën, kritische kanttekeningen en een praktische blik bijgedragen aan veel aspecten van dit onderzoek, van de modellering van gasproductie en de simulatie, tot de uitvoering van de veldproef in Noorwegen. Bauke Deinum heeft een grote inbreng gehad met zijn grote expertise van verteerbaarheidsonderzoek bij grassen. Mijn promotor Leendert 't Mannetje dank ik voor zijn steun gedurende het project en het zorgvuldig lezen van de manuscripten.

Voor de gasproductiemetingen is intensief samengewerkt met de vakgroep Veevoeding van de Landbouwwuniversiteit. In het bijzonder dank ik Barbara Williams hartelijk voor haar hulp bij het uitvoeren van de metingen en de prettige samenwerking bij het vervaardigen van verschillende manuscripten. Tevens bedank ik Wiebe Koops voor zijn grote bijdrage aan de statistische analyse van de gasproductiecurves.

Leidulf Nordang en het Noorse onderzoeksinstituut Planteforsk bedank ik voor het mogelijk maken van de veldproef die in Bodø werd uitgevoerd.

... en natuurlijk wil ik degenen bedanken die al het gras in handen hebben gehad. Gedurende de uitvoering van de experimenten is André Maassen zeer actief betrokken geweest. Zowel in de kassen, het ruwlab, het chemisch lab als bij de gasproductie-metingen, waarbij hij 's avonds in de pauzes voorbijgangers op de Haagsteeg tracteerde op 'n saxofoonconcert. Rinus van de Waard en John van der Lippe van Unifarm worden bedankt voor de goede organisatie rondom de proeven. Grote inspanningen zijn ook geleverd door verscheidene andere medewerkers van Unifarm, zoals Gerrit Besselink, Henk van Roekel, Wim van der Slikke, Evert Verschuur, Eddy de Boer, Jan van der Pal, Ton Blokzijl en anderen... Chemische analyses en verteerbaarheidsmetingen zijn uitgevoerd door Hennie Halm (Agronomie) en Marianne van 't End en Jane-Martine Muijlaert (Veevoeding). In het

kader van afstudeervakken en na-doctorale onderzoekprojecten zijn delen van het onderzoek uitgevoerd door Luuk Hagting, Arno Oostdam, André van Schaik en Simon Kloostra.

Collega's van de vakgroep Agronomie bedank ik voor de plezierige samenwerking. Een bijzondere plaats wordt ingenomen door twee toppers: Bert Bos, mijn kamergenoot in de halve cirkel van Agronomie, en Jacco Wallinga, mijn toenmalig huisgenoot. Met genoeg denk ik terug aan de gezelligheid en de leuke maar ook inspirerende gesprekken over planten en alle andere belangrijke top-onderwerpen.

Het onderzoek is uitgevoerd onder de paraplu van de onderzoeksschool Productie Ecologie. Zeer leerzaam waren de bijeenkomsten op vrijdagmorgen, waarin de promovendi elkaars manuscripten beoordeelden. De deelnemers aan deze sessies en de begeleiders wil ik hartelijk bedanken.

Grote dank gaat ook uit naar mijn familie en vrienden, die altijd belangstelling toonden. En natuurlijk naar Olga, die alle geduld had, mij steunde wanneer dat nodig was, maar ook op de juiste momenten hielp te relativeren en te ontspannen.

Jeroen.



## ***CONTENTS***

1	General introduction	1
Part I	Composition and digestibility of consecutively formed plant organs on the main shoot of grass	
2	Spaced vs. sward plants	7
3	Defoliation	21
4	Temperatures and populations	33
5	Simulation model	49
Part II	The use of the cumulative gas production technique	
6	Multiphasic analysis of gas production kinetics	71
7	Fermentation of cell walls and contents	85
8	General discussion	97
	References	105
	Summary	113
	Samenvatting	117
	Curriculum vitae	121

## **ACCOUNT**

Parts of this thesis have been or will be published elsewhere:

### *Chapter 2*

Groot J C J, Neuteboom J H 1997 Composition and digestibility during ageing of Italian ryegrass leaves of consecutive insertion levels. *J Sci Food Agric* **75** 227-236.

### *Chapter 3*

Groot J C J, Neuteboom J H, Deinum B 1999 Composition and digestibility during ageing of consecutive leaves on the main stem of Italian ryegrass plants, growing undisturbed or regrowing after cutting. *J Sci Food Agric* **79** 1691-1697.

### *Chapter 4*

Groot J C J, Neuteboom J H, Lantinga E A, Deinum B Composition and digestibility during ageing of vegetative and reproductive perennial ryegrass tillers, grown at three temperatures. Submitted.

### *Chapter 6*

Groot J C J, Cone J, Williams B A, Debersaques F D, Lantinga E A 1996 Multiphasic analysis of gas production kinetics for in vitro fermentation of ruminant feedstuffs. *Anim Feed Sci Technol* **64** 77-89.

### *Chapter 7*

Groot J C J, Williams B A, Oostdam A J, Boer H, Tamminga S 1998 The use of cumulative gas and volatile fatty acid production to predict in vitro fermentation kinetics of Italian ryegrass leaf cell walls and cell contents at various time intervals. *Brit J Nutr* **79** 519-525.

## **1. GENERAL INTRODUCTION**

### **1.1 Changing grassland use in farming systems**

Grass is an important component of the diet of agricultural livestock in The Netherlands. As such it provides the ruminant with energy and nutrients for maintenance, growth and/or milk production, but it also plays a crucial role in the stabilization of fermentative and degradative processes in the reticulo-rumen (Tamminga & Van Vuuren 1996). Moreover, it provides the farmer with a feed of low cost. Consequently, grass species and cultivars are extensively evaluated for their productivity, persistence and quality as ruminant feed (e.g., Anonymous 1998).

Digestibility of forage grass in intensive farming systems in the temperate regions is usually high. Highly digestible grass species such as *Lolium perenne* are used. Moreover, high fertilizer inputs support rapid (re-)growth. Consequently, swards can be grazed or cut in a young stage, so that maturation and reduction of digestibility are limited. Under more sustainable agricultural practices, the N fertilizer rate has to be reduced from an economical optimum of 420 kg ha<sup>-1</sup> per year (Deenen 1994) to an ecological optimum in the order of 150-250 kg ha<sup>-1</sup> per year, depending on grassland management system (Lantinga & Groot 1996). This will result in either longer growth periods, and hence harvesting of older and more mature grass, or more frequent harvesting at lower herbage yield, but with high crop digestibility. Irrespective of the management system, maintenance of similar levels of animal performance is desired. Thus, the grass digestibility should remain at a high level, as also the use of concentrates will decline (Tamminga & Van Vuuren 1996).

### **1.2 Plant aspects determining digestibility**

An important measure of quality is digestibility, which depends on the ratio between cell contents (CC) and cell wall (CW), and on cell wall digestibility (CWD). CC consist mainly of soluble carbohydrates, proteins and organic acids, which are readily soluble in the rumen after cell rupture, and is assumed to be degraded rapidly and completely. CWD is variable and

dependent on the chemistry and physical arrangement of the cell walls (Wilson 1994). Directly after synthesis CW polymers are completely digestible. Their digestibility declines primarily through cross-linking of CW polymers (Chesson 1993), *i.e.* changes in the chemical characteristics. Physical limitations are important in intact plant material ingested and only partly comminuted by ruminants. Indigestible cell wall layers such as the primary cell wall-middle lamella (Engels 1989) can form a barrier to digestion of CC and potentially digestible CW that they enclose (Wilson & Hatfield 1997). Digestibility can also be negatively affected by the slow movement of rumen bacteria and fungi through cell structures (Wilson & Mertens 1995) and the limited possibilities for microbial attachment (McAllister *et al.* 1994). However, these physical limitations are largely removed when the analysed material is ground before *in vitro* digestibility measurement, as in the experiments presented in this thesis.

Plant organs differ in cell wall content (CWC) and CWD due to differences in anatomical structure and chemical composition and cell wall thickness (Wilson 1994). Generally, leaf blades have lower CWC and higher CWD than leaf sheaths, and stem internodes have the highest CWC and lowest CWD (Hacker & Minson 1981). The proportions of the different plant organs and their composition and digestibility can vary considerably, depending on plant development stage and age, environmental factors (light, temperature) and grassland management.

### ***1.3 A mechanistic approach for simulation of grass digestibility***

For maintaining a high level of grass digestibility during longer regrowth periods, improvements of digestibility are being pursued through breeding and efforts are being made to identify correlations between quality characteristics and plant morphology and physiology (*e.g.* Masaoka *et al.* 1991; Buxton and Lentz 1993; MacAdam *et al.* 1996). However, changes in herbage quality are complex, because they occur through the rate of plant development and ageing, dry weight of plant organs (leaf blades, leaf sheaths, stem internodes) and composition and digestibility of these organs. Therefore, results from breeding for one plant character to improve the feeding quality have to be related and evaluated for other plant characteristics, and during the growing season. An explanatory mechanistic approach would enable separation of the various processes governing herbage quality.

The development of an integrating model necessitates the quantification of developmental characteristics of plants and their organs and the effects of environmental factors and management practices. The main objective of the study described in this thesis is a thorough investigation of both the composition and digestibility of individual plant organs consecutively formed on grass shoots. First the general trends are determined for the leaf blades of spaced and sward grown plants (Chapter 2). The effects of cutting on composition and digestibility of leaf blades and whole shoots during regrowth are investigated in Chapter 3. The most important factors determining composition and digestibility of grass are reproductive development (Nelson & Moser 1994) and temperature (Buxton & Fales 1994), because they affect plant development rate as well as CWC and CWD. In Chapter 4 the consequences are evaluated of differences in temperature on vegetative and reproductive shoots of two populations of perennial ryegrass, selected for differences in leaf digestibility. The experimental findings are incorporated into a simulation model of grass growth and digestibility, which is presented in Chapter 5.

#### ***1.4 Gas production as an alternative for 48 h in vitro digestibility***

The 48 h *in vitro* digestibility measurement is very useful for practical reasons, as it can be related to the *in vivo* digestibility through regression. However, it is a static measure, that is based on the assumption that the average retention time of feed particles in the rumen is ca. 48 h, whereas the rumen retention time *in vivo* can vary from 20 h to 70 h, depending on the forage. For more detailed analysis of the degradation process and the causes of differences in digestibility between feeds, the kinetics of degradation can be determined from differences in the residues after various incubation times. However, this approach is laborious, expensive and not always accurate enough. Moreover, the course of fermentation of soluble substrate components cannot be quantified (Pell & Schofield 1993).

Alternatively, the kinetics of feedstuff degradation can be determined from the fermentative gas production, which measures the amount of gas released directly as a product of the fermentation and indirectly from buffered rumen fluid (Beuvink & Spoelstra 1992; Pell & Schofield 1993; Cone *et al.* 1994; Theodorou *et al.* 1994). The kinetics of gas production are dependent on a sequence of processes. Upon incubation, substrates are partly solubilized. The

soluble components are rapidly fermentable after incubation. A gradual shift subsequently occurs towards the fermentation of the insoluble parts, that need to be hydrated and colonized by rumen microorganisms, before they can be fermented (Van Milgen *et al.* 1993). The rates at which these processes can take place, depend on the initial concentration and composition of the microbial population, and on the ability of the microorganisms present in the mixture to colonize, ferment and utilize the fermentation products for growth (Demeyer 1981; Hidayat *et al.* 1993). Substrates and their components can be resistant to these processes to different extents, resulting in substantially different gas production profiles.

Gas production experiments were carried out to obtain information additional to the standard 48 h *in vitro* digestibility measurements and to explore the possibilities for using the gas production method in elaborate studies of forage quality evaluation. In Chapter 6 a statistical model and a method for curve fitting of the gas production profiles are presented. The model is used in Chapter 7 to evaluate the contrasts in gas production from CC and CW.

***PART I.***

***Composition and digestibility of consecutively formed plant organs  
on the main shoot of grass***

## 2. SPACED VS. SWARD PLANTS

with Jan H. Neuteboom

### 2.1 Abstract

Organic matter digestibility (OMD) is determined from the proportion of indigestible cell wall (ICW) in the total plant organic matter. To improve understanding of processes governing the proportion of ICW, plant morphological development, and leaf composition and digestibility were studied for Italian ryegrass (*Lolium multiflorum*). Since grass is usually grown in swards, a comparison was made between spaced and sward grown plants.

The time course of ICW accumulation in individual leaves on the main shoot (MS) could be described by a negative exponential saturation curve. Remarkably, the curvature and the asymptotic ICW as a proportion of total leaf cell wall mass were the same for all leaves in both the spaced and the sward plants. Under both conditions, leaves consecutively formed on the MS have lower cell wall digestibility (CWD) at leaf appearance and lower rate of CWD decline during ageing, which could be explained from the longer period between the estimated start of ICW formation and the moment of leaf appearance. The higher cell wall content for consecutive leaves and for leaves of the sward plants enhanced the effect of lower CWD on OMD at leaf appearance, but counteracted the lower CWD decline rate, so that all leaves had the same rate of OMD decline with age. The observed trends clearly demonstrate the close link between morphological development and leaf composition and digestibility.

### 2.2 Introduction

Few workers have investigated the composition and digestibility characteristics of individual leaves, consecutively formed on grass shoots. In spaced plants of *Panicum maximum* var. *trichoglume* (Wilson 1976), *Zea mays* (Deinum 1981) and *Hordeum vulgare* (Nordang *et al.* 1992), gradients along the MS have been observed. Later formed leaves showed higher cell wall content (CWC) and lower digestibility at ligule appearance. The rate of decline of digestibility



with ageing was lower in later formed leaves. Because grass is usually grown in a sward, the characteristics of leaves not only of spaced plants, but also of sward plants need to be quantified. Therefore, in this experiment, gradients in characteristics of consecutive leaves on the MS of grass were determined for spaced and sward plants.

### 2.3 Experimental

The experiment was carried out in a well-controlled glasshouse with day/night temperatures of 18/13°C, natural daylength and 70% relative humidity. Italian ryegrass (*Lolium multiflorum*) cv. Multimo (2n = 4x) was seeded on July 7, 1994, into 1.5 litre pots with square surface (0.0169 m<sup>2</sup>). Seeding rates per pot were 1 (spaced) and 13 at equal distances (sward). The number of pots was 7 (harvests) times 80 giving 560 for spaced plants and 5 (harvests) times 10 giving 50 for sward plants. Pots were placed adjacent to each other with a border row around the sward. Spacing between pots containing 1 plant was increased throughout the experiment, because pots were removed for harvesting. Spaced plants were randomly placed within the glasshouse. The sward was placed in the centre of the glasshouse. Within the sward pots for different harvest dates were randomly allocated. The sward arrangement was restored after removal of pots for harvest. Pots contained a mixture of sand and peat (1:1 v/v). The pots were placed in large trays and were flushed twice daily with nutrient solution (Steiner 1984). Radiation data were obtained from the nearby Wageningen weather station. Daily irradiance was calculated from global radiation corrected for the transmission coefficient (0.7) of the glasshouse.

The appearance of leaves on the MS was recorded, based on the date of ligule appearance. Leaves were counted from the base to the top of the shoot. After the ligule of the third leaf had appeared plants were harvested at each leaf appearance interval. Leaf blades were dissected from the MS, and separated into leaf insertion classes. Leaves of ca. 80 plants were bulked to form a sample. Leaf blade and leaf sheath length, leaf blade width, leaf blade area and the dry weight of leaf blades and total plants were determined. For each harvest, per treatment, leaves of the same insertion level were bulked for chemical analysis. Samples were oven dried at 70°C for 24 h and subsequently ground to pass a 1 mm screen in a hammer mill.

Samples were analysed for cell wall content in organic matter (CWC) using neutral

detergent solution (Goering & Van Soest 1970) with an additional protease treatment to remove undissolved protein (Wilson *et al.* 1991). *In vitro* true digestibility was determined after a 48 h *in vitro* incubation of 0.5 g air dry matter in rumen fluid from fistulated steers fed medium quality grass hay (Goering & Van Soest 1970) and true digestibility of cell walls and organic matter (respectively CWD and OMD) were determined, assuming complete digestibility of the cell contents.

Regression analyses were performed for cell wall content in organic matter (CWC), cell wall digestibility (CWD) and organic matter digestibility (OMD), and nitrogen content (NC) in dry matter (all units g kg<sup>-1</sup>). To discern constituents causing differences in these relative quantities, regression analyses were carried out for the following characteristics of individual leaves: specific leaf mass of dry matter ( $s_{dm}$ ), organic matter ( $s_{om}$ ), cell contents ( $s_{cc}$ ), cell wall ( $s_{cw}$ ), indigestible cell wall after 48 h incubation ( $s_{icw}$ ) and nitrogen ( $s_n$ ) per unit of leaf area (all units mg cm<sup>-2</sup> leaf area). Parameters were analysed for effects of leaf number on the MS ( $I$ ), time ( $t$ ) and  $t^2$ , and in cases of combined regressions for spaced and sward plants, for effects of spacing ( $S$ ). Interaction terms were also included in the full model which was analysed by stepwise multiple regression using Genstat 5.3 (Genstat 5 Committee 1993). The specific leaf area (SLA, cm<sup>2</sup> g<sup>-1</sup> dry matter) was also calculated.

## 2.4 Results

### 2.4.1 Growth and leaf appearance rate

Global radiation at plant level was high until 50 days after emergence (DAE), but showed a general decline over the whole experiment (Fig 1a). The spaced and sward plants had the same leaf appearance rates until leaf stage 3 (0.277 (SE 0.015) leaves per day), then leaf appearance rate gradually declined to 0.104 (SE 0.004) per day for spaced plants and 0.076 (SE 0.001) per day for sward plants (Fig 1b).

Growth of the spaced plants in terms of dry matter was near-exponential until 50 DAE (0.14 (SE 0.02) g g<sup>-1</sup> per day), but declined sharply thereafter. The sward had already reached the linear growth phase by 15 DAE (Fig 1c). In this treatment, the growth rate declined after 25

DAE. The average growth rate of the sward amounted to  $0.31$  (SE  $0.03$ )  $\text{g pot}^{-1}$  per day; *i.e.*  $18.8$   $\text{g m}^{-2}$  per day. Nitrogen in the total herbage mass declined throughout the experiment in both treatments (Fig 1*d*). However, according to the criteria developed by Burns (1992), NC never fell below the critical level for optimal growth.

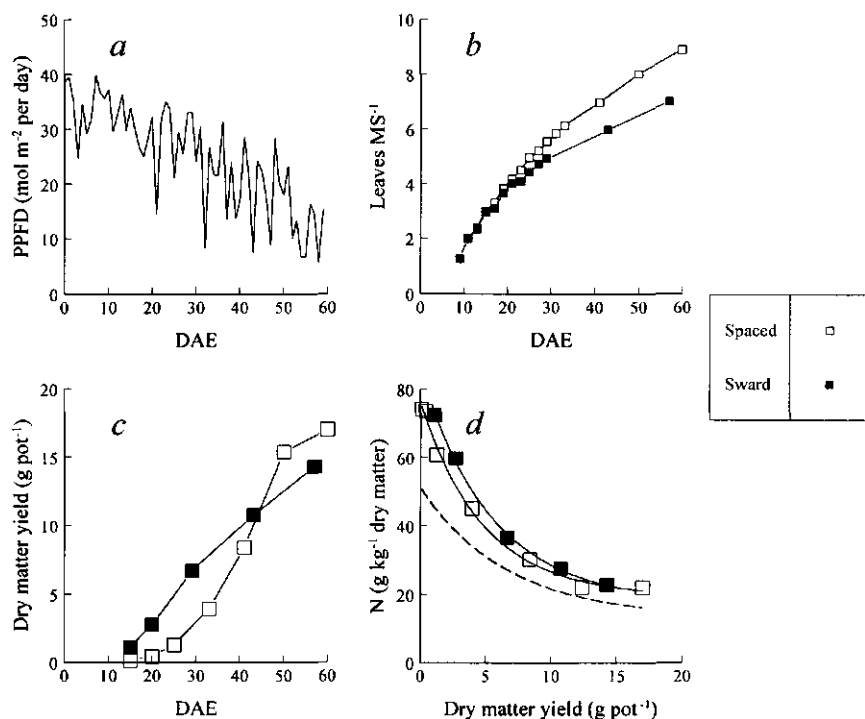


**Fig 1.** *a.* Daily photosynthetic photon flux density (PPFD) at plant level throughout the experiment. Number of leaves per main shoot (MS) (*b*) and dry matter accumulation (*c*) at different days after emergence (DAE) for the spaced and the sward plants. *d.* Relation between nitrogen content in the dry matter and dry matter yield per pot. The dashed line indicates the critical level of nitrogen (Burns 1992).

#### 2.4.2 Leaf dimensions, organic constituents and nitrogen

In the spaced plants, leaf blade width of leaves on the MS reached a maximum for leaf 7 (Fig 2*a*). The length of the leaf blade (Fig 2*b*) and the resulting leaf area (Fig 2*c*) increased for consecutive leaves of spaced plants up to and including leaf 8, as did leaf blade dry matter mass (Fig 2*d*). The

sward plants had longer but narrower leaf blades than the spaced plants, however, they had the same leaf blade area until leaf 5. After leaf 3, leaves on the MS of sward plants had a lower leaf blade dry matter mass and from leaf 5 onward a smaller leaf area. This resulted in a higher SLA for the sward plants:  $413 \text{ cm}^2 \text{ g}^{-1}$  vs.  $321 \text{ cm}^2 \text{ g}^{-1}$  on average for spaced plants (Fig 2e). The leaf sheath length reached a maximum for leaf 7 and was higher for the sward plants than for the spaced plants (Fig 2f).

Regression analyses were performed on the data of leaves 4 to 6 of the spaced plants. Of these leaves, data over the time span of 3 leaf appearance intervals from ligule appearance were available, *i.e.* data of 4 consecutive sampling dates per leaf. For the sward plants fewer data were available per leaf and combined regression analyses for spaced and sward plants for the same leaves 4 to 6 were only possible over the time span of two leaf appearance intervals from ligule appearance, *i.e.* data from 3 consecutive sampling dates per leaf.

*Spaced plants.* At the time of ligule appearance  $s_{dm}$  and  $s_{om}$  increased for consecutive leaves caused by an increase in  $s_{cw}$ , while leaves did not systematically differ in  $s_{cc}$  (Fig 3a, Table 1). Later leaves also started with a higher  $s_{icw}$ .  $s_{dm}$  and  $s_{om}$  decreased linearly in time due to a reduction of  $s_{cc}$ , while  $s_{cw}$  remained unchanged (Fig 3c, Table 1). All leaves showed the same linear rate of decline in  $s_{cc}$  as indicated by the absence of any  $t.l$  interaction (Table 1). Slight  $t.l$  and  $t^2.l$  interactions occurred in the increase in time of  $s_{icw}$  probably caused by a stronger  $s_{icw}$  increase in time in the earlier formed leaves (see below). At ligule appearance, CWC (Table 3, see below) and OMD (Fig 3e), were respectively higher and lower for consecutive leaves. During leaf ageing CWC increased as can be deduced from  $s_{om}$  and  $s_{cw}$  in Fig 3c. OMD decreased over time with the same rate in consecutive leaves (Fig 3e). However, later leaves had a lower initial CWD (see Table 3 below) and CWD showed a lower rate of decline in later leaves ( $t.l$  interaction).

NC in dry matter at ligule appearance had decreased for consecutive leaves (Table 1) together with the NC in the total dry matter (Fig 1d). Up to 30 DAE when leaf 5 had emerged, NC for the whole plant mass was  $> 40 \text{ g kg}^{-1}$ , which suggests that, until then, N had not been limiting for leaf growth and tillering.

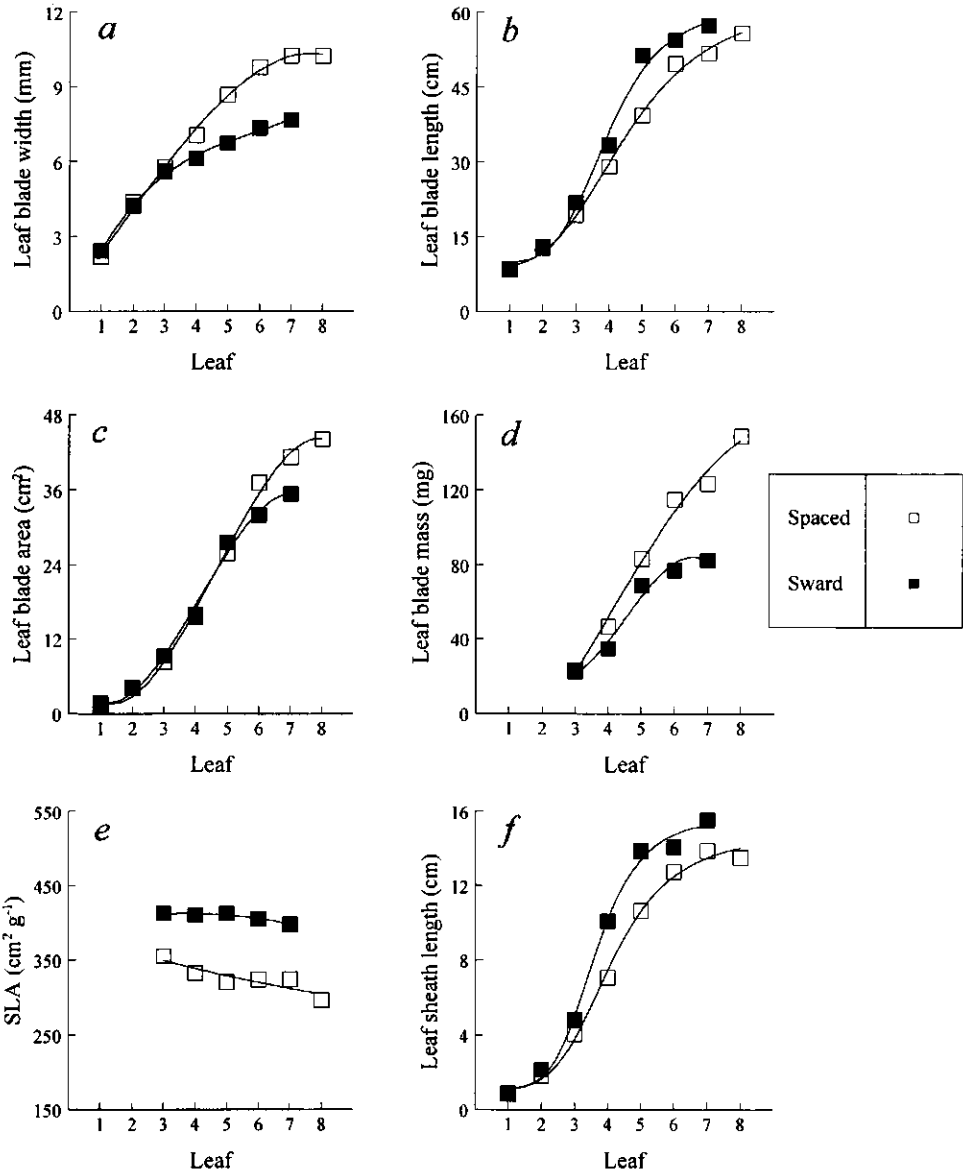


**Fig 2.** Leaf dimensions of consecutive leaves on the main shoot of the spaced and the sward plants at ligule appearance. Leaf blade width (a), length (b), area (c), mass (d), specific leaf area (SLA, e) and leaf sheath length (f).

**Table 1.** The contributions to the  $r^2$  of the components of the regression on three leaf appearance intervals after ligule appearance of leaves 4 to 6 of spaced plants <sup>a,b</sup>.

Variate	$t$	$t^2$	$l$	$t.l$	$t^2.l$
$s_{dm}$	31.7b	ns	35.4a	ns	ns
$s_{om}$	24.8a	ns	49.6a	ns	ns
$s_n$	62.3b	ns	ns	ns	ns
$s_{cc}$	59.3b	ns	ns	ns	ns
$s_{cw}$	ns	ns	92.9c	ns	ns
$s_{icw}$	48.7c	ns	48.7c	0.7a	1.7a
CWC	37.9a	ns	56.8c	ns	ns
CWD	82.9c	ns	13.8b	1.9a	ns
OMD	72.4c	ns	26.4c	ns	ns
NC	73.4c	ns	19.4c	6.2b	ns

<sup>a</sup> Regression analysis was performed for mass of dry matter ( $s_{dm}$ ), organic matter ( $s_{om}$ ), nitrogen ( $s_n$ ), cell contents ( $s_{cc}$ ), cell walls ( $s_{cw}$ ) and indigestible cell walls ( $s_{icw}$ ) per unit of leaf area (all units  $\text{mg cm}^{-2}$ ), and cell wall content in organic matter (CWC), cell wall and organic matter digestibility (CWD and OMD), and nitrogen content in organic matter (NC) (all units  $\text{g kg}^{-1}$ ). Terms included in the full model were: time ( $t$ ; days) and  $t^2$ , and leaf ( $l$ ) and their interactions.

<sup>b</sup> Significance: a =  $p < 0.05$ ; b =  $p < 0.01$ ; c =  $p < 0.001$ .

*Spaced vs. sward plants.* At ligule appearance the sward plants had lower initial values than the spaced plants for  $s_{dm}$ ,  $s_{om}$ ,  $s_{cc}$ ,  $s_{cw}$  and  $s_{icw}$  but showed the same tendencies of higher values for consecutive leaves (Figs 3b & 3d; Table 2). The absence of a  $t.S$  interaction for  $s_{dm}$ ,  $s_{om}$  and  $s_{cc}$  suggests that these parameters decreased linearly in time with the same rate in the spaced and the sward plants (cf. Figs 3c & 3d; Table 2). The sward plants had leaves with higher CWC and lower OMD than for the spaced plants (Table 3; cf. Figs 3e & 3f). The  $t.S$  interaction from the regression on CWD indicated a slower decline of CWD in the spaced plants vs. the sward plants after ligule appearance. The sward plants had lower leaf NC at comparable leaf stages than the spaced plants which has to be attributed to their faster dry matter accumulation per pot.

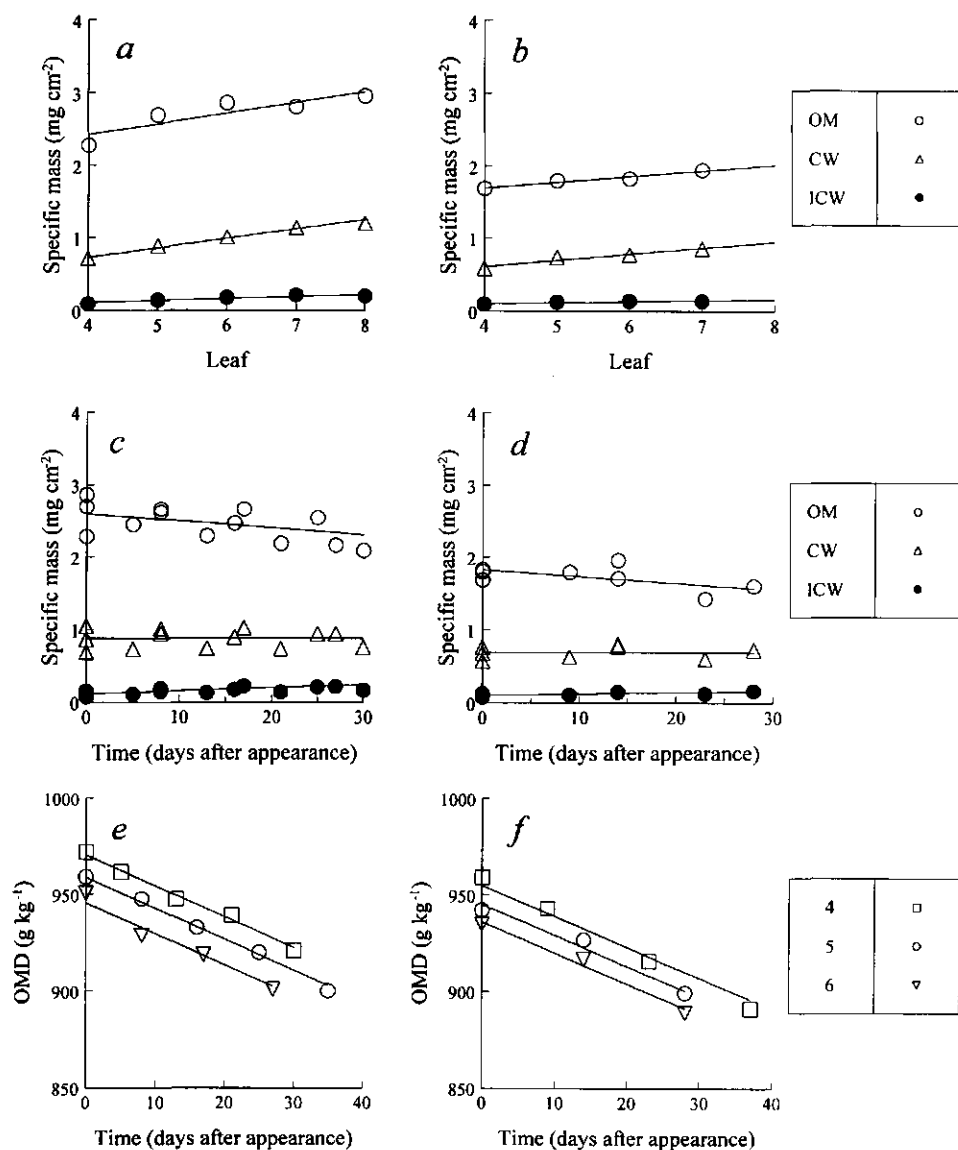


**Fig 3.** Specific mass of organic matter (OM), cell wall (CW) and indigestible cell wall (ICW) for consecutive leaves at the moment of ligule appearance (*a*, spaced and *b*, sward), from the moment of ligule appearance (*c*, spaced and *d*, sward), and organic matter digestibility (OMD) of leaves 4, 5 and 6 of the spaced plants (*e*) and the sward (*f*) plants. Lines derived from regression analyses are plotted.

**Table 2.** The contributions to the  $r^2$  of the components of the regression on two leaf appearance intervals after ligule appearance of leaves 4 to 6 of spaced and sward plants<sup>a,b</sup>.

Variate	<i>T</i>	<i>S</i>	<i>l</i>	<i>t.S</i>	<i>t.l</i>
<i>s<sub>dm</sub></i>	9.5b	82.5c	ns	ns	ns
<i>s<sub>om</sub></i>	10.7b	76.8c	7.1b	ns	ns
<i>s<sub>n</sub></i>	44.2c	6.5a	25.6b	10.2a	ns
<i>s<sub>cc</sub></i>	17.7c	76.6c	ns	ns	ns
<i>s<sub>cw</sub></i>	ns	43.0c	49.3c	ns	ns
<i>s<sub>icw</sub></i>	26.2c	17.4c	46.9c	3.3b	4.5b
CWC	33.7c	27.9c	34.1c	ns	ns
CWD	76.6c	ns	13.1b	3.8a	ns
OMD	68.3c	8.0c	21.8c	ns	ns
NC	50.8c	12.4c	24.0c	2.8a	6.4a

<sup>a</sup> Regression analysis was performed for mass of dry matter (*s<sub>dm</sub>*), organic matter (*s<sub>om</sub>*), nitrogen (*s<sub>n</sub>*), cell contents (*s<sub>cc</sub>*), cell walls (*s<sub>cw</sub>*) and indigestible cell walls (*s<sub>icw</sub>*) per unit of leaf area (all units mg cm<sup>-2</sup>), and cell wall content in organic matter (CWC), cell wall and organic matter digestibility (CWD and OMD), and nitrogen content in organic matter (NC) (all units g kg<sup>-1</sup>). Terms included in the full model were: time (*t*; days), spaced or sward plants (*S*), leaf (*l*) and their interactions. *t.S.l* interactions were never significant and therefore excluded from the Table.

<sup>b</sup> Significance: a =  $p < 0.05$ ; b =  $p < 0.01$ ; c =  $p < 0.001$ .

#### 2.4.3 Further analysis of cell wall digestibility from *s<sub>icw</sub>*

This analysis was motivated by the significant interactions for *s<sub>icw</sub>* and CWD. The increase in time of *s<sub>icw</sub>* (mg cm<sup>-2</sup>) could be satisfactorily described by a negative exponential saturation curve:

$$s_{icw} = \alpha_s (1 - e^{-\beta(t - \tau)}) \quad \text{Eqn 1}$$

In this equation  $\alpha_s$  (mg cm<sup>-2</sup>) denotes the asymptotic value and  $\beta$  (per day) is a rate constant. *t* is time (days) and  $\tau$  the intersection between the curve and the time axis. The  $\tau$  could be theoretically associated with the time at which CW starts to become indigestible. Values of  $\alpha_s$ ,  $\beta$  and  $\tau$  were found iteratively by nonlinear regression.

The values of  $\alpha_s$  increased for consecutive leaves and differed for same leaves of the spaced and the sward plants (Figs 4a & 4b) but not when expressed as a proportion ( $\alpha_p$ ) of the total cell wall mass of the leaf after ligule appearance (Figs 4c & 4d). Also  $\beta$  did not systematically differ for consecutive leaves and for leaves within the same class of the spaced and the sward plants. Therefore, the curves for *p<sub>icw</sub>* (the proportion of indigestible cell walls in



the total cell wall mass of the leaf after ligule appearance) against time for consecutive leaves and for the leaves of the spaced and the sward plants were almost identical when corrected for  $\tau$  as the time of initiation of ICW increase (Figs 4e & 4f).

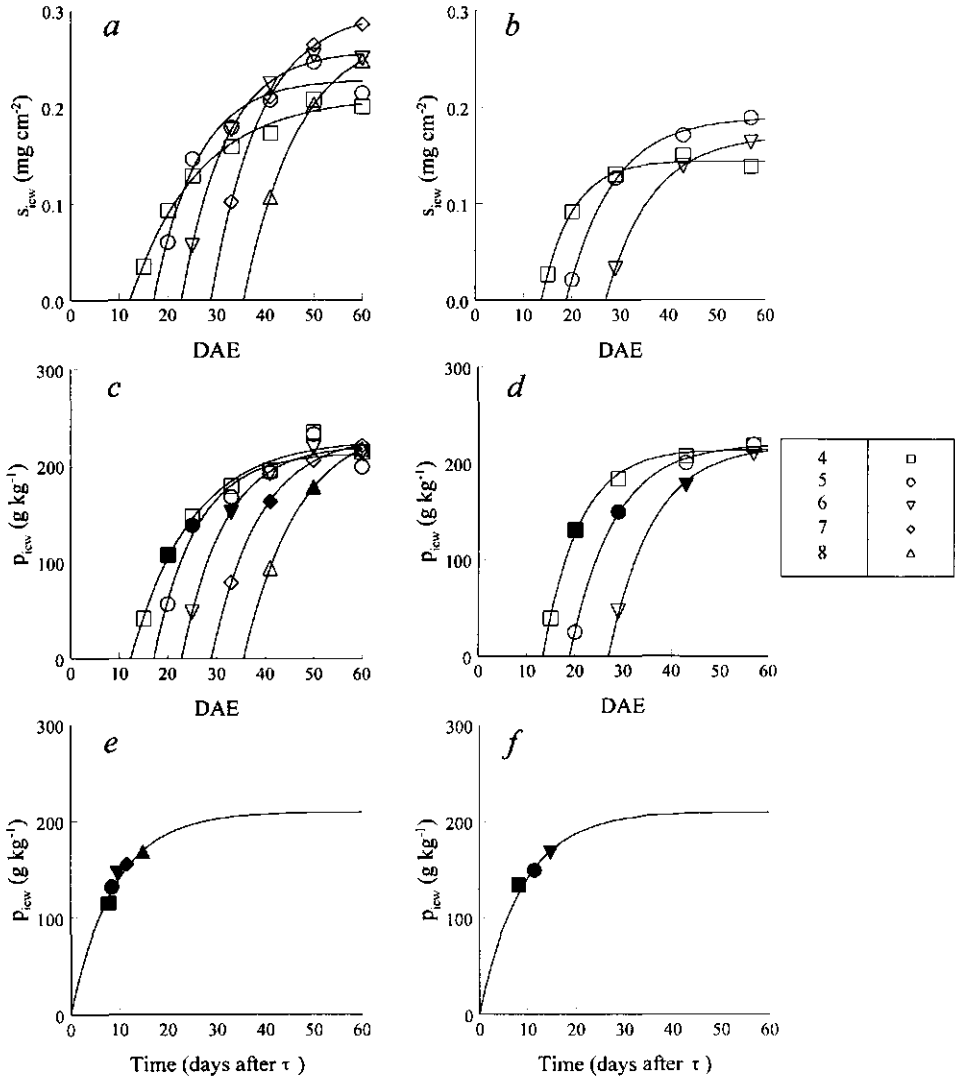


**Fig 4.** The curves of indigestible cell wall accumulation: specific mass in leaves 4, 5, 6, 7, and 8 ( $s_{icw}$ ) (*a*, spaced and *b*, sward), expressed as a proportion of cell wall mass ( $p_{icw}$ ) (*c*, spaced and *d*, sward) and after correction for the time of intersection with the time axis (*e*, spaced and *f*, sward). Solid markers indicate the moment of ligule appearance of leaves.

The points in Figs 4e & 4f indicate the time of ligule appearance for consecutive leaves. They clearly suggest that the higher  $p_{icw}$  at the moment of ligule appearance in later produced leaves had been due to the fact that this moment occurred in a more advanced stage of leaf growth, when calculated from the estimated time of the initiation of  $s_{icw}$  increase ( $\tau$ ). From the same background also the leaf differences and the differences between the spaced and the sward plants in the CWD at ligule appearance (Table 3) and the rate of CWD decline during ageing could be explained.

**Table 3.** Cell wall content and digestibility at ligule appearance (CWC and CWD; g kg<sup>-1</sup>) of consecutive leaves on the main shoot of plants grown spaced or in a sward.

Treatment	Leaf	CWC	CWD
Spaced	4	304	889
	5	321	868
	6	365	854
	7	401	845
	8	412	832
Sward	4	340	866
	5	380	839
	6	417	833

## 2.5 Discussion

During the experiment, the level of irradiance and the crop nitrogen concentration declined. However, until 50 DAE, light intensity was not limiting for photosynthesis of individual leaves when corrected for daylength and thus calculated as average PPFD in  $\mu\text{mol m}^{-2} \text{s}^{-1}$  (critical value of ca. 400  $\mu\text{mol m}^{-2} \text{s}^{-1}$ ; Gaastra 1959), while, up to 30 DAE, the spaced plants had high total plant NC of 60 g kg<sup>-1</sup> or more. We therefore assume that, at least for the spaced plants until then the changing light intensity and nitrogen concentrations had not been limiting for leaf growth and leaf and shoot development up to that time. After 30 DAE the spaced plants had produced 6 leaves on the MS and until then they had kept a high and constant site filling of 0.555 shoots shoot<sup>-1</sup> per day.

### 2.4.1 Leaf appearance rate

After an initial period of slow leaf growth by cell division, a leaf of ca. 1 to 5 mm length enters a phase of rapid growth when cell elongation commences. After cell elongation, cells reach a maturation zone where secondary CW is synthesized (Skinner & Nelson 1995). This process may be accompanied by lignification of the primary cell wall as was observed in stem tissues of *Zea mays* by Engels & Schuurmans (1992). Therefore, the calculated time of initiation of  $s_{icw}$  increase ( $\tau$ , Eqn 1) may be associated with the start of rapid leaf growth. The values of  $\tau$  show that the intervals between the moments of initiation of this leaf growth stage increased. Moreover, the time span between  $\tau$  and ligule appearance increased. This may have been related to the increasing length of the sheath tube through which leaves have to grow (Wilson & Laidlaw 1985). This suggests that the declining leaf appearance rate had two causes. These could also explain the difference in the leaf appearance rate between the spaced and the sward plants although the number of observations of  $\tau$  for the sward plants may be too limited to draw firm conclusions.

### 2.4.2 Leaf dimensions and composition

The photomorphogenetic response of plants to crop shading, as observed in the sward plants when compared to the spaced plants, first led to reduced leaf dry weight. Leaf area remained the same until leaf 5 in both treatments because a reduction in width of leaf blades of the sward plants was compensated by increased length. Leaf area was gradually smaller in later leaves of the sward plants and SLA of the leaf blades at ligule appearance was higher in the sward plants (Fig 2).

Both  $s_{cw}$  and  $s_{cc}$  were lower in the sward plants than in the spaced plants. However, the reduction of the  $s_{cc}$  was stronger than for  $s_{cw}$  (Figs 3a & 3b) and consequently CWC was higher in the sward plants (Table 3). The reduction in leaf width and in  $s_{cw}$  and  $s_{cc}$  was probably related to declining width and depth, and increasing length of cells as observed by Rahim & Fordham (1991) in *Allium sativum* in response to shading. Moreover, the intercellular air volume can be higher in more heavily shaded leaves (Deinum B pers comm).  $s_{cc}$  was probably further reduced by the lower N and assimilate amounts in leaves of the sward plants.

After ligule appearance  $s_{om}$  declined due to loss of CC. The decline in  $s_{cc}$  can be attributed to a decreasing rate of photosynthesis, to respiratory losses and to translocation of assimilates or N to growing leaves (Robson & Deacon 1978). The rate of decline in  $s_{cc}$  during the ageing of leaves was constant and the same for consecutive leaves and for the spaced and the sward plants (Figs 3c & 3d). This may be an indication of a closely balanced control of metabolic processes rather independent of leaf light interception, although the leaves of the sward plants yellowed earlier than leaves of the spaced plants.

$s_{cw}$  remained unchanged during ageing, although changes occurred in this fraction as reflected in the increasing  $p_{icw}$ , until an asymptotic value of ca. 210 g kg<sup>-1</sup> CW (Fig 4) was reached. This  $\alpha_p$  was remarkably constant for consecutive leaves and for the spaced and the sward plants which indicates that the tissue composition was essentially independent of leaf number and light. The increase of  $s_{icw}$  during ageing can be attributed to continued lignification of the primary and part of the secondary CW in xylem and sclerenchyma, as described by Engels & Schuurmans (1992).

#### 2.4.3 Digestibility

Differences in OMD at ligule appearance were observed but the rate of OMD decline during ageing was the same for leaves 4 to 6 (Figs 3e & 3f). A longer time span between  $\tau$  and ligule appearance lowered CWD at ligule appearance due to the more advanced stage of ICW synthesis, resulting in lower OMD. The higher CWC of consecutive leaves and of leaves of the sward plants had a further reducing effect on OMD at ligule appearance. Moreover, the rate of CWD decline during ageing was lower if the period between  $\tau$  and appearance had been longer. However, the effect of this reduction on the rate of OMD decline was counteracted by higher CWC, resulting in virtually the same OMD decline rate for all leaves.

The lower OMD at ligule appearance for consecutive leaves has also been observed by Wilson (1976), Deinum (1976) and Nordang *et al.* (1992). However, a higher OMD decline rate is often observed for leaves 1 to 5 on the MS. As demonstrated in this experiment, various parameters can contribute to the latter trend, such as a lower CWC, a higher  $s_{cc}$  decline rate and a higher  $\alpha_p$ . These parameters may be influenced by environmental factors (e.g. temperature) and plant species characteristics. Further analysis of these factors is required.

It can be concluded that analysis of  $s_{cc}$  and  $s_{cw}$  ( $\text{mg cm}^{-2}$ ) improved insight into CWC dynamics. The CWC is an important factor in determining OMD at ligule appearance and OMD decline rate during ageing. These quantities were further strongly affected by  $s_{icw}$  increase in leaves. The  $\alpha_p$  was remarkably constant. Lower CWD at ligule appearance and CWD decline rate of consecutive leaves and leaves of the sward plants resulted from the longer period of growth of the leaf through the sheath tube indicating the importance of plant morphology in relation to plant digestibility.

### 3. DEFOLIATION

with Jan H. Neuteboom & Bauke Deinum

#### 3.1 Abstract

The characteristics of individual leaf blades on regrowing grass shoots were quantified. A glasshouse experiment was carried out with Italian ryegrass (*Lolium multiflorum*) grown from seed. Half of the plants were grown undisturbed until leaf stage 8, while the other half were cut at leaf stage 4, after which they were allowed to grow until leaf stage 9. The composition and digestibility characteristics of leaves 6, 7 and 8 on the main shoot (MS) of plants from both treatments were quantified.

In the uncut plants, leaf blade length and mass and specific cell wall (CW) and organic matter mass ( $s_{CW}$  and  $s_{OM}$ , mg cm<sup>-2</sup>) was higher for consecutive leaves. During leaf ageing  $s_{CW}$  remained unchanged, while  $s_{OM}$  and cell wall digestibility (CWD) declined, resulting in a decline of organic matter digestibility. CWD of leaves decreased to ca. 780 g kg<sup>-1</sup>, a value also found in an earlier experiment.

The newly formed leaves after cutting had a reduced leaf size and specific leaf mass ( $s_{dm}$ , mg cm<sup>-2</sup>). Leaf 6, that was damaged by cutting, showed a lower initial cell wall content and a rapid decline of  $s_{CW}$  and  $s_{OM}$  and of CWD during ageing. Its low  $s_{CW}$  and CWD could have been related to cessation of CW synthesis during its growth after cutting, as was evidenced by the lower cell wall thickness of sclerenchyma cells. The later formed leaves, 7 and 8, had digestibility characteristics similar to those of the uncut plants. Since leaf 6 hardly contributed to the total plant dry matter mass, the cut and the uncut plants differed only slightly in digestibility of the total leaf fraction. It can be concluded that cutting sets back leaf size and growth rate but has little effect on composition and digestibility characteristics during ageing.

#### 3.2 Introduction

Herbage consumed by the grazing ruminant primarily consists of leaf blades (Brereton & Carton

1988), grown in a frequently defoliated sward. Most studies on individual leaf blade digestibility have been carried out with undisturbed growing plants (Wilson 1976; Deinum 1976; Nordang *et al.* 1992). In Chapter 2 the time course of digestibility of consecutive leaves on the MS of Italian ryegrass grown as spaced plants and simulated swards was compared. In this Chapter, a comparison of the effects of defoliation on consecutive leaves on the MS of Italian ryegrass plants grown undisturbed or defoliated once in the fourth leaf stage is made. Defoliation has a strong effect on leaf blade size of later leaves (Hill & Pearson 1985; Van Loo 1993) and could, in principle, also have particular effects on tissue and cell wall characteristics of consecutive leaves.

### 3.3 Experimental

#### 3.3.1 General

Italian ryegrass (*Lolium multiflorum*) cv. EIRT58 was sown on August 10, 1992. This experimental cultivar was selected for its large leaf size. The seeding rate was 25 per 1.5 litre pot (surface area 0.0169 m<sup>2</sup>). Pots contained a mixture of sand and peat (1:1 v/v), and were filled to the same weight. When the plants had emerged (ca. 1 week after sowing), they were thinned to 16 plants per pot. The experiment was carried out in a glasshouse (day/night temperature 18/13°C, daylength 14 h, rel. humidity ca. 70%). The transmission coefficient of the glasshouse for outdoor irradiance was 0.7. Additional photosynthetically active light was supplied by Philips 400W SON-T lamps (207  $\mu\text{mol m}^{-2} \text{s}^{-1}$  at ground level for 14 h).

The pots were placed in 4 replicate blocks. The blocks were split for 2 treatments (sub-blocks): half of the plants were cut at 2 cm above ground level 28 days after emergence, when plants had reached the 4-leaf stage on the MS (ligule leaf 4 appeared), while the other half remained uncut. Within the sub-blocks 4 rows of 6 pots were formed, to which consecutive harvests were randomly assigned. One randomly selected row of the cut treatment served for the first dry matter measurement of the uncut plants. Uncut plants were harvested at average leaf-stages 5, 6, 7, and 8. The cut plants were harvested at average leaf-stages 6, 7, 8 and 9. Material of replicate blocks 1&2 and 3&4 was bulked, to give 2 replicates for chemical analysis of

individual leaves.

The pots were placed in large trays, which were flushed twice daily with nutrient solution containing 1.068 g  $\text{Ca}(\text{NO}_3)_2 \cdot 4 \text{H}_2\text{O}$  litre<sup>-1</sup> and 0.535 g  $\text{KNO}_3$  litre<sup>-1</sup> and sufficient amounts of other nutrients. The nutrient solution was replenished weekly.

### *3.3.2 Sample collection and measurements*

The plants were harvested by cutting shoots at 2 cm above ground level. Main shoots (MS, first shoot appearing after germination) were separated into individual leaf blades and sheaths and dry matter mass was determined. Blade area and blade and sheath length were measured on 10 main shoots per series of 6 pots. Leaf area was measured using a LI-COR 3100 Leaf-Area Meter® (Li-Cor Inc., Lincoln, NE, USA). Samples were dried at 70°C for 24 h. After weighing, samples were ground to pass a 1 mm screen in a hammer mill. At each harvest 4 plants were stored in 50% alcohol solution and stored at 4°C for anatomical studies.

### *3.3.3 Chemical analyses*

Samples were analysed for cell wall content in organic matter (CWC), using the Neutral Detergent method (Goering & Van Soest 1970). Additionally undissolved protein was removed by incubation of the cell wall residues with alcalase (0.75 ml in 40 ml buffer solution) for 1 h at 40°C. *In vitro* true organic matter and cell wall digestibility (OMD and CWD) was determined after 48 h incubation of 0.5 g dry matter in rumen fluid from oxen fed medium quality grass hay (Goering & Van Soest 1970).

### *3.3.4 Anatomical measurements*

Leaves 6 and 7 of cut and uncut plants were analysed for anatomical characteristics after ligule appearance. 25 mm portions were taken from the midpoint of the leaf and from it a series of 100 µm thick transverse sections were cut using a sliding arm microtome. Of these sections, the width, average thickness and area were determined. The cross sectional area of vascular bundles (VB) and the parenchyma bundle sheath (PBS) was also measured. The sclerenchyma (SCL)



bundles in the leaf were counted. These bundles were classified, according to the number of cells per bundle; class 1 comprised bundles containing 1 to 5 cells, class 2 bundles with 6 to 10 cells, class 3 bundles with 10 or more cells. Thus, a class index could be calculated for SCL bundles. In a well-developed sclerenchyma bundle adjacent to the midrib bundle, cell diameter and cell wall thickness were measured.

### 3.4 Results

#### 3.4.1 Biomass accumulation, leaf appearance and tillering

The canopy growth parameters were significantly different between undisturbed seedling growth and regrowth after cutting. The linear growth rate calculated from the expo-linear curve of Goudriaan & Monteith (1990) was lower after cutting than for undisturbed seedling growth (19.7 vs 24.7 g m<sup>-2</sup> per day) (Fig 1).

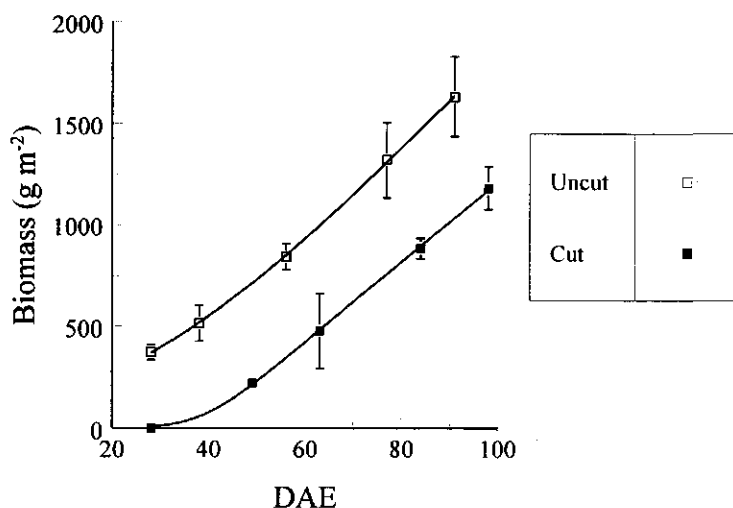


**Fig 1.** Biomass above cutting height for uncut plants and cut plants vs days after emergence (DAE). An expolinear curve is fitted (—).

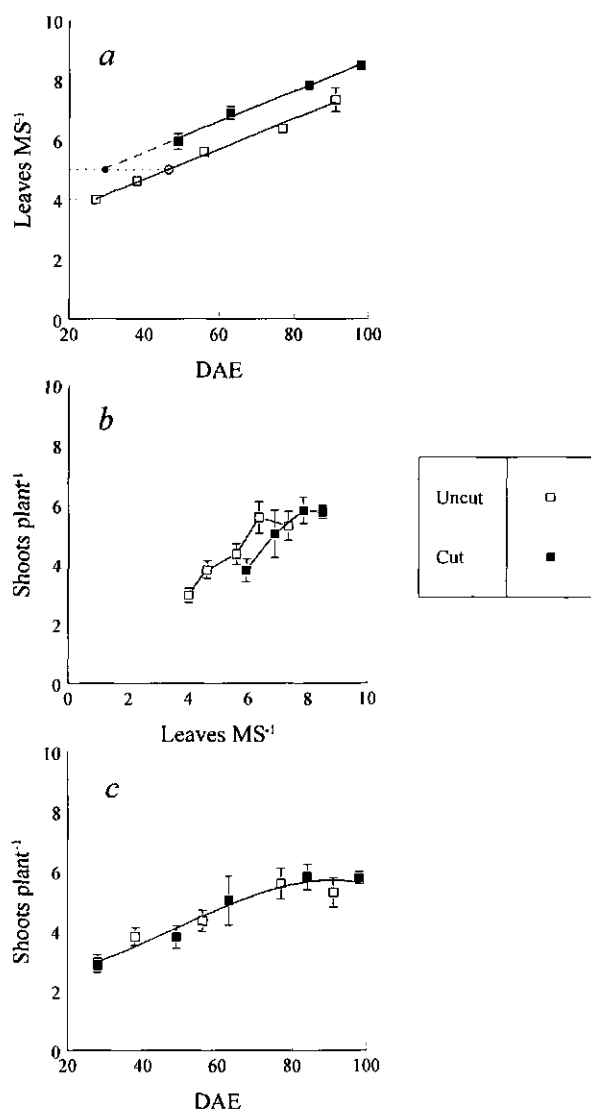


**Fig 2.** Leaf appearance and tillering of uncut and cut plants. *a.* The mean leaf stage of the main shoot ( $MS$ ) vs days after emergence (DAE). A linear regression line was fitted through the observations (—). From this line, the moment at which leaf stage 5 (indicated by ----) was reached was calculated (indicated by ○ and ● for uncut and cut plants, respectively). *b.* Number of shoots per plant vs mean leaf stage. *c.* Number of shoots per plant vs DAE.

Cutting at the low height of 2 cm had reduced the sheath tube length and therefore quickened the appearance of leaf 5. Fig 2*a* shows that, adjusted for this effect, the leaf appearance rate was not

affected by cutting, and that from the second harvest onward, the cut and the uncut plants had the same leaf appearance rate (0.050 and 0.051 per day, respectively). Also tillering, in terms of site filling, was in fact not affected by cutting because, if the shoot number increase plotted against the number of leaves of the MS in Fig 2*b* is put back for the cut plants by one leaf, then the cut and uncut plants had the same site filling (0.250 and 0.236 shoots shoot<sup>-1</sup> per leaf appearance interval, respectively). After the total number of shoots stabilized at ca. 6 per plant (ca. 57 dm<sup>-2</sup>) first shoot death was observed (Fig 2*c*).

### 3.4.2 Leaf dimensions

Leaf blade dimensions of consecutive leaves on the MS are presented in Table 1. These dimensions were determined immediately after ligule appearance. During undisturbed growth in the uncut plants, leaf blade lengths increased to a maximum for leaf 7, while leaf blade area increased up to and including leaf 8. As leaf dry matter mass increased more strongly than leaf blade area, specific leaf mass ( $s_{dm}$ , mg dry matter cm<sup>-2</sup>) increased slightly for consecutive leaves.

Cutting reduced the sizes and mass of the following newly formed leaves compared with undisturbed growth. This was most pronounced for leaf 6, which was damaged by cutting. Cutting reduced the leaf lengths, areas and dry matter masses, averaged for leaves 7 and 8, by 25%, 37% and 57%, respectively. Due to the stronger effect of cutting on leaf mass, leaves 7 and 8 had a 39% and 23% lower  $s_{dm}$  compared with undisturbed growth, respectively.

### 3.4.3 Specific leaf mass

Table 1 also presents the specific mass (mg cm<sup>-2</sup>) of total organic matter ( $s_{om}$ ) and cell wall ( $s_{cw}$ ). The higher  $s_{dm}$  and  $s_{om}$  for consecutive leaves during undisturbed growth (the uncut plants) resulted mainly from a higher  $s_{cw}$ , because all leaves had virtually the same specific cell contents mass ( $s_{cc}$ ), calculated as  $s_{om}$  minus  $s_{cw}$ . This also resulted in a slightly higher CWC for consecutive leaves.

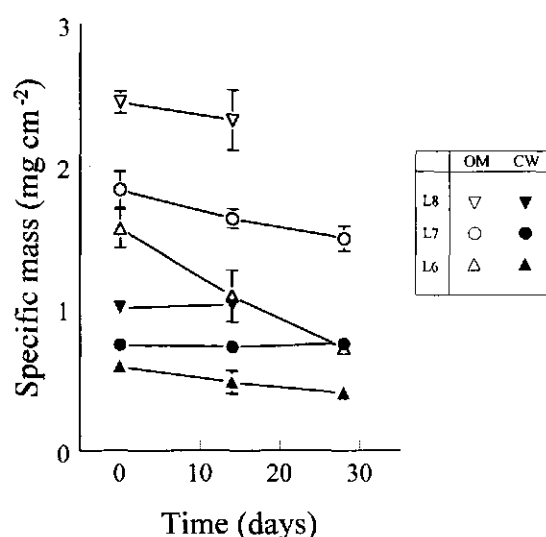


Fig 3. Specific mass of organic matter (OM) and of total cell wall (CW) of the blades of consecutive leaves 6, 7 and 8 on the main shoot of the cut plants vs days after ligule appearance.

Table 1. Dimensions of consecutive leaf blades on the main shoot of uncut and cut plants<sup>a,b</sup>.

	Leaf	DW mg	Length cm	Area cm <sup>2</sup>	$s_{dm}$ mg cm <sup>-2</sup>	$s_{om}$ mg cm <sup>-2</sup>	$s_{cw}$ mg cm <sup>-2</sup>	CWC g kg <sup>-1</sup>
Uncut	6	119	67	38	3.1	2.7	1.0	323
	7	161	74	45	3.5	3.0	1.2	344
	8	178	72	49	3.7	3.3	1.5	403
Cut	6	40	34	22	1.9	1.6	0.6	326
	7	68	53	31	2.2	1.9	0.8	365
	8	78	56	28	2.8	2.4	1.0	357
LSD		19.0	13.5	3.7	0.22	0.39	0.12	16
Cut as	6	34	51	58	61	59	60	100
%	7	42	72	69	63	63	67	106
of uncut	8	44	78	57	76	73	67	90

<sup>a</sup> Dry weight (DW), length, area, specific leaf mass of dry matter ( $s_{dm}$ ), organic matter ( $s_{om}$ ) and cell wall ( $s_{cw}$ ), and cell wall content (CWC).

<sup>b</sup> LSD indicates least significant difference ( $\alpha=0.05$ , Tukey test).

The lower  $s_{dm}$  and  $s_{om}$  of the newly formed leaves after cutting was due to lower  $s_{cw}$  and  $s_{cc}$ . Since both were lowered to the same extent, CWC of the new leaves was not affected by cutting.

Both the uncut (not shown) and the cut plants (Fig 3) showed a tendency of declining  $s_{om}$  after ligule appearance.  $s_{om}$  of leaf blades of the uncut plants and of leaves 7 and 8 of the cut plants declined significantly during ageing. This was due to a decline in cell contents, because  $s_{cw}$  hardly changed.  $s_{cw}$  declined after ligule appearance only for leaf 6 of the cut plants.

#### 3.4.4 Digestibility

In the uncut plants, CWD of the leaf blades after ligule appearance decreased from 850 g kg<sup>-1</sup> to 769 g kg<sup>-1</sup> for leaves 6 and 7 (Fig 4a). Leaf blades 7 and 8 of the cut plants reached similar values of 771 g kg<sup>-1</sup> and 787 g kg<sup>-1</sup> CWD (Fig 4b). However, in leaf 6 of the cut plants, CWD declined to a low level below 400 g kg<sup>-1</sup>. This together with its relatively low  $s_{cc}$  explains its low final OMD of 642 g kg<sup>-1</sup> (Fig 4b). The cut and the uncut plants showed a similar decline of OMD for leaves 7 and 8 (Figs 4a & 4b).

The low CWD of leaf 6 was the reason for the lower CWD (708 vs 757 g kg<sup>-1</sup>) of the total leaf fraction of the cut vs the uncut plants 10-15 days after cutting (Fig 4c). However, due to the increasing mass and normal digestibility characteristics of the newly formed leaves 7 and 8, this hardly affected OMD of the total leaf fraction of the cut vs the uncut plants (Fig 4c).

#### 3.4.5 Leaf anatomy

The cross sectional areas of leaf blades contained 90-92 % of thin-walled mesophyll and epidermis tissues. However, the largest part (ca. 80%) of total cell wall mass was found in sclerenchyma cell walls. Characteristics of the cross sections of leaves 6 and 7 of the uncut and the cut plants are presented in Table 2. During undisturbed growth (the uncut plants) leaf width, thickness, and VB and PBS cross sectional area increased from leaf 6 to leaf 7. The same was true for the cross sectional area of sclerenchyma tissue, although the sclerenchyma bundle number and cell wall thickness hardly increased. Cutting reduced the cross sectional dimensions of VB, PBS and sclerenchyma of leaf 7, whereas in leaf 6 especially cell wall thickness of the sclerenchyma cells was reduced (Table 2).

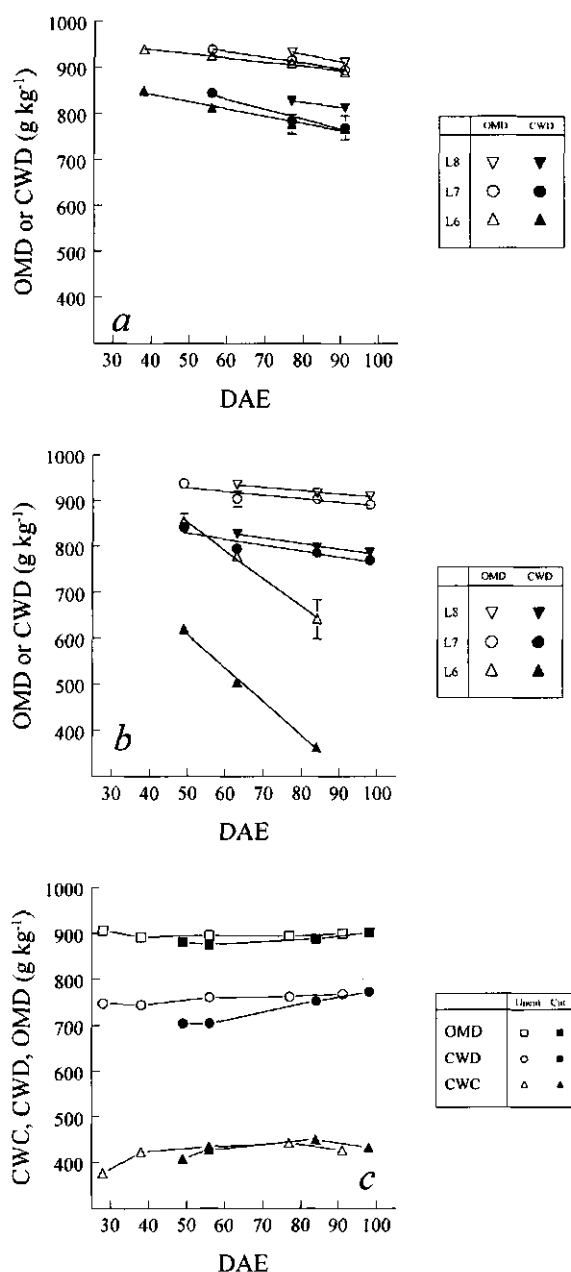


**Fig 4.** Cell wall and organic matter digestibility (CWD and OMD) of leaf blades 6, 7 and 8 on the main shoot of uncut and cut plants (*a*, *b*) vs days after emergence (DAE). *c*. Weighed average cell wall content (CWC), CWD and OMD of the total leaf blade fraction on the main shoot of uncut and cut plants.

**Table 2.** Characteristics of the leaf cross sections of leaves 6 and 7 of uncut and cut plants<sup>a,b</sup>.

	Leaf	Leaf cross section					Sclerenchyma			
		Width	Thick- ness	Area	VB	PBS	Bundle nmb.	Bundle class	Cell diam.	Wall thickn.
		$\times 10^2 \mu\text{m}$	$\mu\text{m}$	$\times 10^4 \mu\text{m}^2$					$\mu\text{m}$	$\mu\text{m}$
Uncut	6	88.8	246	220	8.8	11.9	35	1.71	8.6	1.47
	7	96.7	299	289	9.8	13.1	36	1.95	10.1	1.35
	6	81.3	257	209	6.9	10.7	32	1.84	9.1	1.00
	7	70.2	263	182	5.5	8.8	29	1.59	7.8	1.21
LSD		11.47	31.3	46.7	2.10	3.02	6.3	0.238	1.67	0.424
Cut as % of uncut	6	92	104	95	78	90	91	108	106	68
	7	73	88	63	56	67	81	82	77	90

<sup>a</sup> Width, thickness and total area and the cross sectional area of vascular bundles (VB), and parenchyma bundle sheath (PBS). For sclerenchyma the number of bundles, the average bundle class (index for the number of cells per bundle), the cell diameter and cell wall thickness are presented.

<sup>b</sup> LSD indicates least significant difference ( $\alpha=0.05$ , Tukey test).

### 3.5 Discussion

Van Loo (1993) also observed no effect of cutting on leaf appearance rate and site filling, except under frequent low cutting (weekly at 2.5 cm). In the present experiment, shoot numbers had doubled between cutting and the end of the experiment. The regrowing defoliated shoots contributed ca. 650 g kg<sup>-1</sup> to the total crop dry matter, assuming that all regrowing shoots had the same leaf appearance rate and leaf dry matter mass as the MS. Considering the calculated linear growth rates of ca. 20 g m<sup>-2</sup> per day, light had not been limiting for dry matter production.

Cutting reduced the leaf dimensions (area,  $s_{dm}$ ,  $s_{om}$  and  $s_{cw}$ ) of newly formed leaves 6, 7 and 8 when compared with undisturbed growth. Despite the reductions in leaf dimensions, the CWC had not changed. Moreover, leaves 7 and 8 showed the same decline rates of OMD and CWD as the leaves of the uncut plants. Therefore, it is concluded that composition in terms of  $s_{cc}$  and  $s_{cw}$ , and the digestibility characteristics, of newly formed leaves are not affected when the growth of the plant is interrupted by cutting.

Only leaf 6, which was damaged by cutting, clearly differed from leaves 7 and 8. The width and cross section tissue area of leaf 6 of the cut plants were the same as in the uncut plants. These dimensions were probably already fixed at the moment of cutting. In contrast, sclerenchyma cell walls had developed poorly. Moreover,  $s_{CW}$  declined during ageing, possibly due to breakdown by endogenous cell wall degrading enzymes as observed in senescing leaves of other plants after wounding and in the abscission zone of tree leaves (Parthier 1989) or degradation of cell wall and cell contents at the cut end of the leaf by bacteria and fungi.

The thin sclerenchyma cell walls of leaf 6 of the cut plants can explain the lower CWD of this leaf. The large fraction of indigestible cell walls at ligule appearance could indicate a sudden arrest of cell wall formation for leaves damaged by cutting, when it is assumed that the primary cell wall had been formed and lignified (Engels & Schuurmans 1992) but the process of secondary cell wall deposition was interrupted. The lignification of the small digestible cell wall fraction and decline in  $s_{CW}$  will then result in a high rate of CWD decline, as observed. The rate of decline in OMD of leaf 6 was high due to the described changes in CWD and the rapid loss of cell contents during ageing, which was probably due to the great sink strength of expanding leaves (Richards 1993). Leaf 7 of the cut plants was narrower and thinner than leaf 6, which can be considered as a morphological response to cutting. The thickness of sclerenchyma cell walls was similar to that of leaf 7 of the uncut plants, indicating that cell wall synthesis was re-established.

In conclusion, contrarily to the plant morphology, the physiology rapidly recovers after defoliation (cf. Chapman & Lemaire 1993). Assuming that all regrowing shoots had a cut leaf similar to leaf 6, the cut leaves contributed only ca. 10% to total crop dry matter at the final harvest. Consequently, the differences in the composition and the digestibility characteristics of the whole leaf fraction between the cut and the uncut plants were limited. Larger changes in crop digestibility might occur in the reproductive development stage, when less digestible stem internodes are formed.



## 4. TEMPERATURE AND POPULATIONS

with Jan H. Neuteboom, Egbert A. Lantinga & Bauke Deinum

### 4.1 Abstract

Temperature and reproductive development are the most important factors determining composition and digestibility of grass. The effects of these factors on digestibility characteristics of individual plant organs were quantified, for two perennial ryegrass (*Lolium perenne*) populations. Two glasshouse experiments were conducted at day/night temperatures of 13/8°C, 18/13°C and 23/18°C with vegetative and reproductive crops. The populations were selected for differences in leaf blade digestibility. Cell wall content (CWC) and true cell wall and organic matter digestibility (CWD and OMD) of vegetative and reproductive shoots were related to dimensions, mass, CWC and digestibility of separate plant organs.

Compared to the vegetative shoots, the reproductive shoots had higher daily rates of leaf appearance, organic matter growth and CWD decline. Strikingly, for both shoot types no direct effect of temperature on whole shoot CWD was observed as temperature effects could be eliminated completely by relating CWD to shoot development stage ( $d_t$ ) expressed as number of appeared leaves on the main shoot. Hence, temperature effects on CWD were restricted to its influence on shoot development rate only. The increase of the proportion of indigestible cell wall ( $p_{icw}$ , g kg<sup>-1</sup>) of individual organs with  $d_t$  in the reproductive shoots could be described satisfactorily with a negative exponential curve, which approached an asymptote ( $\alpha_p$ ) that was lower for leaf blades (245 g kg<sup>-1</sup>) than for leaf sheaths (509 g kg<sup>-1</sup>) and stem internodes (770 g kg<sup>-1</sup>).  $\alpha_p$  and the fractional CWD decline rate of 0.395 per  $d_t$  of all organs in both shoot types were not affected by plant organ insertion level, temperature or population. As the distribution of whole shoot cell wall mass between the plant organ fractions converged for all treatments, temperature and population had also no effect on whole shoot CWD decline rate. Differences between temperature treatments in OMD were caused by the higher CWC of plant organs at higher temperature, due to the stronger decline of specific organic matter mass than of specific cell wall mass of plant organs at higher temperature. Differences in whole shoot OMD between populations were observed only for vegetative shoots and were also caused by differences in CWC.

It is concluded, that temperature accelerates both the shoot development rate and the CWD decline rate during ageing to the same extent, whereas plant organs corresponded in CWD decline pattern as a function of  $d_f$ . These trends offer unique possibilities for modelling grass digestibility under contrasting temperature regimes.

## ***4.2 Introduction***

In the experiments described in this Chapter a new contribution to an explanatory mechanistic approach of changes in grass feeding quality is proposed. Changes in cell wall content and digestibility of vegetative and reproductive shoots were quantified and related to the dimensions, mass, composition and digestibility of the plant organs, in particular the leaf blades of vegetative shoots and the leaf blades, leaf sheaths and stem internodes of reproductive shoots. Since temperature is the most important environmental factor that influences digestibility of grasses (Buxton & Fales 1994), plants were grown at three temperature regimes. To study the possible causes of differences in digestibility between perennial ryegrass populations, two populations which were selected for differences in leaf blade dry matter digestibility were used.

## ***4.3 Experimental***

### ***4.3.1 General***

Two experiments with vegetative (experiment 1) and reproductive (experiment 2) perennial ryegrass were carried out in three well-controlled glasshouses, with day/night temperatures of 13/8°C, 18/13°C and 23/18°C. In both experiments, two ryegrass populations differing in leaf blade digestibility were included. Day temperatures were maintained between 8.00 h and 20.00 h. Relative humidity was on average 70%. The experimental periods and average radiation intensities are summarized for both experiments in Table 1. Radiation data were obtained from the nearby Wageningen weather station. Daily irradiance was corrected for the transmission coefficient (0.7) of the glasshouse.

Seeds were sown into pots containing a mixture of sand and peat (1:1 v/v). The pots were placed in large trays, which were flushed with mineral solution (Steiner 1984) daily. Seeds of two populations of perennial ryegrass, differing in leaf blade digestibility (population 1: high; population 2: low), were used (seed kindly supplied by Barenbrug BV, Oosterhout, The Netherlands). Plants were harvested 5 times, based on development stage. Four replicate blocks were placed in each glasshouse. Within the blocks, 10 rows of 6 pots were randomly assigned for each population x harvest time combination. Border pots were placed adjacent to the experimental pots. Harvested material of replicate blocks 1&2 and 3&4 was bulked to give two replicates for chemical analyses of individual leaf blades, leaf sheaths and stem internodes.

**Table 1.** Experimental periods and the average daily incoming solar radiation corrected for the transmission coefficient (0.7) of the glasshouse in the experimental periods (standard deviations between brackets), for vegetative (1993) and reproductive (1994) perennial ryegrass grown at three day/night temperatures.

Shoot type	Temperature °C	Period days after Jan. 1	Radiation MJ m <sup>-2</sup> d <sup>-1</sup>
Vegetative	13/8	129-214	11.8 (4.9)
	18/13	127-176	12.2 (5.0)
	23/18	123-155	12.5 (4.5)
Reproductive	13/8	149-192	12.6 (4.7)
	18/13	129-157	10.9 (4.3)
	23/18	112-136	10.9 (4.6)

#### 4.3.2 Experiment 1: vegetative shoots

In March 1993, pots for the three temperature regimes were seeded at weekly intervals, so that plants would reach the 4-leaf stage on the main shoot appearing after plant emergence at approximately the same moment. Daylength was natural. Plant density was 20 dm<sup>-2</sup>. Plants were cut at 3.5 cm above ground level in the 4-leaf stage. Harvests were made at each leaf appearance interval from leaf stage 6 onwards. Consecutive leaf blades from the main shoot were dissected and analysed.

#### 4.3.3 Experiment 2: reproductive shoots

In September 1993, seeds were sown and placed in an unheated glasshouse for vernalization during winter. Plant density was 15 per dm<sup>2</sup>. Plants were cut on 28 October 1993 in the 4-leaf stage. In March 1994, pots were transferred to heated glasshouses with day/night temperatures of 13/8°C. For the 18/13°C and 23/18°C regimes, the temperature was increased by 1°C per day until the required temperatures were reached, to avoid loss of vernalization. Moreover, daylength was extended to 17 h by low radiation (25 W) light bulbs to initiate inflorescence development and stem elongation at the same moment at every temperature. In the early stages of the experiment, two harvests were taken for determination of whole crop characteristics. Thereafter, for analyses of individual organs, plants were harvested at the moment of flag leaf appearance and after 1 and 2 intervals of 21 d, 14 d and 10 d thereafter for the 13/8°C, 18/13°C and 23/18°C temperature regimes, respectively. From each pot the 15 largest shoots were selected and dissected into separate leaf blades, leaf sheaths and stem internodes. Leaves and internodes were numbered from the bottom to the top of the shoot, starting with the first leaf formed after transfer (= leaf 1).

#### 4.3.4 Measurements

In both vegetative and reproductive plants the moment of appearance of leaves on the main shoot was recorded, to determine the rate of shoot development. The leaf appearance rate was used to calculate the development stage of shoots ( $d_i$ , in leaf appearance intervals). The age of plant organs ( $d_j$ ) was expressed in leaf appearance intervals after their full expansion. Although in reproductive shoots no new leaves are formed after flag leaf appearance, the leaf appearance rate before that stage was used to calculate  $d_i$  and  $d_j$ . Two harvests were made before flag leaf appearance. These were made at different development stages in the three temperature treatments, because the development stage relative to the flag leaf was not known before its appearance. Consequently, comparisons between insertion levels and temperature treatments after ligule appearance were not possible.

The length and width of leaf blades and stem internodes was recorded. Leaf area was calculated from length and width using a calibration factor to correct for leaf shape (cf. Bos & Neuteboom 1998). The leaf sheaths in the vegetative plants were not analysed, because

these form only a minor part of the animal diet. In a reproductive crop leaf sheaths are elevated along with the internodes and thus will be harvested, at least with silage cuts.

Samples of consecutive leaf blades, sheaths and stem internodes were oven-dried for 24 h at 70°C and subsequently weighed to determine the dry matter mass. Samples were ground to pass a 1 mm screen in a hammer mill and analysed for cell wall content in organic matter (CWC) using neutral detergent solution (adjusted after Goering & Van Soest 1970). Undissolved protein was removed by incubation of the cell wall residue with alcalase (0.75 ml in 40 ml buffer solution) for 1 h at 40°C. Cell wall digestibility after 48 h (CWD) was measured according to the method of Goering and Van Soest (1970), using an incubation of 0.5 g air dry matter in rumen fluid from fistulated steers fed medium quality grass hay. True organic matter digestibility (OMD) was calculated assuming complete digestibility of the cell contents. From the mass of organic matter (OM; dry matter minus ash) and CWC ( $\text{g kg}^{-1}$  OM), cell wall (CW) mass was calculated. From the data on area, length, OM mass and CW mass, specific mass of OM and CW was calculated for each organ ( $s_{om}$  and  $s_{cw}$ ,  $\text{mg cm}^{-2}$  for leaf blade,  $\text{mg cm}^{-1}$  for leaf sheaths and stem internodes).

#### 4.3.5 Statistical analyses

To determine the effects of development stage, temperature and populations on OMD, CWD, CWC of whole shoots, and on the CWD and  $s_{om}$  and  $s_{cw}$  of plant organs, stepwise multiple regression analyses were carried out using Genstat 5.3 (Genstat 5 Committee, 1993). Terms included in the models for whole shoot composition were temperature ( $T$ ), population ( $P$ ), replicates ( $R$ ), development stage ( $d_i$ ),  $d_i^2$  and interactions terms (full model:  $(d_i + d_i^2) * T * P * R$ ). For the plant organs,  $d_i$  and a term for insertion level ( $I$ ) were included in the model, which resulted in the full model:  $(d_i + d_i^2) * T * P * I * R$ . Terms were added to the model provided they resulted in a significant ( $p < 0.05$ ) reduction in the residual mean square.

The curves of decline of CWD of individual organs were fitted non-linearly with a negative exponential decline curve, adjusted after Eqn 1 given in Chapter 2:

$$\text{CWD} = 1000 - \text{ICW} = 1000 - \alpha_p (1 - e^{-\beta(d_i - \delta)}) \quad \text{Eqn 1}$$

In this equation,  $\alpha_p$  denotes the asymptotic indigestible cell wall fraction ( $\text{g kg}^{-1}$ ),  $\beta$  is the fractional rate of decline of CWD per  $d_b$ , and  $\delta$  is the development stage at which ICW increase commences.

#### 4.4 Results

First, growth and development characteristics and the general trends in plant organ dimensions and composition in terms of  $s_{om}$  and  $s_{cw}$  are presented. Subsequently, the changes in whole shoot composition and digestibility and the effects of temperature and population are demonstrated on the basis of multiple regression analysis. Finally, the changes in shoot characteristics are related to those observed in separate plant organs.

##### 4.4.1 Shoot growth and development

Individual reproductive shoots showed considerably higher OM growth rates than vegetative shoots (Figs 1a & 1b). Growth and development rates were higher at higher temperature for both shoot types and only for reproductive shoots these rates were higher in population 1 than in population 2. The accelerated development rate at higher temperature is reflected in shorter growth periods for reaching the chosen development stage of the last harvest (Figs 1a & 1b) and increasing leaf appearance rate with temperature (Fig 1c). At final harvest, stem internodes and ears formed ca. 75% of total harvested shoot OM in the reproductive shoots (data not shown).

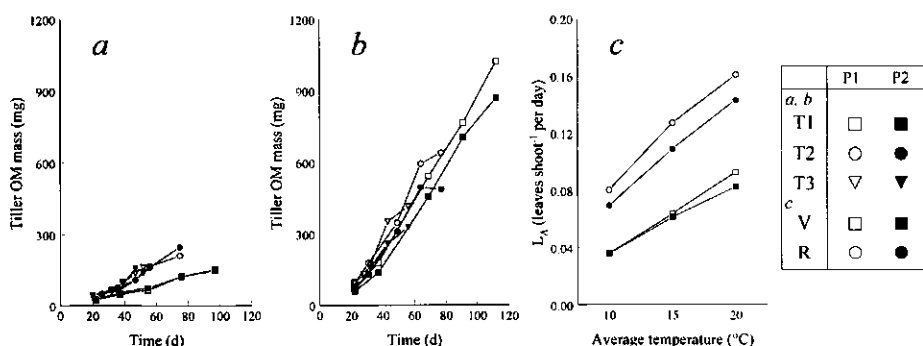


**Fig 1.** Shoot organic matter (OM) mass of vegetative (a) and reproductive (b) shoots and leaf appearance rate ( $L_A$ , c). Vegetative and reproductive shoots (V, R). Temperatures 13/8°C, 18/13°C and 23/18°C (T1, T2, T3). Populations 1 and 2 (P1, P2).

#### 4.4.2 Plant organ dimensions, mass, composition and digestibility

The consecutively formed plant organs increased in dimensions. In vegetative shoots the organs were larger at higher temperature, but this was reversed in reproductive shoots (Fig 2). In the vegetative shoots, the leaf blades of consecutive insertion levels had higher  $s_{om}$  and  $s_{cw}$ .  $s_{om}$  declined after ligule appearance at more or less similar rates for all leaf blades (Fig 3a). Also in the reproductive shoots, the leaf blades and sheaths of consecutive insertion levels had a higher  $s_{om}$  (Fig 3b). After flag leaf appearance,  $s_{om}$  of lower leaf blades declined, but it increased for the flag leaf (L6).

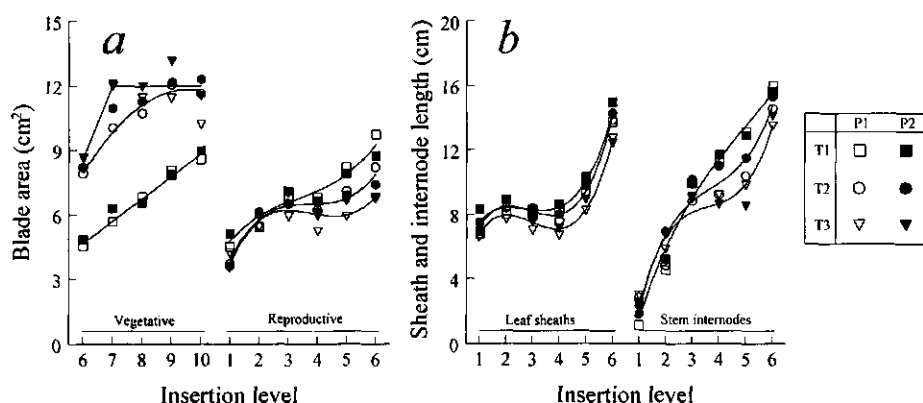


**Fig 2.** Leaf blade area (a), leaf sheath and stem internode length (b) for consecutive insertion levels on vegetative and reproductive shoots. Temperatures 13/8°C, 18/13°C and 23/18°C (T1, T2, T3). Populations 1 and 2 (P1, P2).

The leaf blade  $s_{cw}$  remained constant after flag leaf appearance (Fig 3b). Leaf sheath 6 (flag leaf) and the youngest stem internodes (5 and 6) were not fully grown at flag leaf appearance, and continued to increase in  $s_{om}$  and  $s_{cw}$ , while  $s_{cw}$  of the sheaths and internodes of lower insertion levels remained unchanged (Figs 3c & 3d). The final  $s_{cw}$  of leaf sheaths was higher for consecutive insertion levels (Fig 3c), while  $s_{cw}$  of stem internodes seemed to converge to the same level for all internodes (Fig 3d).

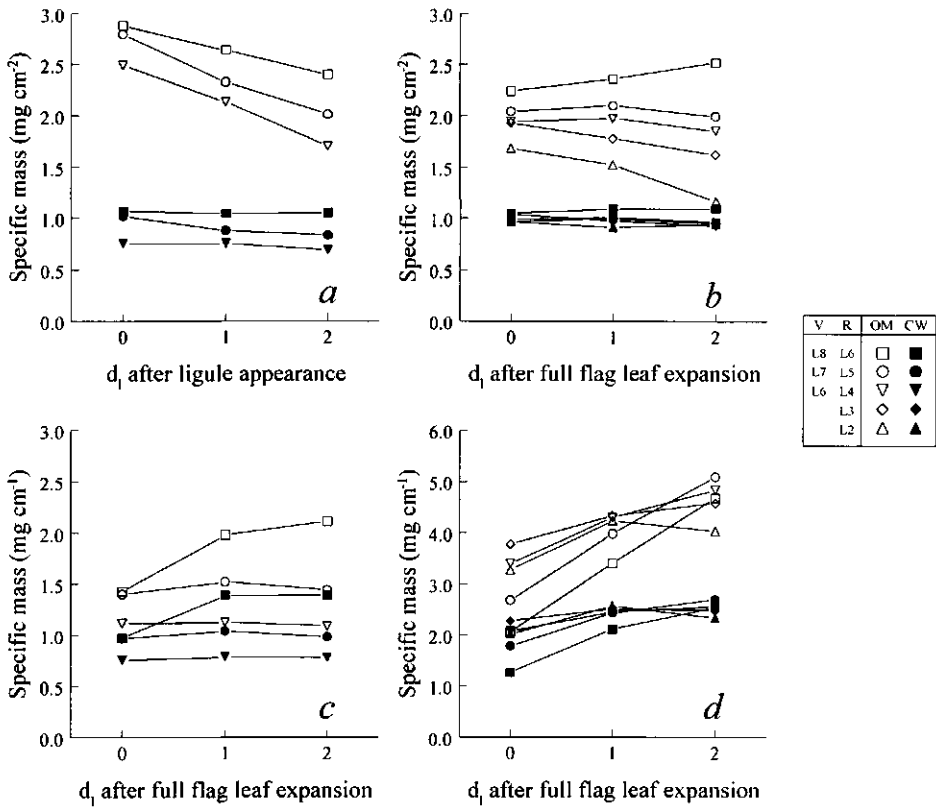


**Fig 3.** Specific OM and CW mass of leaf blades of vegetative shoots (a) of insertion levels 6 to 8 (L6 to L8) and leaf blades (b), and leaf sheaths (c) and stem internodes (d) of insertion levels 2 to 6 (L2 to L6) of reproductive shoots vs. plant organ development stage ( $d_1$ ). Vegetative and reproductive shoots (V, R). Averaged for temperatures and populations.

The pattern of CWD decline  $d_1$  of leaf blades, leaf sheaths and stem internodes is illustrated for the reproductive shoots in the 18/13°C temperature treatment in Fig 4a. The fitted curves were obtained with Eqn 1. Leaf blades, leaf sheaths and stem internodes differed in  $\alpha_p$  (Fig 4b), but had the same  $\beta$  of 0.395 per  $d_1$  (Fig 4c).  $\alpha_p$  was lower for leaf blades (245 g kg<sup>-1</sup>) than for leaf sheaths (509 g kg<sup>-1</sup>) and stem internodes (770 g kg<sup>-1</sup>). Both  $\alpha_p$  and  $\beta$  were not affected by temperature or populations (Figs 4b & 4c).



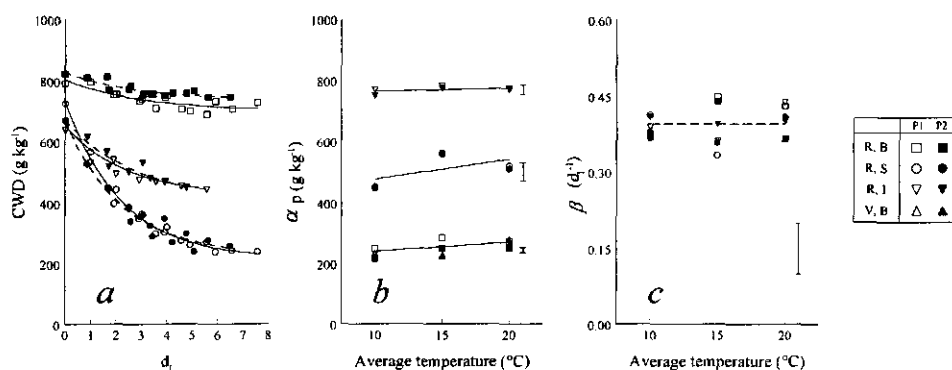


Fig 4. *a*. Plant organ cell wall digestibility (CWD) vs. leaf development stage ( $d_I$ ) of reproductive shoots at 18/13°C. The lines indicate the fitted curves. Asymptotic indigestible cell wall fraction ( $\alpha_p$ , *b*) and fractional indigestible cell wall increase rate per  $d_I$  ( $\beta$ , *c*) of plant organs at different average temperatures. Blades, sheaths and internodes (B, S, I). Vegetative and reproductive shoots (V, R). Populations 1 and 2 (P1, P2).

#### 4.4.3 Whole shoot composition and digestibility

A stepwise multiple regression analysis was carried out to discern the most important trends in composition and digestibility of whole shoots (Table 2). OMD was predominantly affected by shoot development stage ( $d_I$ ) and its quadratic component ( $d_I^2$ ), which is reflected in a decline of OMD with increasing development stage (Figs 5e & 5f). Minor effects were present of temperature and in vegetative shoots of population. Strikingly, whole shoot CWD declined linearly with  $d_I$  in both vegetative and reproductive shoots, although at a higher rate in the latter (Figs 5a & 5b).

In the vegetative shoots CWC was higher at higher temperature, and increased with development stage in the 18/13 and 23/18°C temperature treatments (Fig 5c) after  $d_I = 7$ , resulting in significant  $d_I$ ,  $d_I^2$  and  $T.d_I$  terms (Table 2). In the reproductive shoots, CWC increased before flag leaf ligule appearance ( $d_I = 6$ ) and faster at higher temperature (Fig 5d), which led to significant  $d_I$  and  $T.d_I$  terms in the regression analysis. However, CWC stabilized after flag leaf appearance and at higher levels at higher temperature (Fig 5d;  $d_I^2$  and  $T$  terms in Table 2).

The proportion of shoot CW mass in leaf blades decreased slowly in the vegetative shoots (Fig 6a), but rapidly in the reproductive shoots (Fig 6b). In the reproductive shoots

stem internodes and ears eventually comprised up to ca. 70% of whole shoot CW mass (Figs 6d & 6e).

**Table 2.** Results of the regression analysis for organic matter digestibility (OMD), cell wall digestibility (CWD) and cell wall content (CWC) of whole vegetative and reproductive shoots. The contribution of the significant terms to the  $r^2$  (%) of the regression model, and total  $r^2_{adj}$  (%) of the final model are presented<sup>a,b</sup>.

Term	Vegetative			Reproductive		
	OMD	CWD	CWC	OMD	CWD	CWC
T	7.83a	1.68b	56.32a	0.66b		20.91a
P	4.21a					
$d_i$	1.54a	82.14a	11.96a	88.94a	96.67a	59.19a
$d_i^2$	74.22a		12.44a	1.00a		8.15a
T.P	1.11b					
T. $d_i$			3.44a	6.19a		4.95a
T. $d_i^2$	1.30b					0.59b
P. $d_i$		1.50b	5.71a		0.33b	
P. $d_i^2$						0.39b
T.P. $d_i$						
T.P. $d_i^2$						0.56b
$r^2_{adj}$	89.4	84.8	89.2	96.6	96.9	94.2

<sup>a</sup> Terms: T, temperature; P, population;  $d_i$ , development stage;  $d_i^2$ , quadratic stage.

<sup>b</sup> Significance: a,  $p < 0.001$ ; b,  $p < 0.01$ ; c,  $p < 0.05$ .

#### 4.4.4 Temperature and populations

In all plant organs  $s_{om}$  and  $s_{cw}$  was lower at higher temperature, but the relative reduction of  $s_{om}$  was larger, resulting in higher CWC (Fig 7). CWC of stem internodes increased in the whole range of temperatures from 10 to 20°C, while in leaf blades and sheaths CWC mainly increased from 10 to 15°C. This was reflected in shoot CWC, which was higher (vegetative shoots, Fig 5c) or increased faster (reproductive shoots, Fig 5d) at higher temperature.

Remarkably, for both shoot types no direct effect of temperature on whole shoot CWD was observed since temperature effects could be eliminated completely by relating CWD to  $d_i$  (Figs 5a & 5b). Hence, temperature effects on CWD were restricted to its influence on shoot development rate only. The  $\alpha_p$  and  $\beta$  of 0.395 per leaf appearance interval of all organs in both shoot types were not affected by temperature or population.

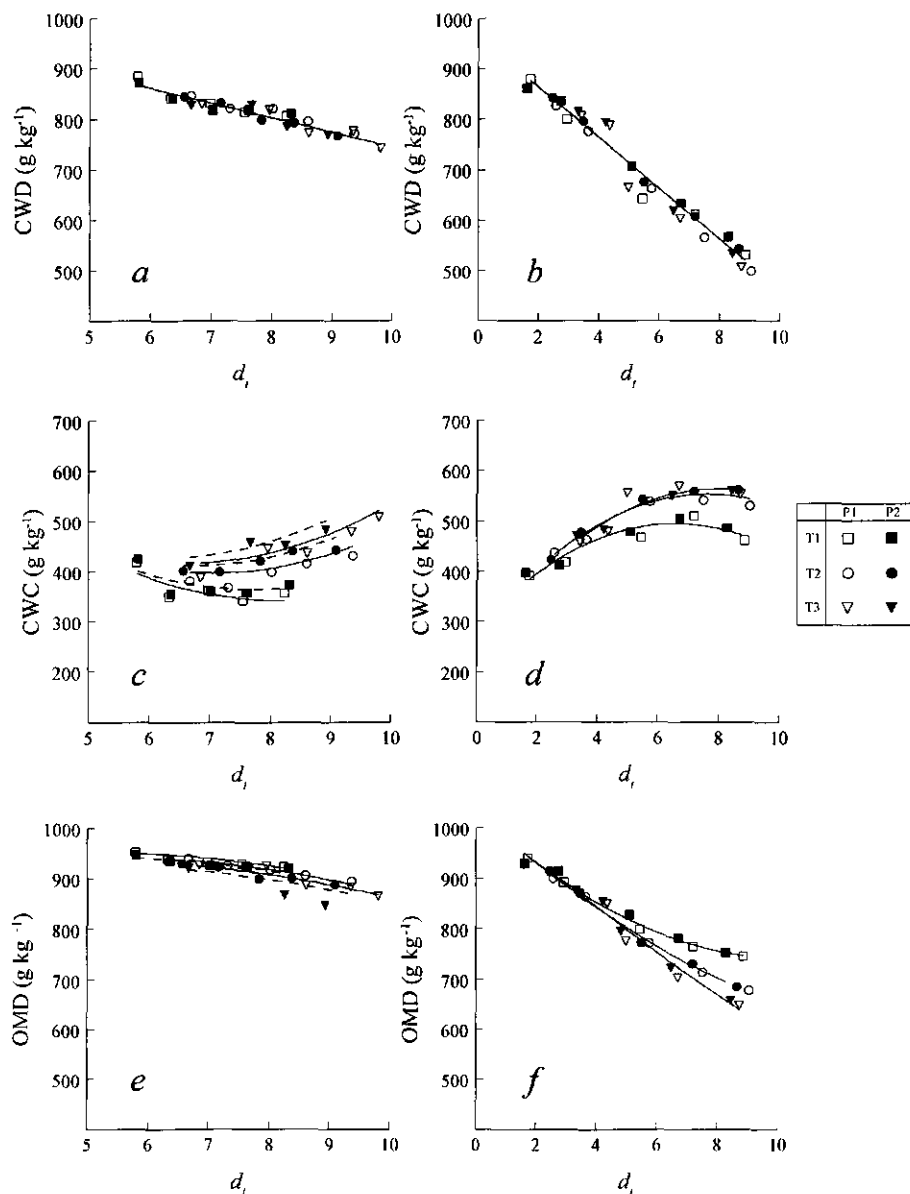


**Fig 5.** Whole shoot cell wall digestibility (CWD: *a, b*), cell wall content (CWC: *c, d*), and organic matter digestibility (OMD: *e, f*) of vegetative (*a, c, e*) and reproductive (*b, d, f*) shoots vs shoot development stage ( $d_i$ ). Temperatures 13/8°C, 18/13°C and 23/18°C (T1, T2, T3). Populations 1 and 2 (P1, P2). Solid and dashed lines indicate significant differences between temperatures and populations, respectively.

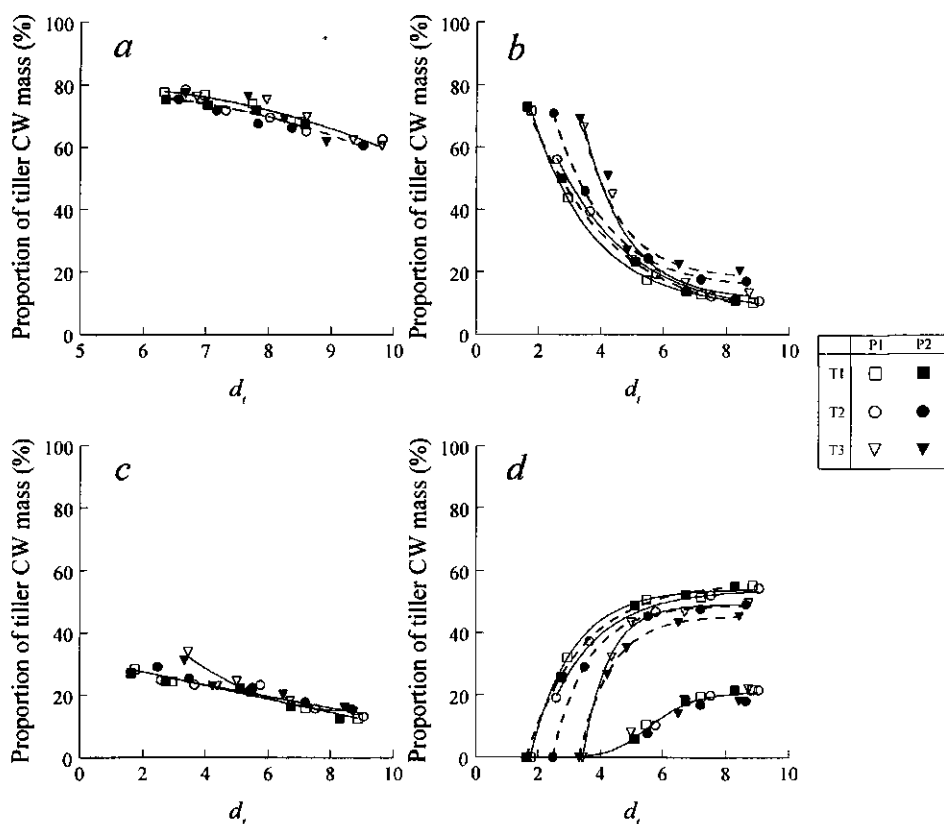


**Fig 6.** The proportion of fractions of plant organs in total shoot cell wall mass vs development stage: leaf blades of vegetative shoots (a), and of reproductive shoots leaf blades (b), leaf sheaths (c), stem internodes and ears (d). Temperatures 13/8°C, 18/13°C and 23/18°C (T1, T2, T3). Populations 1 and 2 (P1, P2).

Although in all plant organs there was a trend to a higher CWC in population 2 at all temperatures (Fig 7), regression analysis only showed a significant population effect on whole shoot CWC for the vegetative shoots ( $P.d_i^2$  interaction in Table 2). Consequently, only the vegetative shoots of population 2 had a lower OMD than population 1. The only significant difference in CWD between populations concerned leaf blades of reproductive shoots at 18/13°C, which showed higher CWD for population 2 than for population 1 (Figs 5a

and 5b). This had no effect on whole shoot CWD because the leaf blade fraction in total CW mass was low (Fig 6b).

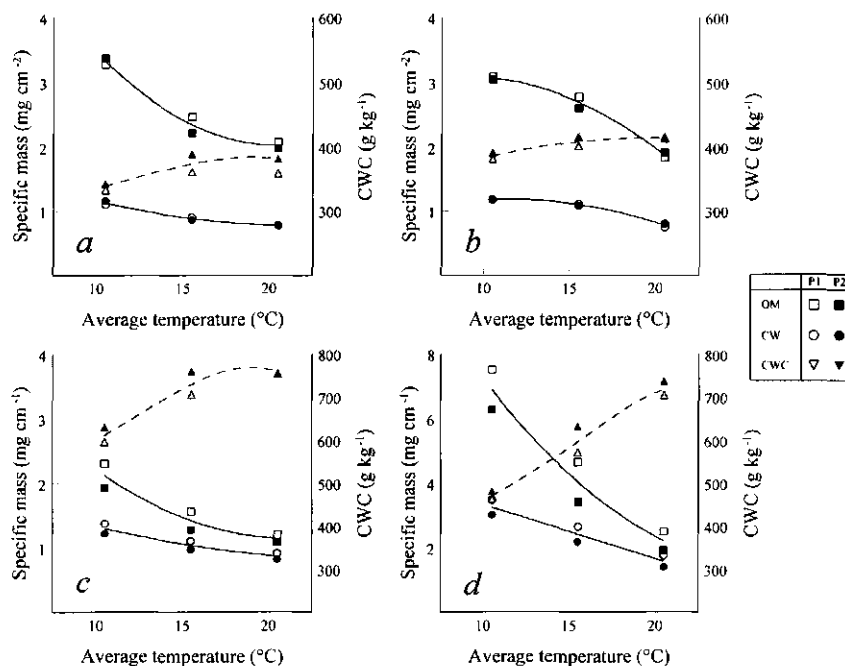


Fig 7. Specific OM and CW mass and cell wall content (CWC) of leaf blades of vegetative shoots (a), and of leaf blades (b), leaf sheaths (c) and stem internodes (d) of the reproductive shoots at different average temperatures. Populations 1 and 2 (P1, P2).

#### 4.5 Discussion

The observed differences between the vegetative and the reproductive shoots could not be analysed statistically, because the data were obtained from separate experiments. Furthermore, in the vegetative shoots changes in leaf characteristics were measured after ligule appearance, whereas in the reproductive shoots these changes were monitored for all organs from the moment of flag leaf appearance onwards. Nevertheless, the contrasts between both shoot types in morphological development, CWC and digestibility were very clear. The reproductive shoots had a higher leaf appearance rate and formed stem internodes. A higher leaf appearance rate (Fig 1c) and higher OM growth rates (Figs 1a and 1b) for

reproductive shoots than for vegetative shoots is generally observed (Parsons & Robson 1980). The more rapid growth of reproductive shoots has been attributed to the cessation of root growth and tillering (Ryle 1970; Parsons & Robson 1981b), remobilisation of reserves from the roots (Davies 1971) and the enhanced photosynthetic rate in leaves of vernalized shoots (Parsons & Robson 1981a; Stapleton & Jones 1987).

Most important information on generally applicable relationships for modelling purposes obtained in this experiment were those of the size, the CW mass and CWD of leaf blades and sheaths, and stem internodes. In both the vegetative and the reproductive shoots the  $s_{cw}$  remained constant for fully expanded leaf blades (Figs 3a & 3b), which is in accordance with the observations in Chapters 2 and 3. In leaf sheaths  $s_{cw}$  stabilized one leaf appearance interval later than in leaf blades, as far as measured in the reproductive shoots (Fig 3b). Stem internodes reached their final length and  $s_{cw}$  after approximately two leaf appearance intervals following ligule appearance of the leaf blade of the same phytomer (Fig 3c). This corresponds to the coordinated pattern of shoot development described for *Festuca arundinacea* by Skinner & Nelson (1994).

Important trends were found in ICW increase of plant organs. The ICW curves of not only the leaf blades, but also of the leaf sheaths and stem internodes in the reproductive shoots could be fitted satisfactorily with the same equation as used in Chapter 2 for the leaf blades of *Lolium multiflorum*. The  $\alpha_p$  for both leaf sheaths and stem internodes was higher than for leaf blades (Fig 4b). As a consequence, the strong decline of the leaf blade fraction in whole shoot CW mass and the increase in the proportion of internodes and ears resulted in faster CWD decline vs. development stage in reproductive shoots (Fig 5b) than in vegetative shoots (Fig 5a).  $\alpha_p$  of plant organs was not significantly affected by insertion level (Fig 4a) or temperature (Fig 4b). This is probably related to the virtually unchanged tissue proportions in the cross sectional area of organs at contrasting temperatures (Akin *et al.* 1987; Da Silva *et al.* 1987; Wilson *et al.* 1991). The absence of temperature effects on  $\alpha_p$  and  $\beta$ , and the convergence between temperature treatments in the proportions of organ types in the whole shoot CW mass (Fig 6) explains that the relation between shoot CWD and  $d_i$  decreased linearly for all treatments (Figs 5a & 5b).

Consequently, the effects of temperature on OMD have to be fully explained from differences in CWC. These can result from differences in the proportions between plant organs (leaf blade, sheath and stem internode, of which internodes have the highest CWC) or

the differences in CWC in plant organs as a result of temperature. Since the contributions of plant organ fractions to whole shoot CW mass converged for temperature treatments (Fig 6), the higher CWC of plant organs at higher temperature (Fig 7) was the sole cause of the temperature effect on OMD. Probably, the higher development rate and higher maintenance respiration rate at higher temperature resulted in lower availability of assimilates per organ formed on a shoot.

Also the differences in whole shoot OMD between populations were limited and only significant in vegetative shoots (Table 2, Fig 5e). As can be seen in Figs 5a & 5c they were caused only by differences in CWC. No significant relations with morphological characteristics were observed, although population 2 tended to have longer and narrower leaves (data not presented) and a lower leaf appearance rate (Fig 1c). It has been demonstrated that these characteristics can be correlated to digestibility (Masaoka *et al.* 1991; Buxton & Lentz 1993). However, these correlations were never strong.

The present experiments revealed that temperature accelerates both the  $d_i$  and the CWD decline rate during ageing to the same extent, whereas plant organs corresponded similarly in ICW increase pattern as a function of  $d_i$ . These trends offer unique possibilities for modelling grass digestibility under contrasting temperature regimes. Moreover,  $d_i$  (leaf appearance rate) and the pattern of increase of ICW during ageing of the various plant organs seem to be most appropriate to relate to herbage digestibility in breeding programs.

## 5. SIMULATION MODEL

with Egbert A. Lantinga

### 5.1 Abstract

An object-oriented simulation model was developed to integrate detailed analyses of perennial ryegrass (*Lolium perenne*) plant organ dimensions, and their mass, cell wall content (CWC) and digestibility (CWD). The model was validated against data from two field experiments, carried out in The Netherlands (52 °N) and Norway (67 °N). In the experiments, the effects of temperature x daylength interactions on development, growth and digestibility were determined. Three cultivars differing in heading date were used, and undisturbed growth and regrowth after early (only The Netherlands) and late cutting were studied. The sensitivity of the model was tested for changes in parameters determining morphological development.

A grass plant was modelled as an aggregation of shoot objects. A shoot is an aggregation of phytomers, plus an inflorescence in the reproductive development stage. A phytomer consists of a leaf blade, a leaf sheath, a stem internode and a root. Each phytomer has an axillary bud, which can develop into a new shoot.

Morphological development, organic matter (OM) growth and composition were simulated well by the model. Only for regrowing crops in The Netherlands CWC was lower and CWD was higher in the simulations than observed in the field, and the differences increased when stem development was more advanced at the moment of cutting. This was attributed to residual stem in the stubble after cutting due to difficulties with machine cutting of lodged crops on the experimental plots. The model can be considered as sufficiently accurate to simulate OM yield and composition of grass cultivars differing in heading date and growing under strongly contrasting environmental conditions. When the leaf appearance rate, width or length of the leaf blade were increased in the sensitivity analysis, OM yield enhanced, but composition and digestibility of the reproductive grass crops were not systematically affected.



## **5.2 Introduction**

For a simulation model of grass growth, composition and digestibility, the characteristics of individual plant organs in relation to whole plant morphological development are crucial. In morphological terms, grasses are collections of shoots, which are in turn aggregations of phytomers plus an inflorescence in the reproductive development stage. A phytomer consists of a leaf blade, a leaf sheath, a stem internode and a root. Each phytomer has an axillary bud, which can develop into a new shoot. Whether or not a plant organ is formed as well as its shape and dimensions depends on plant species, development stage and external factors. Object-oriented simulation provides new opportunities to support a morphological modelling approach, as it enables simulation of plant organs as discrete units and in dependence of their position in the plant (Sequeira *et al.* 1991).

The building of a mechanistic simulation model of grass growth, development, composition and digestibility, requires a detailed analysis of plant organ dimensions, mass, cell wall content (CWC) and digestibility (CWD) in relation to morphological development. The effects of environmental factors (in particular temperature) and management (in particular cutting) also need to be quantified. These analyses have been made in the experiments described in Chapters 2, 3 & 4 under controlled conditions in glasshouse experiments and have been used to calibrate the object-oriented simulation model presented in this Chapter. The model calculations are validated against measurements from two field experiments, carried out in Wageningen (The Netherlands) and Bodø (Norway). With the model, evaluations are made of the sensitivity of grass composition and digestibility to changes in the morphological parameters leaf blade width and length, and leaf appearance rate.

## **5.3 Model description**

### **5.3.1 Model structure**

In an object-oriented design, the system is modelled in terms of relevant classes. These classes form the abstract framework of objects, which can be created during a simulation run.

The classes describe the 'attributes' and 'methods' of the objects that are created during the simulation run. Attributes are characteristics, usually directly observable, such as length and mass of a plant organ. Methods are functions that enable an object to perform operations on its attributes. Examples of methods are elongation and photosynthesis.

The classes identified in the simulation model are presented in Fig 1. Objects from the 'seed' class can produce an object from the 'plant' class, *i.e.* germination. Each plant is an aggregation of 1 to  $n$  objects from the 'shoot' class, which in turn contains a collection of 1 to  $n$  objects from the 'phytomer' class, and can contain an object from the 'inflorescence' class during the reproductive development stage.

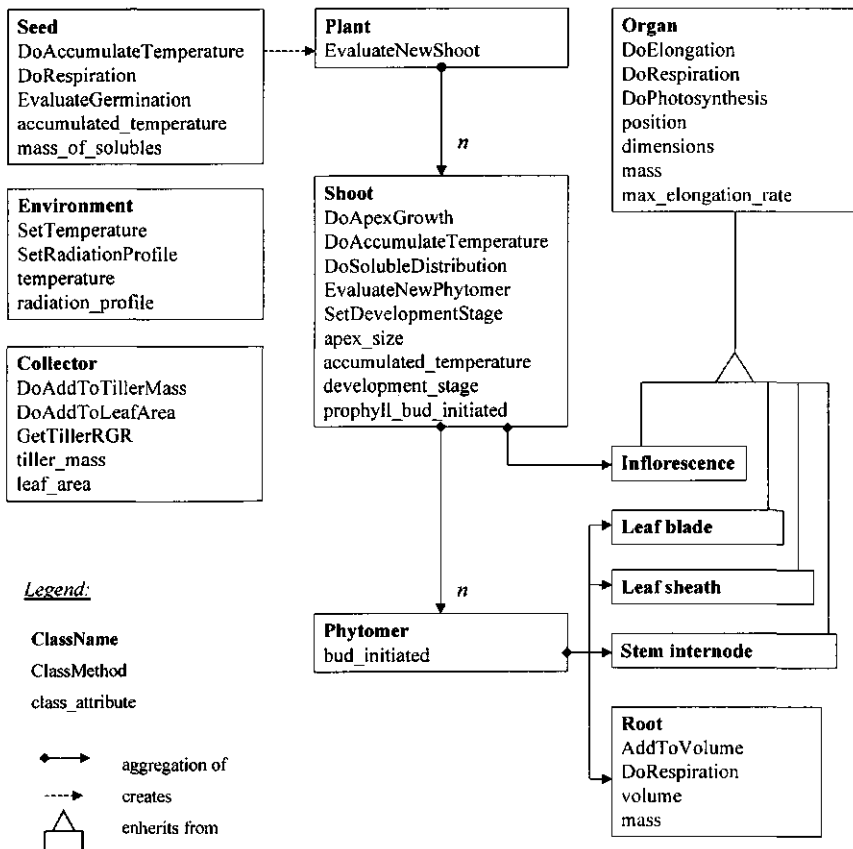


Fig 1. Class diagram of the model.

A phytomer is an aggregation of objects from the 'leaf blade', 'leaf sheath', 'stem internode' and 'root' classes. The leaf blades, leaf sheaths, stem internodes and inflorescence are considered as above ground plant organs and inherit characteristics from the class 'organ'. Whole shoot cell contents, cell wall and indigestible cell wall mass, and leaf area in 1 cm canopy layers are monitored by an object from the 'collector' class. The temperature and the radiation profile in the canopy are managed by an object from the 'environment' class.

### 5.3.2 Morphological development

The simulation starts with one or more seed-objects. Germination occurs when a critical temperature sum has been exceeded. The plants that are produced from the seed consist of one shoot with one phytomer.

Shoots have an apex that can vary in size, proportional to the relative growth rate of the shoot, as shown in Eqn 1 (see Appendix 1 for definitions and values of model parameters and variables). The apex size  $S$  determines phytomer width ( $w_j$ , cm of phytomer  $j$ ) and elongation rate ( $E_{20j}$ , cm h<sup>-1</sup> at 20°C), see also §5.3.3.  $S'$  is the rate of change in apex size, with units cm h<sup>-1</sup> for phytomer width and cm h<sup>-1</sup> h<sup>-1</sup> for elongation rate.  $r_g$  is the relative growth rate of the shoot (h<sup>-1</sup>) and  $c$  is a proportionality constant.

$$S' = S \cdot r_g \cdot c \quad \text{Eqn 1}$$

The apex size of branch shoots is set at 0.5 times the apex size of the shoot of origin at the moment of initiation of the subtending phytomer. Newly formed shoots are 'vegetative'. Shoots present at the end of the vernalization period enter the 'double ridge' development stage. The 'double ridge' shoots become 'reproductive' in order of their appearance at a linear rate during a transition period. The estimated date of completion of vernalization and length of the transition period ( $D_T$ ), and the observed date of onset of reproductive growth and maximum final number of elongated stem internodes on a shoot ( $n_m$ ) are included as model parameters.

A coordinated fashion of development is assumed, adjusted after the findings of Skinner & Nelson (1994) for *Festuca arundinacea*. In the model, the development of the phytomers consecutively formed on grass shoots is divided into two or three distinct phases of one leaf appearance interval for elongation of leaf blade, sheath and stem internode, respectively (Table 1). The latter occurs only in reproductive shoots. After the last phase of

organ elongation, a 'window of opportunity' for shoot formation occurs, *i.e.* a new shoot develops from an axillary or prophyll bud when the density of cell contents in a phytomer is above a critical value ( $C_b$ ). Because the prophyll and the axillary bud are not modelled as separate objects, the shoot and phytomer objects contain an indicator for the development of the shoot. The elongation of the inflorescence starts when flag leaf elongation begins and ceases when the internode of the flag leaf stops elongating.

The phytomers that have reached the adult phase no longer elongate or form axillary shoots. When a new phytomer is formed on top of the shoot, after a critical temperature sum ( $T_{crit}$ ) has been exceeded, the phytomers already present shift to the next development stage. The critical temperature sum is 0.5 times lower in reproductive shoots than in vegetative shoots, resulting in a higher leaf appearance rate (cf. Chapter 4).

**Table 1.** The developmental phases of phytomers of vegetative and reproductive grass shoots, from the top phytomer ( $x$ ) downward. Each phase lasts one leaf appearance interval.

Phytomer	Vegetative	Reproductive
$x$	leaf blade elongating	leaf blade elongating
$x-1$	leaf sheath elongating	leaf sheath elongating
$x-2$	window for new shoot	stem internode elongating
$x-3$	adult	window for new shoot
$x-4$	adult	adult

### 5.3.3 Plant organ dimensions

In the model, the apex size at the moment of phytomer initiation determines the phytomer elongation rate ( $E_{20,j}$  at 20°C, cm h<sup>-1</sup>) and width ( $w_j$ , cm). Initial values of these parameters, that apply to the first phytomer produced from seed, are given as model input (Appendix 1).

The elongation rate of the leaf blades, sheaths and stem internodes are proportional to  $E_{20}$ , using proportionality constant  $q_i$  (Eqn 2). The elongation rate of the inflorescence is determined by the apex size (1.18 times  $E_{20,j}$ ) at the moment of onset of its growth. The elongation rate of plant organ  $i$  ( $L_i$ , cm h<sup>-1</sup>) is influenced by temperature, with a  $Q_{10}$  of 3 (Peacock 1975; Thomas & Stoddart 1984), and is not influenced by the current assimilate supply (Sambo 1983). In Eqn 2,  $T$  is temperature (°C). The final lengths of the plant organs

are determined by organ elongation rate and the duration of the elongation interval. Each plant organ records its position in the canopy (only in vertical direction).

$$L_i' = E_{20j} \cdot q_i \cdot 3^{(T-20)/10} \quad \text{Eqn 2}$$

The width of leaf blades and sheaths is equal to the phytomer width. Stem internodes and inflorescences are considered to be cylinders with a circumference equal to 1.5 and 1.0 times the phytomer width, respectively. Leaf blades and sheaths are assumed to have a rectangular shape and a thickness equal to 0.10 times the width of the organ. From these dimensions the volume  $V_i$  of each plant organ can be calculated.

The increase in root volume is proportional to that of blade, sheath, internode, and inflorescence assuming a constant shoot to root volume growth ratio (Eqn 3). In Eqn 3,  $V_i'$  denotes the rate of change in plant organ volume ( $\text{cm}^3 \text{ h}^{-1}$ ), and  $q_r$  is the ratio between shoot and root growth.

$$V'_{\text{root}} = \frac{V'_{\text{blade}} + V'_{\text{sheath}} + V'_{\text{internode}} + V'_{\text{inflorescence}}}{q_r} \quad \text{Eqn 3}$$

The ratio  $q_r$  is four times higher in the 'reproductive' development stage than in the 'vegetative' and 'double ridge' stages. This reflects the increased allocation of assimilates to shoots in reproductive shoots (Davies 1971; Parsons & Robson 1981b).

#### 5.3.4 $\text{CO}_2$ assimilation, respiration and distribution

The distribution of LAI over canopy height is calculated from leaf blade area and plant density ( $15 \text{ dm}^{-2}$ ), for each 1 cm layer of the canopy, using leaf blade position and a leaf blade zenith angle of  $60^\circ$  for all leaf blades. From the LAI profile the amount of absorbed photosynthetically active radiation (PAR) within layer  $h$  of the canopy ( $I_{a,h}$ ,  $\text{J m}^{-2} \text{ s}^{-1}$ ) can be calculated:

$$I_{a,h} = (1 - \rho) I_0 (1 - e^{-k L_h}) \quad \text{Eqn 4}$$

In Eqn 4,  $I_0$  is the PAR entering the top of layer  $h$  ( $\text{J m}^{-2} \text{s}^{-1}$ ),  $\rho$  is the reflection coefficient of the canopy,  $L_h$  is the LAI within layer  $h$  and  $k$  is the light extinction coefficient.

Leaf blade gross  $\text{CO}_2$  assimilation rate in each layer  $h$  ( $A_h$ ,  $\text{g CO}_2 \text{m}^{-2} \text{s}^{-1}$ ) can be calculated according to Eqn 5, where  $A_m$  is the gross  $\text{CO}_2$  assimilation rate at light saturation ( $\text{g CO}_2 \text{m}^{-2} \text{s}^{-1}$ ) and  $\varepsilon$  is the initial light use efficiency ( $\text{g CO}_2 \text{J}^{-1}$ ).

$$A_h = A_m \left( 1 - e^{-\varepsilon I_h / A_m} \right) \quad \text{Eqn 5}$$

The production rate of organic matter (cell contents,  $P_{cc}$ ,  $\text{g OM h}^{-1}$ ) is calculated for individual leaf blades from gross  $\text{CO}_2$  assimilation within each layer (Eqn 6), using the conversion factor from  $\text{CO}_2$  to  $\text{CH}_2\text{O}$  ( $\chi$ ) and the conversion efficiency for cell contents ( $\chi_{cc}$ ,  $\text{g OM g}^{-1} \text{CH}_2\text{O}$ ).

$$P_{cc} = \sum A_h \cdot \chi \cdot \chi_{cc} \quad \text{Eqn 6}$$

The maintenance respiration rate is calculated for individual organs ( $R_i$ ,  $\text{g OM h}^{-1}$ , where  $i$  denotes organ type) as a fraction of the mass of cell contents ( $M_{cc,i}$ ,  $\text{g OM}$ ) (Eqn 7). The fractional respiration rate ( $r_m$ ,  $\text{g CH}_2\text{O g}^{-1} \text{OM h}^{-1}$ ) is dependent on temperature ( $T$ ,  $^{\circ}\text{C}$ ), with a  $Q_{10}$  of 2 (Goudriaan & Van Laar 1994).

$$R_i = M_{cc,i} \cdot r_{m,20} \cdot 2^{(T-20)/10} \quad \text{Eqn 7}$$

Cell contents can be distributed between the phytomers of a shoot, but only in the apical direction. For axillary shoots also the subtending phytomer can contribute. When the cell contents density ( $\text{g OM cm}^{-3}$ ) in the lower phytomer is higher than in the upper phytomer the densities are equalized, which results in a positive or negative flow of cell contents from the phytomer ( $\Phi_d$ ). The total flow of cell contents for a phytomer ( $\Phi$ ,  $\text{g OM h}^{-1}$ ) can be calculated as:

$$\Phi = P_{cc} - \sum R_i + \Phi_d \quad \text{Eqn 8}$$

In addition, within a phytomer the concentration of cell contents is equalized between individual organs. For an individual organ with volume  $V_i$  ( $\text{cm}^3$ ) and cell contents mass  $M_{cc,i}$  ( $\text{g OM}$ ) the flow of cell contents ( $\Phi_i$ ,  $\text{g OM h}^{-1}$ ) is simulated as:

$$\Phi_i = (\Phi + \Sigma M_{cc,i}) \frac{V_i}{\Sigma V_i} - M_{cc,i} \quad \text{Eqn 9}$$

The phytomer decays when the cell contents mass of a phytomer drops below a critical fraction ( $f_{crit}$ ) of its highest mass, which is generally reached at ligule appearance (Chapter 2). It is assumed that the remaining cell contents and cell wall mass of the leaf blade and sheath are completely lost by decay and the blade and sheath are removed.

### 5.3.5 Cell wall synthesis and digestibility

In elongating plant organs a fixed fraction ( $f_{cw,i}$ , where  $i$  denotes organ type) of the assimilated and imported cell contents is used for cell wall production ( $P_{cw,i}$ , g OM h<sup>-1</sup>, Eqn 10). This fraction is higher for leaf sheaths and stem internodes than for leaf blades.

$$P_{cw,i} = \Phi_i \cdot f_{cw,i} \cdot \chi_{cw} / \chi_{cc} \quad \text{Eqn 10}$$

where  $\chi_{cw}$  (g OM g<sup>-1</sup> CH<sub>2</sub>O) is the conversion efficiency for cell wall. After plant organ elongation has ceased, no more cell wall is synthesized (Chapters 2, 3 & 4). The cell wall of plant organs becomes indigestible at a rate ( $F'_{icw,i}$ , g kg<sup>-1</sup> h<sup>-1</sup>), that is determined by the asymptotic ( $\alpha_{p,i}$ , g kg<sup>-1</sup>) and the current proportion of indigestible cell wall, and the fractional rate ( $\beta$ , g kg<sup>-1</sup> °C<sup>-1</sup> h<sup>-1</sup>), that is linearly related to temperature ( $T$ , °C):

$$F'_{icw,i} = (\alpha_{p,i} - F_{icw,i}) \cdot \beta \cdot T \quad \text{Eqn 11}$$

### 5.3.6 Cutting

At a cutting event leaf sheaths and stem internodes above the cutting height are removed and dimensions and weights of sheaths and internodes below the cutting height are adjusted proportionally to the length of the organ removed. Leaf blades are completely removed in a reproductive crop, except the elongating leaf blade within the sheath tube, as was observed in the current field experiments. The apex size is reduced by a factor 0.6 after cutting (cf. Chapter 3). When the growing point of a shoot had been elevated above the cutting height, the rates of elongation of leaf blade and sheath are set to zero, *i.e.* decapitation.

### 5.3.7 Implementation

The model was built in the programming language Visual C++, MicroSoft Developer Studio, version 4.0. The growth of five plants was modelled simultaneously, using 0.20 h timesteps. The sets of shoots per plant and phytomers per shoot were implemented as linked object lists.

## 5.4 Experiments

The data for model validation under field conditions were obtained from two experiments of the same design, carried out in spring and early summer of 1995 in Wageningen, The Netherlands (52 °N) and in Bodø, Norway (67 °N). In the experiments the effects of cultivar heading date and temperature x daylength interactions on growth and digestibility of perennial ryegrass were studied. Also the effects of early and late cutting on regrowth and digestibility were determined.

### 5.4.1 Experimental sites, design and management

In both experiments, three perennial ryegrass cultivars differing in heading dates were used. The cultivars were Barylou, Exito and Kerdion, with average heading dates in The Netherlands of 9 May, 29 May and 16 June, respectively.

Swards were seeded into three replicate blocks of 19 m x 12 m in a latin-square design in June 1994 on both locations. The plots were surrounded by 5 m borders. Moderate rates of fertilizer (60 kg N ha<sup>-1</sup>) were applied and in order to enhance tillering the swards were cut one or two times, in Norway and The Netherlands, respectively. In the experimental year, each plot in The Netherlands was separated into 3 sub-plots, to allow for undisturbed growth, and late (16 May) and early (24 April) cutting treatments. These treatments were fertilized on 25 March 1995 at rates of 120, 80 and 60 kg N ha<sup>-1</sup>, respectively. After cutting, 80 kg N ha<sup>-1</sup> was applied on the same day. In the Norway experiment only two sub-plots were used for undisturbed growth and late cutting (8 June). These treatments were fertilized with 120 kg N ha<sup>-1</sup> and 80 + 80 (after cutting) kg N ha<sup>-1</sup>, respectively. Cuttings were made at 5 cm height above ground level, using a motor scythe.



#### 5.4.2 Measurements

Throughout the experimental periods, the leaf appearance rate was measured on marked shoots, by counting the number of appeared leaves at weekly intervals. Weekly harvests were made by cutting the above ground mass of a 0.5 m x 0.5 m sample screen within the subplots, at 3 cm height above ground level. Harvested material was separated into green leaf blade, leaf sheath and stem, and dead leaf blade fractions. The dry weight was measured after oven drying for 24 h at 70 °C. Samples were ground to pass a 1 mm screen in a hammer mill, and analysed for cell wall content in organic matter (CWC) using neutral detergent solution (adjusted after Goering & Van Soest 1970). Undissolved protein was removed by incubation of the cell wall residue with alcalase (0.75 ml in 40 ml buffer solution) for 1 h at 40 °C. True cell wall digestibility after 48 h (CWD) was measured according to the method of Goering & Van Soest (1970), using an incubation of 0.5 g air dry medium in rumen fluid from fistulated steers fed medium quality grass hay.

Radiation and temperature data were obtained from nearby weather stations. The temperature sum after 1 January was calculated from mean daily air temperatures above 0°C.

### 5.5 Results

#### 5.5.1 Parametrization

The parameters and their estimated values are presented in Appendix 1. Most parameters were measured in the experiments described in previous chapters. Some parameters were adopted from existing literature (Ennik, 1966; Jones *et al.* 1978, Goudriaan & Van Laar 1994). Three parameters and two input variables were obtained by calibration, using data from the experiments described in Chapter 4. These were:

- parameter  $f_{CW,ls}$  using the specific CW mass in the organs;
- parameter  $C_b$ , using tillering rates;
- parameter  $c$  and input variables elongation rate and width of the first leaf, using lengths and widths of consecutive plant organs.

The values were estimated when the calibrated values corresponded to those observed in the experiments ( $\pm 10\%$ ).

The day numbers for model initialization for sites and cultivars were chosen in such a way that modelled shoots had reached leaf stage 1 (one fully expanded green leaf and one elongating leaf) on a day number as was observed in the field. The day numbers for model initialization, the end of the vernalization period and onset of reproductive growth are presented in Table 2. The effect of daylength on development is not directly simulated, since the transition between development stages is determined by the dates presented in Table 2.

**Table 2.** The dates (days after 1 January) for model initialization (*I*), the end of the vernalization period (*V*) and the onset of reproductive development (*R*).

Site	Cultivar	<i>I</i>	<i>V</i>	<i>R</i>
The Netherlands	Barylou	30	85	105
	Exito	40	96	116
	Kerdion	46	107	127
Norway	Barylou	30	121	141
	Exito	40	125	145
	Kerdion	41	130	150

### 5.5.2 Validation

The model was first used to simulate morphological development and changes in crop OM yield, CWC and CWD, and to compare the results with those observed in the two field experiments. Fig 2 presents the observed and simulated developmental characteristics of the crops: leaf number per main shoot, leaf weight ratio (LWR, g leaf blade OM kg<sup>-1</sup> shoot OM) and leaf area index (LAI, m<sup>2</sup> m<sup>-2</sup> ground area) in the initial stages of (re-)growth. Spring growth commenced earlier for Barylou than for Exito and Kerdion, and at a much lower temperature sum in Norway than in The Netherlands (Figs 2a & 2b). The decline in LWR due to stem development also started earlier for Barylou than for the other cultivars (Figs 2c & 2d), whereas no differences in the LAI were observed for undisturbed growth (Figs 2e & 2f). However, during regrowth the LAI increased slower for Barylou than for the later heading cultivars. The trends in the simulations were the same as in the observations.

In Fig 3 the observed and simulated OM yields of the crops are shown. In accordance with the order of average heading dates and morphological development (Fig 2), Barylou

showed at both sites the most rapid spring growth in the undisturbed crop, followed by Exito and Kerdion, respectively (Figs 3a & 3b). In contrast, the regrowth after cutting was slower for Barylou and Exito than for Kerdion, in particular after the late cut in The Netherlands. Many apices had been removed by cutting in the early heading cultivars, because stem elongation had elevated them above the cutting height.

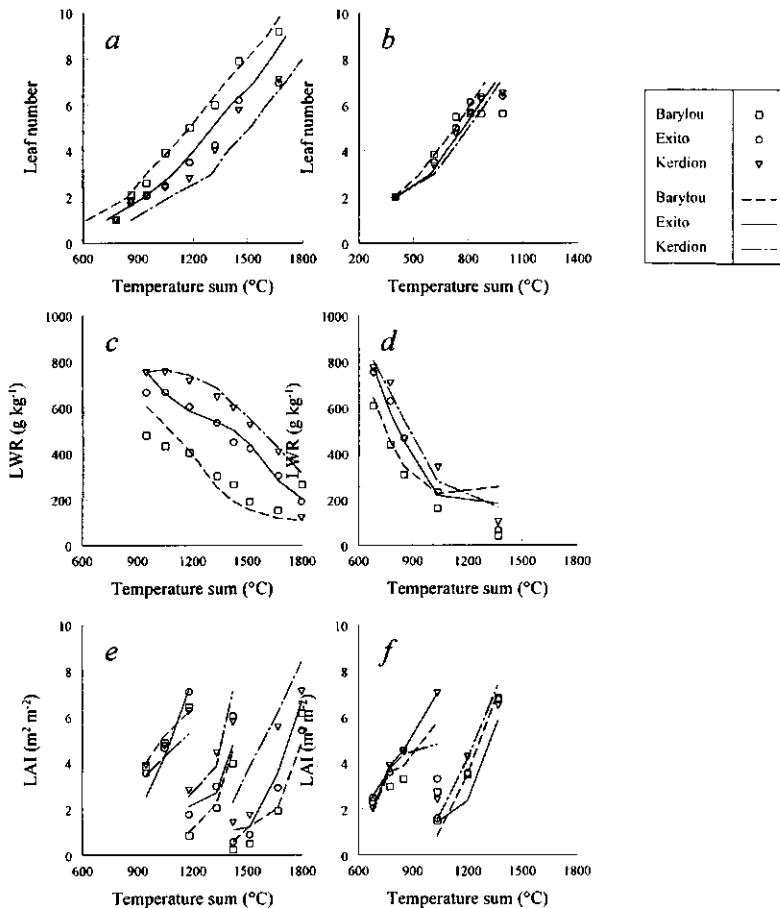


**Fig 2.** The average leaf number per shoot (a, b), leaf weight ratio (LWR: c, d) leaf area index (LAI: e, f) of three *Lolium perenne* cultivars vs temperature sum after 1 January, in Wageningen, The Netherlands (a, c, e) and in Bodø, Norway (b, d, f). Leaf numbers and LWR are only shown for undisturbed crops, LAI also for regrowth after early and/or late cutting. Markers and lines represent observed data and model calculations, respectively. Note the different scale of the x-axis of figure b.

The early onset of stem elongation in Barylou also resulted in faster increase of CWC and decline of CWD during undisturbed growth (Figs 4a & 4b). Also during regrowth in The Netherlands, Barylou had higher CWC and lower CWD than Exito and Kerdion, because stem elongation continued. In contrast, in Norway no more stem elongation occurred after cutting, so that the cultivars had the same CWC and CWD during regrowth.

In general, the simulation results reflected the observed trends of OM growth and the changes in CWC and CWD well. Only OM growth and CWC during regrowth of Kerdion after the early cut in The Netherlands were overestimated and underestimated by the model, respectively.

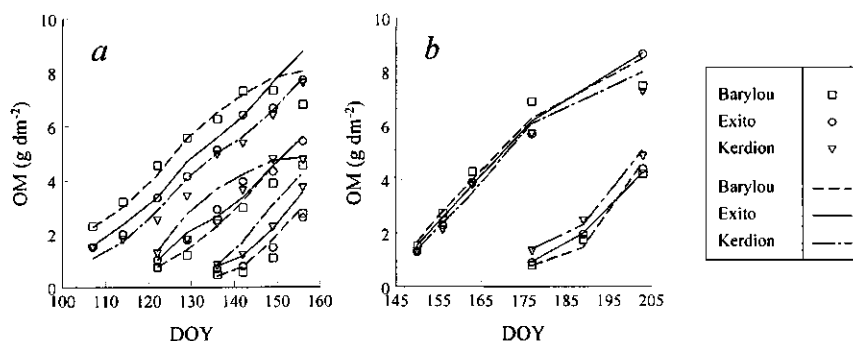


**Fig 3.** Organic matter yield of three *Lolium perenne* cultivars grown in Wageningen, The Netherlands (a undisturbed growth, regrowth after early cut and regrowth after late cut) and in Bodø, Norway (b undisturbed growth and regrowth after late cut) vs days after 1 January (DOY). Markers and lines represent observed data and model calculations, respectively.

### 5.5.3 Sensitivity analysis

The sensitivity of the simulated OM yield, LWR, CWC and CWD to a 10% increase in leaf blade length or width, or leaf appearance rate (through reduction of  $T_{crit}$ ) is shown in Figs 5 & 6. In the undisturbed crops, OM yield increased in all three cases (Figs 5a, c, e). Moreover, LWR was up to  $40 \text{ g kg}^{-1}$  higher after an increase in the length or width of leaf blades (Figs 5b & 5d). When leaf appearance rate was higher, LWR was generally negatively affected during undisturbed growth (Fig 5f). Due to the large variation, no firm conclusions could be drawn from trends in regrowing crops. Changes in the leaf blade dimensions had minor effects on CWC and CWD, with only weak trends for lower CWC and higher CWD during

regrowth (Figs 6a-d). When CWC was low, it tended to be increased due to higher leaf appearance rate, but this was reversed for higher values of CWC (Fig 6e). CWD decreased slightly due to a 10% increase in leaf appearance rate for undisturbed crops (Fig 6f).

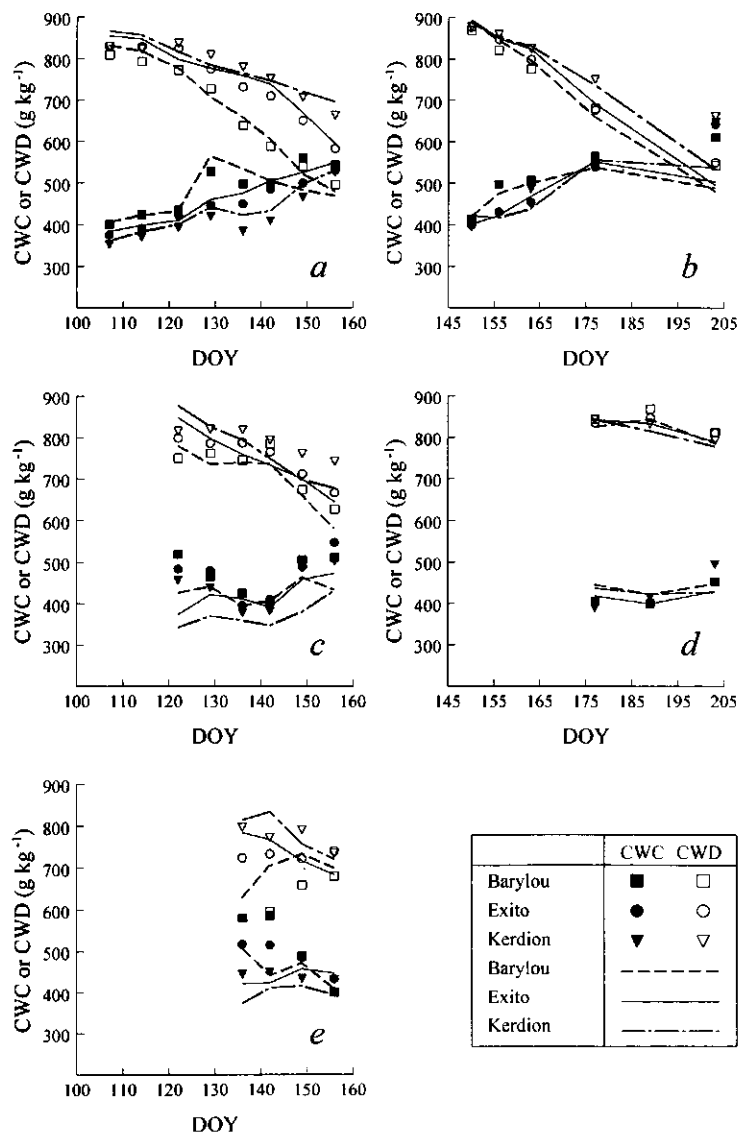


**Fig 4.** CWC and CWD of three *Lolium perenne* cultivars grown in Wageningen, The Netherlands (a undisturbed growth, c regrowth after early cut, e regrowth after late cut) and in Bodø, Norway (b undisturbed growth, d regrowth after late cut) vs days after 1 January (DOY). Markers and lines represent observed data and model calculations, respectively.

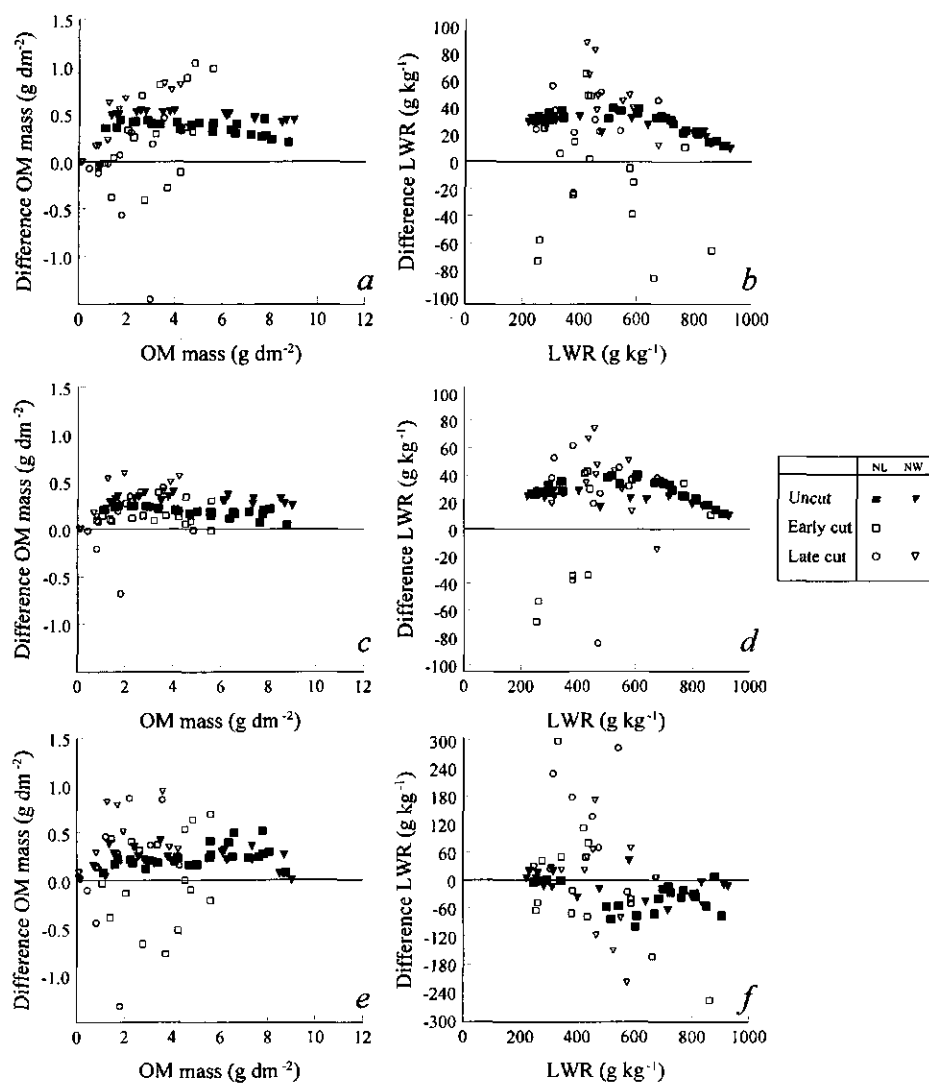


**Fig 5.** The changes in simulated OM yield (*a*, *c*, *e*) and leaf weight ratio (LWR; *b*, *d*, *f*) after a 10% increase in leaf blade length (*a*, *b*) and width (*c*, *d*), and leaf appearance rate (*e*, *f*). Simulations made for grass crops in Wageningen, The Netherlands (NL) and Bodø, Norway (NW), grown undisturbed or regrowing after early or late cut. Note the different scale of the y-axis of figure *f*.

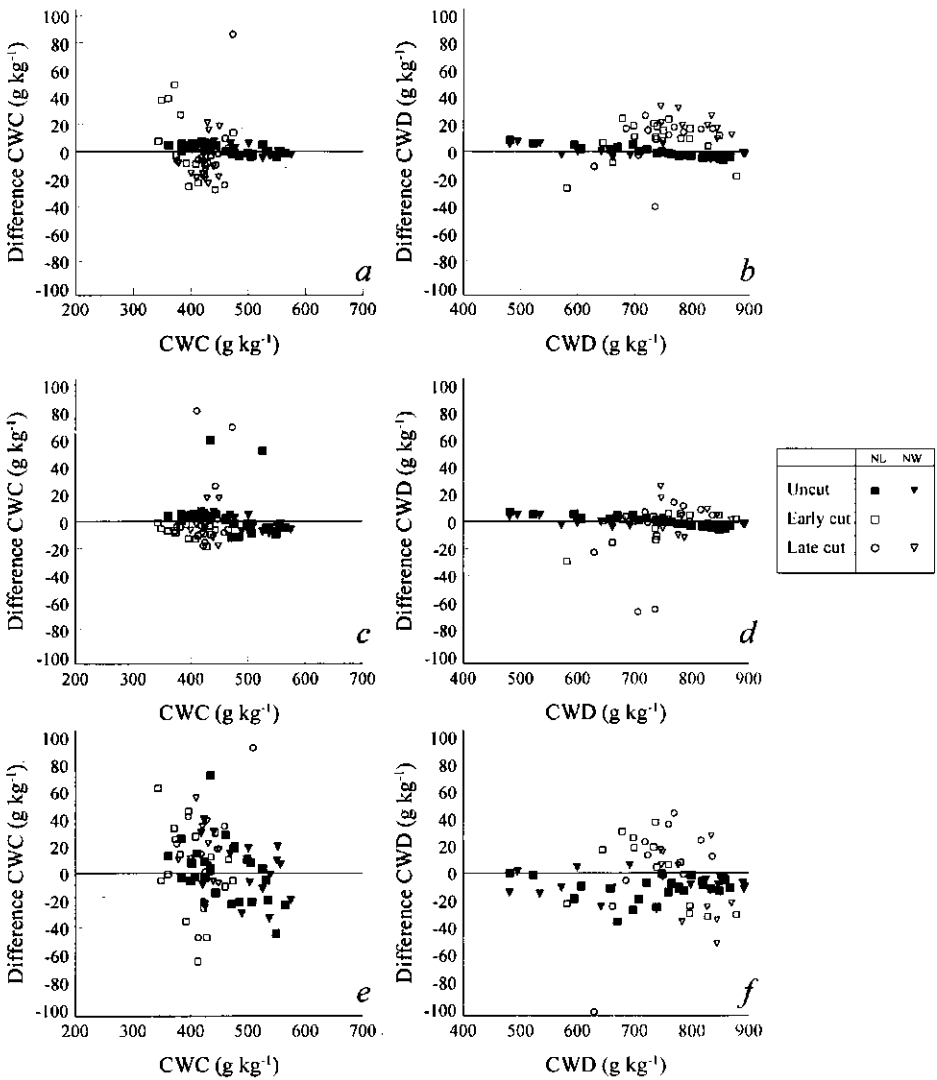


**Fig 6.** The changes in simulated cell wall content (CWC; *a*, *c*, *e*) and cell wall digestibility (CWD; *b*, *d*, *f*) after a 10% increase in leaf blade length (*a*, *b*) and width (*c*, *d*), and leaf appearance rate (*e*, *f*). Simulations made for grass crops in Wageningen, The Netherlands (NL) and Bodø, Norway (NW), grown undisturbed or regrowing after early or late cut.

### 5.6 Discussion

The presented model offers the opportunity to simulate development, growth and digestibility of grass on both a morphological and a physiological basis. The model uses a limited set of parameters. Some of the assumptions over-simplify physiological processes largely, in particular those concerning the distribution of assimilates. In future versions of the model these processes will require a more thorough analysis and implementation, comparable for instance to the concepts presented by Sheehy *et al.* (1995). Such considerations gain importance when plant characteristics such as nitrogen distribution and its effects on the rate of leaf elongation are also incorporated into the model. However, this was outside the scope of the present study and the used approach resulted in sufficiently accurate estimations of cell contents distribution (data not presented).

The simulated trends in changes in composition for the three cultivars and both locations were the same as those observed in the field (Fig 4). This supports the suggestion of Illius (1985) that for modelling of crops under very contrasting conditions, a morphological modelling approach should result in better performance than merely crop physiology based or statistical models. The differences between observed and simulated crop composition were the largest for the early stages of regrowth in The Netherlands. These discrepancies were in all probability caused by cutting of lodged crops and a 2-3 cm difference between the machine cutting height and the harvest height using the sampling screen. This resulted in a high proportion of stem internodes remaining after cutting of crops in a highly advanced development stage, such as Barylou after the early and late cuttings. As a consequence, in the harvested material during early stages of regrowth CWC was higher and CWD tended to be lower than calculated by the simulation model (Figs 4c & 4e). This was not observed in Norway, as the difference between the machine cutting height and the harvest height was there only about 1 cm.

Some of the effects of changes in single model parameters in the sensitivity analysis were as expected, *e.g.*, the higher simulated OM yield after an increase in the leaf blade length or width, or leaf appearance rate (Figs 5a, c, e). The changes in these parameters resulted in a more rapid leaf area expansion in early growth stages (Nelson *et al.* 1977). In the undisturbed crops the higher leaf appearance rate led to a lower LWR (Fig 5f) and a lower



CWD (Fig 6f). This phenomenon corresponds to the strong relationship between development rate and CWD decline in reproductive shoots, as observed in Chapter 4.

The model evaluation of variations in a single parameter value might be inadequate, since plant characteristics can be influenced by multiple parameters. In the sensitivity analysis, no effects of leaf blade width on CWC or CWD were observed, whereas positive correlations between width and dry matter digestibility have been observed in *Bromus inermis* by Sleper & Drolsom (1974) and in *Dactylis glomerata* by Lentz & Buxton (1991). However, width of plant organs is often related to changes in leaf anatomy. Wider leaves and stem internodes with a larger circumference can have a lower proportion of lignified tissue (Lentz & Buxton 1991). This suggests that a larger width of plant organs is associated with a lower asymptotic indigestible cell wall fraction, which results in higher CWD.

From the model calculations it is concluded that morphological characteristics have limited effects on grass composition and digestibility. Direct changes in the composition and digestibility may cause larger effects. Relevant parameters can be the proportion of cell contents used for cell wall synthesis, and cell wall characteristics such as the indigestible cell wall asymptotic proportion ( $\alpha_p$ ) and its fractional rate of increase ( $\beta$ ). Some perspectives are available, as large variability in anatomical characteristics and digestibility has been observed between and within cultivars and populations of perennial ryegrass (Deinum *et al.* in prep).  $\beta$  is probably not affected by selection or breeding, since it reflects the rate of chemical processes such as polymeric cross-linking in the cell walls, which are primarily affected by temperature (see Buxton & Fales 1994).

In conclusion, the model could be accepted as sufficiently accurate to simulate OM yield and composition of grass cultivars differing in heading date and growing under strongly contrasting conditions. The model was effectively used to evaluate the effects of several model parameters on development, growth and digestibility. The studied morphological characteristics had limited effects on composition and digestibility of reproductive grass crops.

# Appendix 1. Model variables and parameters

$A_h$	gross CO <sub>2</sub> assimilation rate in layer $h$		$\text{g CO}_2 \text{ m}^{-2} \text{ s}^{-1}$
$A_m$	gross CO <sub>2</sub> assimilation rate at light saturation		$1.11 \text{ mg CO}_2 \text{ m}^{-2} \text{ s}^{-1}$
$\alpha_{p,i}$	asymptotic fraction of indigestible cell wall for plant organ $i$	$i = \begin{cases} \text{blade} & 0.27 \\ \text{sheath} & 0.52 \\ \text{internode} & 0.77 \\ \text{inflorescence} & 0.77 \end{cases}$	
$\beta$	fractional rate of indigestible cell wall increase		$0.0065 \text{ g kg}^{-1} \text{ }^\circ\text{C}^{-1} \text{ d}^{-1}$
$\chi$	conversion factor from CO <sub>2</sub> to CH <sub>2</sub> O		30/44
$\chi_{cc}$	conversion efficiency for cell contents		$0.79 \text{ g OM g}^{-1} \text{ CH}_2\text{O}$
$\chi_{cw}$	conversion efficiency for cell wall		$0.76 \text{ g OM g}^{-1} \text{ CH}_2\text{O}$
$c$	proportionality constant of $S$ to $r_g$		0.125
$C_b$	critical density of cell contents in a phytomer for branching		$0.10 \text{ g OM cm}^{-3}$
$D_T$	duration of the transition period for reproductive development		20 days
$\epsilon$	initial light use efficiency		$12.5 \mu\text{g CO}_2 \text{ J}^{-1}$
$E_{20,j}$	phytomer elongation rate of phytomer $j$ at 20°C		$\text{cm h}^{-1}$
$E_{20,1}$	elongation rate of the first phytomer		$0.067 \text{ cm h}^{-1}$
$\Phi$	total flow of cell contents for a phytomer		$\text{g OM h}^{-1}$
$\Phi_d$	distribution flow of cell contents from the phytomer		$\text{g OM h}^{-1}$
$\Phi_i$	total flow of cell contents for plant organ $i$		$\text{g OM h}^{-1}$
$f_{crit}$	critical fraction of maximum cell contents mass for decay		0.5
$f_{cw,i}$	fraction of cell contents flow converted to cell wall for plant organ $i$	$i = \begin{cases} \text{blade} & 0.34 \\ \text{sheath} & 0.41 \\ \text{internode} & 0.50 \\ \text{inflorescence} & 0.50 \end{cases}$	
$F_{icw,i}$	indigestible cell wall as a fraction cell wall of plant organ $i$		$\text{g kg}^{-1}$
$I_0$	PAR entering the top of layer $h$		$\text{J m}^{-2} \text{ s}^{-1}$
$I_{a,h}$	absorbed PAR within layer $h$ of the canopy		$\text{J m}^{-2} \text{ s}^{-1}$
$k$	light extinction coefficient		$0.5 \text{ m}^2 \text{ ground m}^{-2} \text{ leaf}$
$L_h$	LAI within layer $h$		$\text{m}^2 \text{ leaf m}^{-2} \text{ ground}$

$M_{cc,i}$	mass of cell contents for plant organ $i$	g OM
$M_{cw,i}$	mass of cell wall for plant organ $i$	g OM
$n_m$	maximum number of elongated stem internodes on a shoot	5
$P_{cc}$	production rate of organic matter (cell contents)	g OM d <sup>-1</sup>
$q_i$	plant organ $i$ to phytomer elongation ratio	$i = \begin{cases} \text{blade} & 1.00 \\ \text{sheath} & 0.80 \\ \text{internode} & 0.87 \end{cases}$
$q_r$	shoot to root ratio for volume growth	1.6 (vegetative), or 6.4 (reproductive)
$\rho$	reflection coefficient of the canopy	-
$r_g$	shoot relative growth rate	h <sup>-1</sup>
$R_i$	maintenance respiration rate for plant organ $i$	g OM h <sup>-1</sup>
$r_{m,20}$	fractional maintenance respiration rate at 20°C	0.025 g g <sup>-1</sup> OM d <sup>-1</sup>
$S$	apex size $\in \{\text{width (cm), elongation rate (cm h}^{-1})\}$	
$T$	temperature	°C
$T_{crit}$	critical temperature sum for new phytomer initiation	140 °C d
$V_i$	volume of plant organ $i$	cm <sup>3</sup>
$w_j$	width of phytomer $j$	cm
$w_1$	width of the first phytomer	0.15 cm

## ***PART II.***

### ***The use of the cumulative gas production technique***

## 6. MULTIPHASIC ANALYSIS OF GAS PRODUCTION KINETICS

*with John Cone, Barbara A. Williams, Filip D. Debersaques & Egbert A. Lantinga*

### 6.1 Abstract

Time related gas production techniques can be an alternative for the 48 h in vitro digestibility measurement. The recently developed methods to quantify the kinetics of ruminant feed fermentation have a high resolution. Consequently, fermentation processes with clearly contrasting gas production kinetics can be identified. Parameterization of the separate processes is possible with a suitable multiphasic model and modelling method. A flexible, empirical, multiphasic model was proposed for parameterization of gas production profiles. This equation was fitted, using a two-step method, to four gas production profiles and the maximum fractional rate of substrate digestion ( $R_M$ ) was calculated for each phase.

In the first step, the number of phases and starting values for parameters of the multiphasic model were derived from a combination of either (1) the measured cumulative gas production profile and its first (rate of gas production) and second (change in rate of gas production) derivative or (2) a fitted monophasic curve and the residuals between this curve and the observations. In the second step, the starting values were used to fit di- or triphasic models. Using approach 1 was complicated by frequent fluctuations in the gas production rate. However, the combined graph of the fitted monophasic curve and residuals (approach 2) gave good results for every profile. The multiphasic model fitted the profiles well. The robustness of the model declined when the number of phases was increased, underlining the importance of accurate estimations of starting values. It is argued that the model parameters and the calculated  $R_M$  are useful for feed quality evaluation. The results show that mathematical description of gas production profiles requires a two-step approach and a multiphasic model.

### 6.2 Introduction

Mathematical description of gas production profiles enables analysis of data and comparison of

substrates or fermentation environment characteristics, and can provide useful information concerning the substrate composition and the fermentability of soluble and slowly fermentable components of the substrate. Various models are available for parameterization of the degradation or fermentation profiles. With early gas production techniques, still being used, using large glass syringes (e.g. Hidayat *et al.* 1993; Khazaal & Ørskov 1994) or a manometric system (e.g. Carg & Gupta 1992; Waghorn & Stafford 1993), only rather simple gas production profiles can be obtained, which can be described with rather simple models. These models are often based on first order kinetics, assuming a constant fractional rate of fermentation (e.g. Ørskov & McDonald 1979).

More recent gas production equipment (e.g. Pell & Schofield 1993; Cone *et al.* 1994; Theodorou *et al.* 1994), supplies much more accurate gas production profiles, in which different underlying processes can be identified, necessitating the use of a more sophisticated model. France *et al.* (1993) postulated an empirical time dependent increase of the fractional rate. In the models of Schofield *et al.* (1994) the fractional rate of fermentation increases to a maximum, dependent on the gas produced in a sigmoidal fashion, following logistic or Gompertz behaviour. Considering the differences between gas production profiles and the possibilities offered by the high resolution measurements using modern equipment, a more flexible model is required. In this paper, we present a new and flexible model for gas production profile parameterization and a flexible approach to quantify the number of phases in such profiles and to attain estimations of the parameter values, to be used as starting values in a computer curvefit program. The model and the modelling approach are tested for a range of profiles.

## **6.3 Experimental**

### **6.3.1 Model**

A sigmoidal equation was adopted to describe the kinetics of the separate phase in the gas production profiles (Eqn 1).

$$G = \sum_{i=1}^n \frac{A_i}{1 + \frac{B_i C_i}{t^{C_i}}} \quad \text{Eqn 1}$$

In this equation,  $G$  ( $\text{ml g}^{-1}$  OM) denotes the amount of gas produced per g organic matter (OM) incubated, at time  $t$  after incubation.  $A_i$  ( $\text{ml g}^{-1}$  OM) represents the asymptotic gas production.  $B_i$  (hours) is the time after incubation at which half of the asymptotic amount of gas has been formed, and  $C_i$  is a constant determining the sharpness of the switching characteristic of the profile. The value of  $i$  indicates the number of phases in the profile ( $i=1,n$ ).

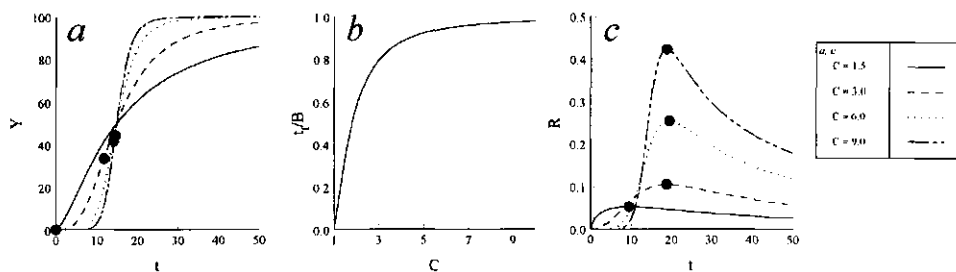


**Fig 1.** Characteristics of the model. *a.* The sigmoidal curve described by Eqn 1, with  $A=100$ ,  $B=15$  and  $C=1, 3, 6$  and  $9$ . ●, Point of inflection of the curves, adjusted after Thornley & Johnson (1991). *b.* The ratio between the point of inflection ( $t_i$ ) and half time ( $B$ ), as affected by the value of  $C$  (Eqn 2). *c.* The relative rate of fermentation (Eqn 3) for parameter values  $B=15$  and  $C=1.5, 3, 6$  and  $9$ . ●, Point of maximum fractional rate ( $t_{RM}$ ,  $R_M$ ) of the curves.

The curvature is determined by  $B$  and  $C$ , resulting in a high flexibility.  $C$  determines the curvature and thereby the position of the point of inflection. The impact of  $C$  is shown in Fig 1a. For  $C \leq 1$ , the profile has no point of inflection ( $t \geq 0$ ). As the value of  $C$  increases, the profile becomes sigmoidal, with increasing slope, until for  $C \rightarrow \infty$  a step function is obtained, with an initial slope of zero. Eqn 2 gives the solution to the second derivative equal to zero, i.e. the point of inflection ( $t_i$ ). Fig 1b illustrates the effect of increasing  $C$ , on the relation between  $t_i$  and  $B$ , expressed as the ratio  $t_i/B$ .

$$t_i = B \left( \frac{C-1}{C+1} \right)^{1/C} \quad \text{Eqn 2}$$

From the parameters B and C, the fractional rate of substrate digestion (R) can be calculated, if a fixed linear relationship is assumed to exist between substrate fermentation and gas production. The proportion of undigested, potentially digestible substrate is given by  $P_i(t) = (A_i - G_i(t))/A_i$ . Thus, R can be calculated as in Eqn 3, for  $C > 1$ .

$$R = -\frac{1}{P} \frac{dP}{dt} = -\frac{C t^{C-1}}{B^C + t^C} \quad \text{Eqn 3}$$

R increases to reach a maximum ( $R_M$ ), when the size of the microbial population no longer limits the fermentation of the particular feedstuff component (Fig 1c). The time after the start of the incubation at which  $R_M$  occurs, i.e.  $t_{RM}$ , solved from  $dR/dt = 0$ :

$$t_{R_M} = B (C - 1)^{1/C} \quad \text{Eqn 4}$$

characterizes the rate of growth of microorganisms and colonization of the feed component.  $R_M$  is reached when the microbial population no longer limits fermentation, and digestion is not hampered by chemical or structural barriers imposed by the feedstuff component at this point.

Gas production profiles can be described with the model using nonlinear curvefitting programmes (e.g. NLREG, Sherrod 1995). However, to do this, the number of phases has to be estimated. To limit the number of calculations and calculation time, estimates of the parameter values can be made and used as starting values.

### 6.3.2 Estimation of the number of phases and parameter values

#### *Approach 1: Cumulative gas production and first and second derivative*

Gas production profiles reflect a concatenation of fermentation processes. Throughout the incubation, these processes either start at their maximum rate, and subsequently decline, or the rate increases to a maximum and declines thereafter. This enables the separation of processes which differ in their maximum fermentation rate and in the time at which this maximum rate is reached. Therefore, characteristics of the different phases in a profile could be deduced from changes in the measured rate of fermentation, using the first and second derivative. Here, the observed smoothed rate, and change in rate of gas production will be used, calculated at time t



as the average of the values at  $t-1$ ,  $t$  and  $t+1$ .

Mathematically maxima in the first derivative and the solution of the second derivative equals zero represent a point of inflection ( $t_i$ ). This  $t_i$  can be used as an estimate of the time after incubation at which half of the asymptotic amount of gas has been formed (see Figs 1a & 1b). This value is used as a starting value for  $B_i$  in the multiphasic curve fitting. The starting value of  $A_i$  can be estimated as twice the gas production at  $B_i$ , subtracting the gas production from previous phases.

#### *Approach 2: Fitted monophasic model and residuals*

Differences between phases are often obscured by limited differences in the fermentation rates of successive phases. An alternative approach is to fit a monophasic model to a gas production profile with different phases. This will result in alternating periods of overestimation and underestimation of the gas production of the separate phases, and will lead to a systematic pattern in the plot of residuals, from which the number of phases can be determined, as will be demonstrated below.

In non-linear curve fitting, the residuals are minimized (Motulsky & Ransnas 1987), so that deviations of observations above and below the fitted monophasic model will be similar. If the phases are symmetrical ( $t_i=B$ ), the monophasic model will intersect the observations at halftime and the plot of residuals intersects with the X-axis. This value is used as starting value for  $B_i$  in the multiphasic curve fitting. From the combined plot of the monophasic model and the residuals, the starting value of  $A_i$  can be estimated from the figure as twice the gas production at  $B_i$ , corrected for gas production in previous phases.

#### *6.3.3 Curve fitting of multiphasic models*

Eqn 1 is used in the second step, in which  $i$  equals the number of phases distinguished in the first step. From the first step, the starting values for the non-linear curve fitting are also estimated as already described. Experimental fermentation profiles of various substrates were fitted to assess the applicability of the two-step method and the multiphasic model. The NLREG package (Sherrod 1995) was used to carry out the nonlinear regression analyses.

The significance of the phases was tested. Phases were added to the model, if the addition

of the extra parameters resulted in a significant improvement of the fit (F-test,  $P < 0.001$ , cf. Motulsky & Ransans 1987) and the parameters were significantly different from zero (t-test,  $P < 0.001$ ) (see also Zwietering *et al.* 1990).

The Durbin Watson coefficient for autocorrelation was used to test if the model approaches the data (goodness of fit), without systematic errors. Significant autocorrelation indicates either that the model lacks one or more key variables or that the model is inappropriate for the data values (Neter & Wasserman 1974).

The robustness, i.e. the sensitivity to different starting values, of the multiphasic model was tested by using deviating starting values (up to 100% from the values estimated in step 1) for the non-linear curve fitting procedure.

#### 6.3.4 Gas production profiles

The gas production profiles of four very different substrates were used to test the model. These profiles contrasted due to the substrates used and the method of incubation, and were selected to demonstrate the wide applicability of the presented model. The substrates were isolated NDF (neutral detergent fiber) from a young regrowth of Italian ryegrass (oven-dried at 70 °C), mature sorghum stems (air dried), whole crop ryegrass regrowth (air-dried) and red clover (freeze-dried), subsequently referred to as ryeNDF, sorghum, grass and clover. All samples were ground to pass a 1 mm screen. The chemical composition of the substrates is given in Table 1.

**Table 1.** The concentration of organic matter (OM), crude protein (CP), neutral detergent fiber (NDF), acid detergent fiber (ADF) and acid detergent lignin (ADL) in the substrates ( $\text{g kg}^{-1}$  DM) used in the gas production experiments.

Substrate	OM	CP	NDF	ADF
Rye NDF	938	47	915	536
Sorghum	829	45	663	376
Grass	887	170	538	251
Clover	871	267	260	230

The grass and clover samples were incubated using the method described by Cone *et al.* (1994), characterised by a high concentration of inoculum (1:2 v/v). The medium used in this method is based on Menke *et al.* (1979) and adjusted by Steingass (1983), and contains minerals, reducing agent and buffer. Gas production was recorded using an automated system.

The ryeNDF and sorghum were tested for gas production according to Theodorou *et al.* (1994). A low inoculum concentration (1:30 v/v) was used. The medium contained minerals, volatile fatty acids, vitamins, protein, reducing agent and buffer. Gas production was measured manually.

## 6.4 Results and discussion

### 6.4.1 Applicability

The gas production profiles of the four samples tested, differed greatly in their curvature and in the total amount of gas produced ( $\text{ml g}^{-1} \text{ OM}$ ). The gas profiles for grass and clover showed rapid gas production in the early stages of fermentation, and the time after which gas production had virtually stopped was shorter than for the other substrates, also due to the incubation of these samples in poorly diluted rumen fluid.

From intersection of the descending part of the curve of the calculated second derivative with the X-axis (Approach 1), a first phase of each profile could be identified (Fig 2) and estimates of the parameter values could be made (Table 2). However, frequent fluctuations occurred in the calculated second derivative after 20h in the ryeNDF and sorghum profiles and after 10h in the grass and clover profiles. Therefore, only intersections of the descending second derivative with the X-axis were used as an indication for a phase after systematic positive ( $\geq 2$  observations) values. Hereby, a second phase was found in the sorghum, grass and clover profiles and a third phase in the grass and clover profiles (Fig 2; Table 2).

The use of a monophasic model (Approach 2) was complicated by the high rate of gas production during a short period immediately following incubation in the grass and clover profiles, resulting in underestimation by the monophasic model, and thus positive residuals, which was not the case with the ryeNDF and sorghum profiles. Here, the end of the first phase was estimated from the first minimum in the plot of residuals and parameter values were estimated at this point

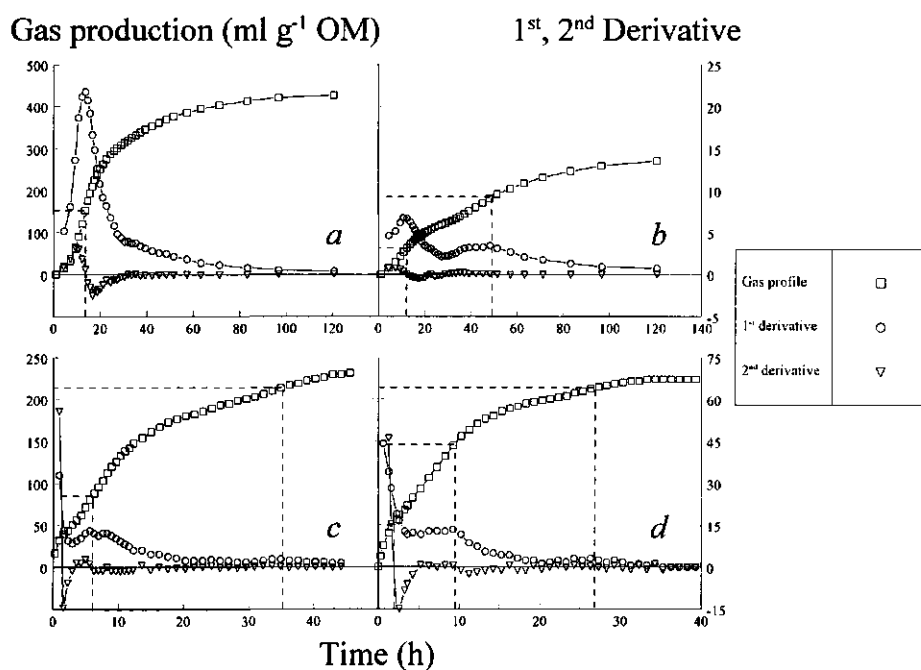


**Fig 2.** Observed gas production profile, with first and second derivative. The dashed lines indicate estimates of respectively ( $B_1$ ,  $0.5A_1$ ), ( $B_2$ ,  $A_1+0.5A_2$ ) and ( $B_3$ ,  $A_1+A_2+0.5A_3$ ). *a.* RyeNDF. *b.* Sorghum. *c.* Grass. *d.* Clover.

**Table 2.** Estimated values of parameters A and B in di- and triphase models<sup>a</sup>.

Substrate	Phase	A (ml g <sup>-1</sup> OM)		B (h)	
		Approach 1	Approach 2	Approach 1	Approach 2
Rye NDF	1	320	320	14	14
	2	n.e.	120	n.e.	59
Sorghum	1	124	114	12	11
	2	122	152	49	48
Grass	1	70	62	1	2
	2	30	104	6	8
	3	228	102	35	37
Clover	1	100	100	2	2
	2	92	97	10	9
	3	44	28	27	25

<sup>a</sup> n.e., Not estimable.

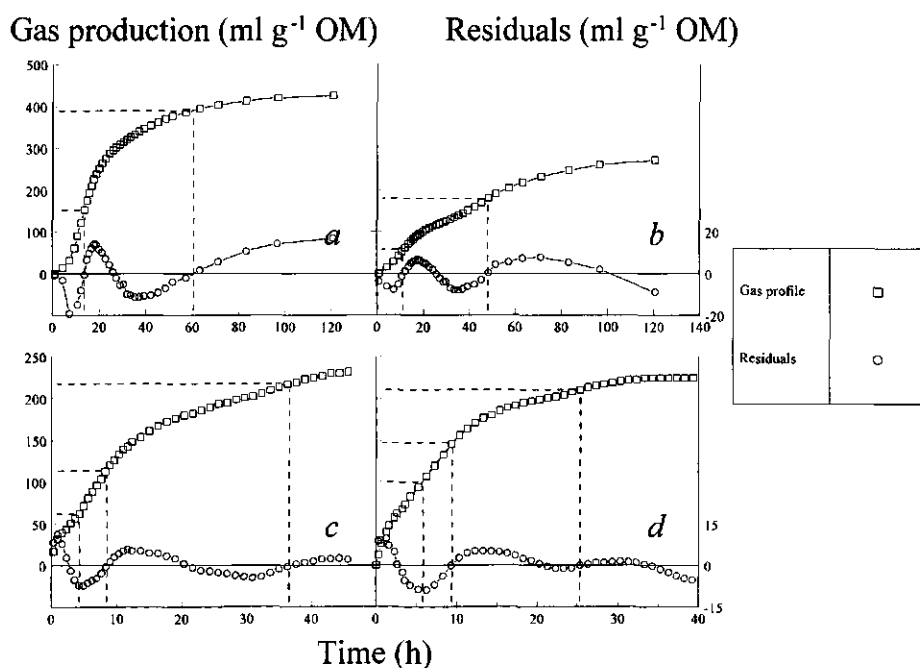


**Fig 3.** Observed gas production profile, fitted with a monophasic model and the residuals. The dashed lines indicate estimates of respectively ( $B_1$ ,  $0.5A_1$  in A and B;  $2B_1$ ,  $A_1$  in C and D), ( $B_2$ ,  $A_1+0.5A_2$ ) and ( $B_3$ ,  $A_1+A_2+0.5A_2$ ). *a.* RyeNDF. *b.* Sorghum. *c.* Grass. *d.* Clover.

**Table 3.** Fitted values of parameters A, B and C in di- and triphase models<sup>a</sup>.

Substrate	Phase	A ml g <sup>-1</sup> OM	B h	C	F-test	DW ( $k_{DW}$ )	$t_{RM}$ h	$R_M$ h <sup>-1</sup>
Rye NDF	1	313	14	3.52	262.9	1.46	18.0	0.140
	2	118	48	3.25		(1.16)	61.6	0.037
Sorghum	1	126	12	2.29	100.8	1.08	13.5	0.095
	2	151	52	3.73		(1.16)	71.7	0.038
Grass	1	44	1	1.13	14.2	1.87	0.1	1.949
	2	152	9	2.40		(0.98)	10.2	0.137
	3	52	37	5.26			48.2	0.088
Clover	1	90	2	1.10	404.8	1.35	0.2	0.557
	2	120	9	3.09		(1.15)	11.1	0.188
	3	17	26	13.8			30.9	0.414

<sup>a</sup> The F-test indicates the improvement to the fit after adding the last significant ( $P < 0.001$ ) phase to the equation. DW indicates the Durbin-Watson coefficient for autocorrelation.  $K_{DW}$  indicates the lower critical value for the Durbin-Watson coefficient ( $\alpha=0.05$ ). The time of occurrence of the maximum fractional rate of substrate degradation ( $t_{RM}$ ) and this maximum fractional rate ( $R_M$ ) are calculated from B and C parameters for each phase.

(2 B<sub>1</sub>, A; Figs 3c & 3d). The systematic fluctuations in the residuals between the fitted monophasic curve and the observations resulted in the identification of 2 phases in the ryeNDF and sorghum profiles and three phases in the grass and clover profiles (Fig 3; Table 2).

The estimations for the number of phases in the profiles and the starting values were compared with results of multiphasic non-linear regression analysis on the profiles. Phases were added to the model, until no significant improvement of the fit or parameter significance could be reached. The final number of phases (i) in the model leading to the last significant improvement of the F-value ( $P < 0.001$ ) and significant parameters (t-test;  $P < 0.001$ ; data not presented) amounted 2 for the ryeNDF and sorghum profiles and 3 for the grass and clover profiles (Fig 4; Table 3). The values of A<sub>1</sub> and B<sub>1</sub> had been estimated accurately using both Approach 1 and Approach 2, except for A<sub>2</sub> and A<sub>3</sub> in the grass profile, which was due to an underestimation of the B<sub>2</sub> in this profile. These results indicate the wide applicability of the two-step method, using approach 2 in the first step and the multiphasic model for parameterization of gas production profiles in the second step.

### Gas production (ml g<sup>-1</sup> OM)

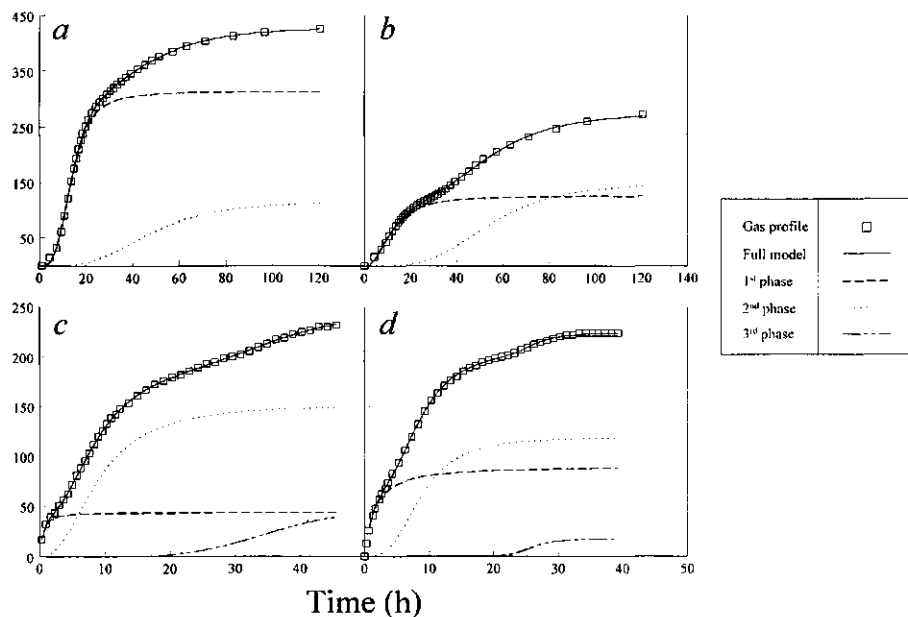


**Fig 4.** Observed gas production profiles, fitted with a diphasic or triphasic model and the curves for phases 1, 2 and 3. *a.* RyeNDF. *b.* Sorghum. *c.* Grass. *d.* Clover.

#### 6.4.2 Goodness of fit

The Durbin-Watson coefficients indicated significant auto-correlation only for the sorghum profile (Table 3). The significant autocorrelation for the multiphasic fit of the sorghum profile was probably due to deviation of the first observation from the curve. This observation may have represented a small first phase, but could not be fitted as such, because the number of observations in the first hours of incubation period was too low.

#### 6.4.3 Robustness

Changing the starting values of parameters had no effect on the outcome of the monophasic curve fitting, although there were differences in the number of iterations before convergence was reached. The sensitivity of the curve fitting procedure to changes in the starting values increased as the number of phases in the model increased. When starting values deviated considerably (> 25%) from those obtained in step 1, were used for fitting multiphasic models, the fitted models sometimes deviated greatly from the data, and in some cases no convergence could be reached.

The declining robustness when the number of phases increases is inherent to the non-linear curve fitting procedure. This procedure iteratively seeks the set of parameters for a model, with the least residual sum of squares. When the number of parameters in the model is increased, the chance of encountering a local minimum increases (Motulsky & Ransnas 1987) and the importance of accurate estimates for initial values increases. By determining good starting values, the proposed two-step method helps to avoid these problems and to detect faulty solutions.

#### 6.4.4 Biological meaning of the parameters

The model presented here is flexible to changes in the fractional rate of fermentation ( $R$ ). As described in the Materials and Methods section, the fractional rate of fermentation is likely to increase in early stages of the incubation, because the microbial population has to multiply and colonize the substrate to form a "biofilm", as in particular the digestion of insoluble feed components is a surface process (France *et al.* 1993; McAllister *et al.* 1994). When this limitation

has been lifted, the maximum fractional rate of fermentation ( $R_M$ ) is reached. The  $R_M$  can be attained rapidly following incubation in the case of fermentation of soluble feedstuff components, which do not require colonization, under high microbial densities, as in the grass and clover profiles analysed in the system of Cone *et al.* (1994). This resulted in low values of  $t_{RM}$  for the grass and clover profiles, when compared to the ryeNDF and sorghum profiles tested, using a different system (Theodorou *et al.* 1994).

After the  $R_M$  has been reached, the fractional rate of fermentation can decline either rapidly or gradually (Fig 1 c). A rapid decline of  $R$  can occur after depletion of the substrate component, which is most likely in the case of soluble components. For insoluble components, associated with the cell wall fraction of substrates,  $R$  is more likely to decrease slowly, when either chemical or structural barriers are encountered. The crystallinity of cellulose, and toxic action of cell wall phenolics can impose chemical barriers to digestion (Kerley *et al.* 1988; Grabber & Jung 1991; Cornu *et al.* 1994). These characteristics are related to factors such as plant species, stage of maturity and chemical pre-treatment. The structural limitations to digestion can also have a diverse nature, e.g., the tube-shape of sclerenchyma fibers (Wilson & Mertens 1995) or the indigestible layers in plant tissues, such as cuticle, warty layer (Engels & Brice, 1985) or middle lamella-primary cell wall (Engels & Schuurmans 1992; McAllister *et al.* 1994). The role of structural barriers depends on the plant anatomy and particle size.

The  $R_M$ , as obtained with the cumulative gas production technique, gives an accurate value of the maximum fractional fermentation rate, if the relationship between organic matter fermentation and gas production is constant for a particular phase. Under the same assumption, the values of  $A$  are related to the amount of fermentation of particular components in the substrate. The assumption is justified, when each phase represents the fermentation of a group of substrate components with corresponding fermentability. However, this relationship does not have to be the same for consecutive phases, since the production of gas per g OM fermented can vary between substrate components differing in fermentability, depending on the fermentation pathways, as demonstrated in stoichiometrical calculations (e.g. Van Soest 1994). However, the relationship between gas production and OM disappearance can be improved by correcting the gas production with measured VFA values and ammonium values. This stresses the importance of the multiphasic analysis of high resolution gas production profiles in detailed studies of feed fermentation.



As already suggested, the differences in the number of phases and the parameter values of the separate phases in the profiles presented in this paper, were probably related to differences in substrate composition and incubation method. The grass and clover substrates, incubated in poorly diluted rumen fluid, contained a high proportion of soluble carbohydrates and protein, which were readily available and were rapidly fermented, leading to a first phase in their triphasic fermentation profiles, with a low  $t_{RM}$  and extremely high  $R_M$ . The first phase of the ryeNDF and sorghum profiles and the second phase of the grass and clover profiles, with a narrow range in the values of  $B_i$ ,  $t_{RM}$  and  $R_M$ , were probably related to an insoluble potentially degradable cell wall fraction, which required colonisation and solubilization by microbial enzymes (Van Milgen *et al.* 1993). The final phase of gas production may have been related to even less degradable substrate components or may have been the consequence of microbial turnover (Theodorou *et al.* 1995), which is currently investigated.

### 6.5 Conclusions

The flexible two-step method to estimate of the number of phases and parameter values, followed by fitting with a multiphasic model is a good alternative to current modelling approaches, and is necessary for highly accurate profiles, being obtained with modern equipment. The best results were obtained when in the first step a combined graph of a fitted monophasic curve and a plot of residuals was used. The value of the parameters of the model and the calculated maximum rate of fermentation in each phase in characterizing the feedstuff composition and degradability need further investigation.

## 7. FERMENTATION OF CELL WALLS AND CONTENTS

with Barbara A. Williams, Arno J. Oostdam, Huug Boer & Seerp Tamminga

### 7.1 Abstract

Differences between the fermentation characteristics of cell contents (CC) and protease-treated cell walls (CW) of young Italian ryegrass leaves (*Lolium multiflorum*) cv. Multimo, were studied *in vitro*. Gas and volatile fatty acid (VFA) production were measured at regular intervals, as was the degradability of organic matter (OM) of CW. The measured VFA were used to predict the gas production and fermentable OM using stoichiometric calculations.

For CW the volume and kinetics of measured gas production were the same as that predicted from the VFA formed. Contrarily, for CC the measured gas production was consistently less than predicted, indicating that the stoichiometric calculations were not valid for rapidly fermenting substrates. For both CC and CW, the relative rate of acetic acid production levelled off more slowly than for other VFA, resulting in an increasing gas yield (in ml g<sup>-1</sup> fermentable OM) after 12 (CW) to 24 (CC) hours of incubation. Consequently, the fermentation of OM was not linearly related to gas production kinetics. The kinetics of decline of degradable OM and fermentable OM were the same, after correction for a constant 'lost fraction' of DOM of 205 g kg<sup>-1</sup> OM.

This work indicates the value of detailed studies of fermentation processes to evaluate herbage quality. In particular the role of CC and the difference between degradation and fermentation require further attention.

### 7.2 Introduction

Fermentation is the anaerobic decomposition of substrates by microorganisms and can be assessed according to the production of end-products, of which volatile fatty acids (VFA) and gas are the most important (Lin *et al.* 1985). The complex interactions within a mixed rumen microbial population leading to conversion of plant components to gas and VFA, have been

summarized in the form of stoichiometric reaction equations (Wolin 1975, 1979; Russell & Wallace 1988; Van Soest 1994). All of the equations show the relationship between the hexose-equivalents fermented, and the proportions of fermentation products produced. Such equations have been used to estimate the extent of digestion of hexose-equivalents on the basis of the fermentation products formed (e.g. Blümmel & Ørskov 1993).

The aim of this work was to gain more insight into the dynamics of degradation and fermentation of the protease-treated cell walls (CW) and cell contents (CC) of Italian ryegrass (*Lolium multiflorum*). Gas and VFA production were both measured at regular intervals during the incubation. The VFA data obtained throughout fermentation were then used in stoichiometric equations to predict both OM fermentation and formation of gas, and the predicted values compared with those measured, to determine whether the measurement of cumulative gas production reflected changes in other fermentation parameters, including the production of VFA and the disappearance of organic matter.

### 7.3 Experimental

#### 7.3.1 Substrates and cumulative gas production

Italian Ryegrass (*Lolium multiflorum*, tetraploid cultivar Multimo) was sown on 28 October 1993. The seeding rate was nine plants per pot (0.0169 m<sup>2</sup> surface area) containing a mixture of sand and peat (1:1 v/v). The plants were grown in a heated glasshouse, at day/night temperatures of 18/13 °C. Day temperatures were maintained between 08.00 and 20.00 hours. Day length was natural, and the relative humidity was approximately 70%. Additional light was supplied by Philips 400W SONT lamps (Philips, Eindhoven, The Netherlands) for 14 h per day. The pots were placed in large trays, which were flushed with nutrient solution (Steiner 1984). The pots were placed in two replicate blocks. Plants were harvested after 113 days of growth, when they had formed eight leaves on the main shoot (18 February 1994). The last fully expanded leaf was dissected from the main shoot of each plant and frozen separately before analysis.

### 7.3.2 Cell wall and contents fractionation, and cumulative gas production

Fresh leaves were first chopped into 10-20 mm pieces using a paper guillotine and then further chopped in a Knifetec Sample Mill (Tecator, Sweden). This material was pressed (HAPA hydraulic press, IKA, Germany; 250 ml) through a double nylon cloth (Nybolt PA 40/30, Zurich, Switzerland) under a pressure of 10100 kPa. The residue was mixed thoroughly with distilled water, and the process repeated three times. The resultant filtrate was cooled with solid CO<sub>2</sub>, while the residue was washed. Both components were freeze-dried and ground through a 1 mm sieve (Retsch mill, Haan, Germany). The residue was then treated with neutral detergent (Goering & Van Soest 1970) and protease (Sigma Protease Type XXIII P-4032, Sigma, St Louis, MO, USA) resulting in the CW fraction. The protease treatment lasted for 1h in 60 ml phosphate buffer containing 0.25 ml protease per gram of dry matter.

Two replicate samples were incubated for cumulative gas production measurements during various incubation periods, according to the method of Theodorou *et al.* (1994). Bottles containing CC were removed at 3, 6, 12, 24, 48 and 120h after inoculation, while the CW removal times were 6, 12, 24, 48, 72 and 120h. The fermentation was stopped by plunging the bottles into iced water for 20 min. A liquid sample was then collected for volatile fatty acid (VFA) analysis and the residual cell walls estimated by filtration through sintered glass crucibles (Schott Duran, porosity #2, Mainz, Germany) and rinsing with hot water. Blank bottles containing only medium and inoculum, but no substrate, were incubated for 120h.

### 7.3.3 Chemical and VFA analysis

Neutral-detergent fibre (NDF; Goering & Van Soest 1970), crude protein, and ash were determined according to standard procedures. VFA were analyzed using gas liquid chromatography (Packard 419, (CE Instruments, Milan, Italy) glass column filled with Chromasorb 101, carrier gas N<sub>2</sub> saturated with formic acid, 190°C with *iso* caproic acid as the internal standard).

### 7.3.4 Stoichiometric calculations

The theoretical stoichiometric calculations used to obtain an approximate indication of OM fermentation, were based on the VFA production measured at each time interval (Van Soest 1994). OM fermentation was expressed in glucose equivalents (g). It was assumed that the glucose equivalents were fermented to form the end-products: acetic (HAc), propionic (HPr), and butyric acids (HBu), and the gases carbon dioxide (CO<sub>2</sub>) and methane (CH<sub>4</sub>), as well as being incorporated into microbial biomass.

To calculate the amount of glucose required for microbial growth, the amount of ATP (mmol) synthesized can be estimated from the VFA production. VFA production results in direct gas production (1 mmol from HAc and 2 mmol from HBu; Hungate 1966; Beuvink & Spoelstra 1992). To estimate ATP production for microbial growth, the molar proportions of CO<sub>2</sub> and CH<sub>4</sub> in the gas produced also need to be derived. From stoichiometric equations it can be calculated that:

$$CO_2 = \frac{HAc}{2} + \frac{HPr}{4} + \frac{3 HBu}{2} \quad \text{Eqn 1}$$

$$CH_4 = HAc + 2 HBu - CO_2 \quad \text{Eqn 2}$$

The production of microbial biomass was estimated from the total ATP production (2, 3 and 3 mol mol<sup>-1</sup> HAc, HPr and HBu, respectively) and the yield of microbial biomass per mol ATP ( $Y_{ATP}$ , assumed to be constant at 10 mg mmol<sup>-1</sup> ATP; Hespell 1979). It was assumed that 80% of bacterial structures are synthesized from glucose skeletons. The glucose consumption for production of biomass ( $Glucose_{biomass}$ ) and for production of products ( $Glucose_{products}$ ) were calculated as:

$$Glucose_{biomass} = 0.8 Y_{ATP} (2 HAc + 3 HPr + 3 HBu + CH_4) \quad \text{Eqn 3}$$

$$Glucose_{products} = 162 \frac{2 HAc + 3 HPr + 4 HBu + CO_2 + CH_4}{6} \quad \text{Eqn 4}$$

Total fermentation of hexose-equivalents was calculated as  $Glucose_{products} + Glucose_{biomass}$ .

Theoretically, one mmol CO<sub>2</sub> should be released from the bicarbonate buffer in the medium, per mmol VFA produced. This was used to calculate the 'indirect' gas production, which was added to the calculated 'direct' gas, to predict the total gas production. This predicted gas production was then compared with the measured values.

### 7.3.5 Statistical analysis

Profiles of cumulative gas (ml g<sup>-1</sup> OM) and VFA (mmol g<sup>-1</sup> OM) production were calculated, as were the degradation and fermentation of OM (g kg<sup>-1</sup> OM). These were fitted iteratively to the model described in Chapter 6 (Eqn 5). In this equation,  $G$  (ml g<sup>-1</sup> OM; mmol g<sup>-1</sup> OM; g kg<sup>-1</sup> OM) denotes the amount at time  $t$  after incubation.  $A_i$  (ml/g OM; mmol g<sup>-1</sup> OM; g kg<sup>-1</sup> OM) represents the asymptote.  $B_i$  (h) is the time after incubation at which half of the asymptotic amount has been formed, and  $C_i$  is a constant determining the sharpness of the switching characteristic of the profile. The value of  $i$  indicates the number of phases in the profile ( $i = 1, n$ ). In this experiment, the mono-phasic curve ( $i = 1$ ) was used, since only six observations were available per profile.

$$G = \sum_{i=1}^n \frac{A_i}{1 + \frac{B_i^{C_i}}{t^{C_i}}} \quad \text{Eqn 5}$$

Significance of the differences of the parameters was determined by ANOVA. Changes in the proportions of acetic, propionic and butyric acid, and the gas yield during the incubation were analyzed by linear regression. Genstat 5.3 (Genstat 5 Committee 1993) was used for all statistical analyses.

## 7.4 Results

The crude protein (258 (SE 18.2) g kg<sup>-1</sup> dry matter) and ash (213 (SE 6.1) g kg<sup>-1</sup> DM) content was higher for CC than for CW, which contained 120 (SE 7.0) g kg<sup>-1</sup> DM crude protein and 18 (SE 0.3) g kg<sup>-1</sup> DM ash. NDF content in CW was 771 (SE 14.7) g kg<sup>-1</sup> DM, while this was negligible for CC and so is not reported here.

#### 7.4.1 Gas and VFA production

The measured cumulative gas production and gas production rates are presented in Fig 1, while the fitted curve parameters for both measured and predicted gas production are shown in Table 1. Although the final measured gas volumes per g OM were not significantly different between CC and CW (Fig 1*a*; Table 1), the maximum gas production rate was higher for CC than for CW (Fig 1*b*). The maximum gas production rate was reached more rapidly for CC than for CW. As a consequence, the half-time of the fitted curve (B parameter) occurred later for CW than for CC.

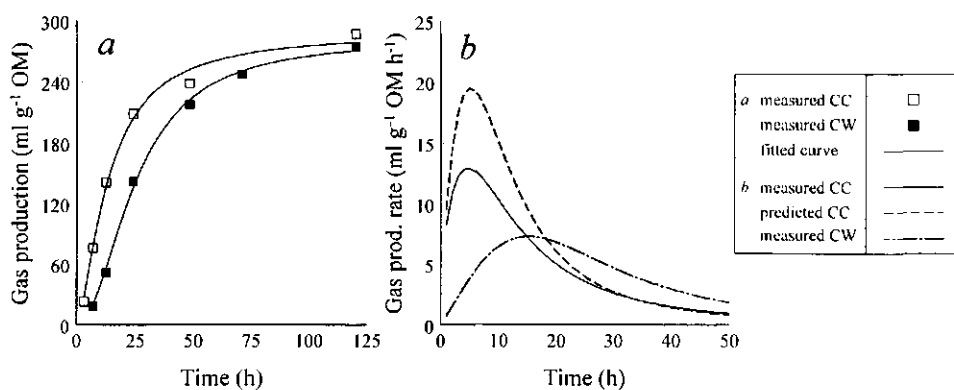


**Fig 1.** *a*. Measured gas production of cell contents (CC) and protease-treated cell walls (CW) of Italian ryegrass during the 120h fermentation and the fitted monophasic curves. *b*. Gas production rate for CC measured and predicted from VFA and for CW measured, during the first 50h of fermentation. Rates were calculated from fitted curves. OM, organic matter.

For the gas production predicted from VFA, the kinetic parameters B and C and, thus, the relative gas production rate were the same as for the measured curves. However, the measured gas volume for CC was considerably lower than predicted from VFA produced, due to a lower absolute gas production rate, which was most evident during the first 24 hours of the incubation (Fig 1*b*). For CW the predicted volume of gas produced corresponded closely with the measured value (Table 1).

**Table 1.** Mean values<sup>a</sup> at 120h incubation and fitted parameter A for measured and predicted gas production (ml g<sup>-1</sup> OM), volatile fatty acid production (mmol g<sup>-1</sup> OM) and OM fermentability and degradability (g kg<sup>-1</sup> OM) for cell contents (CC) and protease-treated cell wall (CW) fractions of the leaves of Italian ryegrass. Fitted half time (B, h) and the shape parameter are also presented<sup>b</sup>.

Variate	Fraction	120h	A	B	C
Measured gas	CC	287	291	13.8	1.50
	CW	275	284	25.6	2.06
Predicted gas	CC	350	362	11.4	1.70
	CW	274	290	26.5	2.11
LSD		21.3	29.4	3.93	0.322
Measured HAc	CC	3.76	3.94	10.2	1.48
	CW	3.95	4.20	28.2	2.02
Measured HPr	CC	3.23	3.32	9.6	2.35
	CW	1.25	1.35	18.6	2.94
Measured HBu	CC	0.71	0.72	13.0	2.76
	CW	0.32	0.37	19.7	2.31
LSD		0.256	0.305	2.65	0.632
Predicted FOM	CC	847	869	10.2	1.92
	CW	597	621	23.7	2.23
Measured DOM <sup>c</sup>	CW	808	928	19.5	1.18
	CW corr. <sup>d</sup>	603	631	23.8	2.05
LSD		94.6	101.1	3.53	0.342

<sup>a</sup> All values corrected for the blank.

<sup>b</sup> LSD, Least significant difference according to the Tukey test ( $\alpha = 0.05$ ).

<sup>c</sup> Not determined for the CC fraction.

<sup>d</sup> CW degradation corrected for the calculated 'lost fraction' of 205 k kg<sup>-1</sup> OM (see text).

After 120 hours of incubation, 11.0 (SE 0.53) and 8.2 (SE 0.29) mmol VFA g<sup>-1</sup> OM had been produced from cell contents and walls, respectively. For both fractions, 89% of the total VFA consisted of acetic, propionic and butyric acids. The amounts and kinetics of VFA production are presented in Table 1 and Fig 2 and molar percentages of these acids are shown in Fig 3.

Two phases could be distinguished in the changes of the percentages of VFA for CC. Until 24 hours of incubation, the percentage of acetic acid declined and propionic and later butyric acid percentages increased (Fig 3a). After 24 hours of incubation, there was a linear increase in the proportion of acetic acid and a decrease in the proportion of propionic acid (both  $P < 0.001$ ). These trends could be related to the changes in the relative rates of VFA production



(Fig 2a). A succession of maxima in the relative production rates of acetic, propionic and butyric acid occurred, after 3, 7 and 10h of incubation, respectively. After the maxima had been reached, the relative production rates declined rapidly for all VFA, though more so for propionic and butyric acid than for acetic acid.

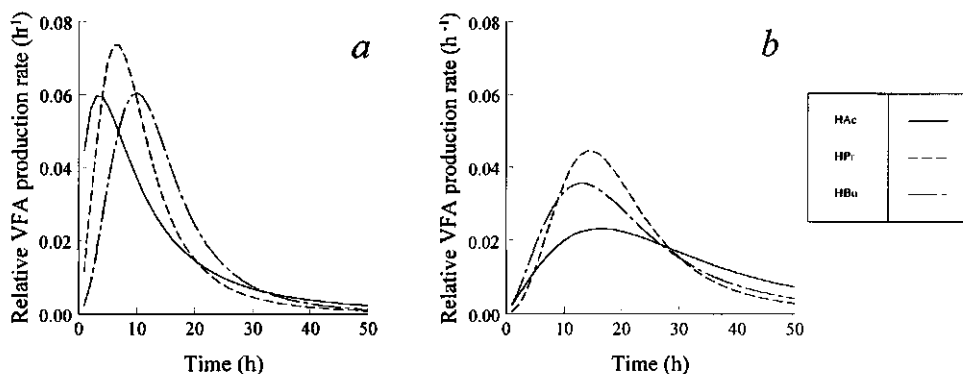


**Fig 2.** Relative production rates of acetic acid (HAc), propionic acid (HPr) and butyric acid (HBu) from (a) cell contents and (b) protease-treated cell walls during the first 50 hours of incubation. Relative rates were calculated from fitted curves. VFA, volatile fatty acids.

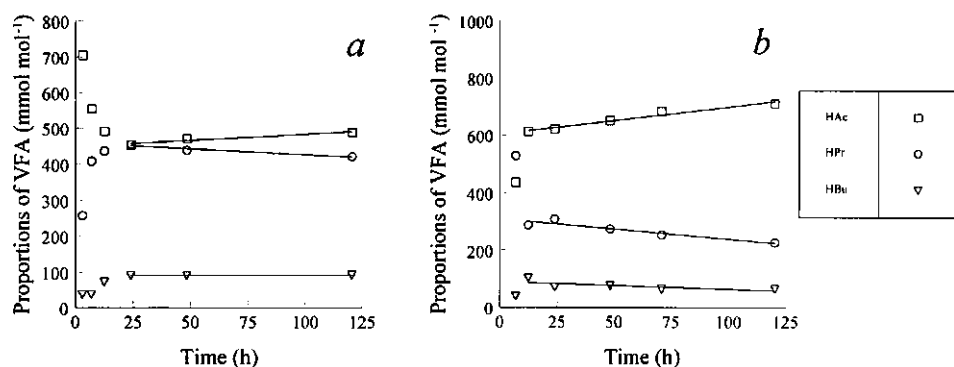


**Fig 3.** Proportions of the total measured volatile fatty acids (VFA) of acetic acid (HAc), propionic acid (HPr) and butyric acid (HBu) during 120 h fermentation of (a) cell contents and (b) protease-treated cell walls of Italian ryegrass. The lines indicate the significant linear relationship determined by regression analysis after 24 h and 12 h of incubation for cell contents and cell walls, respectively.

For CW, rapid changes in the proportions of VFA occurred between 6 and 12 h of incubation (Fig 3b). After 12 h of incubation, changes were more gradual, with an increase in the proportion

of acetic acid, and declining propionic and butyric acid proportions ( $p < 0.001$ ). The propionic acid production was lower than with CC (Table 1). As a result the percentages of acetic and butyric acid in total VFA were higher. The maxima in the relative production rates of VFA occurred almost simultaneously, but the relative rate of acetic acid production levelled off more slowly than for propionic and butyric acids (Fig 2*b*).

#### 7.4.2 Degradation, fermentation, and gas yield

Stoichiometric equations were also used to predict how much organic matter should have been fermented to produce the amounts of VFA measured from CC and CW (Fig 4*a*). The predicted final fermentability of both CC and CW was considerably lower than 100% (Table 1).

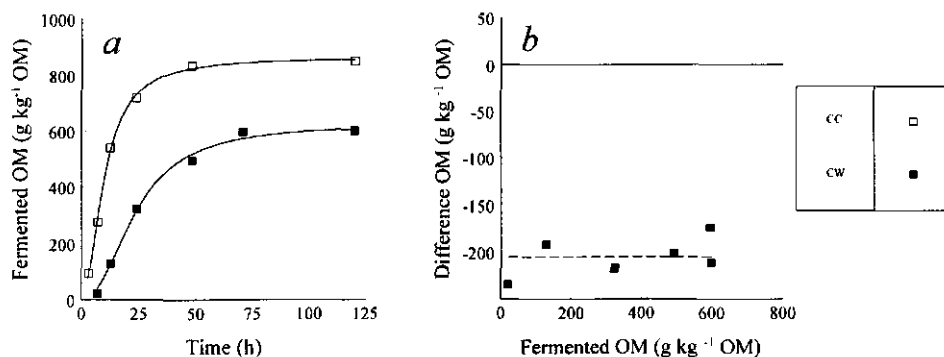


**Fig 4.** *a*. Stoichiometrically calculated organic matter (OM) fermentability for cell contents (CC), and protease-treated cell walls (CW) from Italian ryegrass, and the fitted monophasic curves. *b*. The difference between predicted OM fermentability and measured OM degradability vs predicted OM fermentability. The dashed line indicates the average value.

Fig 4*b* shows that for CW the predicted OM fermentability was 205 (SE 21.0)  $\text{g kg}^{-1}$  OM lower than the measured degradability. This difference was considered to be a 'lost fraction'. Moreover, the asymptotic gas volume A was higher and the kinetic parameters B and C were lower than for the measured degradation. However, when the degradability was corrected for the 'lost fraction' of 205  $\text{g kg}^{-1}$  OM at every point of observation, the fitted parameters of degradability of CW corresponded with those of fermentability (Table 1).

The yield of gas per g fermented OM ( $Y_F$ ) and per g degraded OM ( $Y_D$ ) are shown in Figs

5a and 5b. For CC,  $Y_F$  declined until 24 h of incubation and increased thereafter ( $P < 0.001$ ). The  $Y_F$  from CW increased linearly throughout the incubation.  $Y_D$  for CW (Fig 5b) increased throughout the incubation period to reach a maximum of 340 ml gas g<sup>-1</sup> degradable OM.  $Y_D$  was consistently lower than  $Y_F$ .

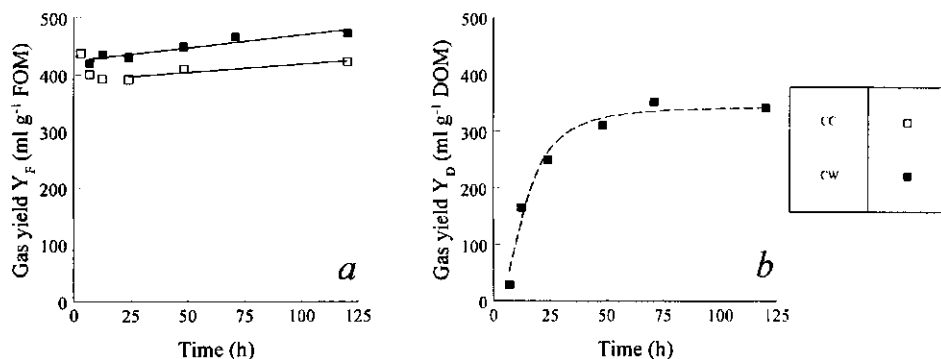


**Fig 5.** *a.* Changes in predicted fermentative yield of gas ( $Y_F$ ; ml g<sup>-1</sup> predicted fermentable organic matter (FOM)) for cell contents (CC) and protease-treated cell walls (CW) of Italian ryegrass. *b.* Changes in measured degradative yield of gas ( $Y_D$ ; ml g<sup>-1</sup> measured degradable organic matter (DOM)) for CW.

### 7.5 Discussion

The results suggest that gas production profiles are not necessarily linearly related to degradation or fermentation of substrate. The higher predicted compared with measured gas production for CC indicated that the stoichiometric relations (Van Soest 1994) are probably not valid for rapidly fermenting substrates.

For CC, the ca. 25% higher gas production predicted by stoichiometric calculations than measured was similar to over-estimations of gas production reported for cellulose (by 20%) and glucose (by 10%) by Beuvink & Spoelstra (1992). Typically, these over-estimations occur for substrates producing high percentages of propionic acid. The use of pure substrates by Beuvink & Spoelstra (1992) seems to rule out the possible mechanism of reduction of gas production by bonding of CO<sub>2</sub> to ammonia. A second process which could reduce the gas produced per mole of VFA, would be the conversion of CO<sub>2</sub> and H<sub>2</sub> to acetate instead of CH<sub>4</sub> (Miller 1995), which

would result in the net consumption of one mole of  $\text{CO}_2$ . This process mainly occurs when low roughage diets containing high proportions of sugars and protein are fed (Leedle & Greening 1988). The possible role of this process could not be estimated for this experiment. However, it demonstrates that deviations from the generally observed stoichiometric relations can occur. Consequently, the estimations of OM fermentation of CC may be inaccurate.

Relatively large amounts of propionic and butyric acid from CC are more frequently reported when easily digestible substrates are supplied to rumen microbes (Van Houtert 1993). When the rate of gas production was high, the percentages of propionic and butyric acid increased and consequently the calculated gas yield ( $Y_F$ ) was low. After 24h of incubation, the gas production rate was lower, and mainly acetic acid was produced which led to an increase in  $Y_F$ . This corresponds with the more frequently observed two-phasic gas production (e.g. Pell & Schofield 1993; Chapter 6). However, multiphasic analysis of the gas production profiles was not possible, due to the limited number of observations per curve.

For CW, the value of  $Y_F$  increased throughout the incubation, due to the higher production of acetic acid compared with other VFA. This resulted in a higher half-time (B parameter) for gas production (26.5 h) than for fermentation of OM (23.7 h). The value of  $Y_D$  increased even more rapidly, and could probably be attributed to the loss of some material when the residual CW was determined by use the NDR method (Goering & Van Soest 1970). This 'lost' cell wall fraction may have been a component such as soluble lignin-carbohydrate complexes (Chesson 1993), which are not fermentable. Such a loss of CW was probably also the cause of the overestimation of gas production by Blümmel & Ørskov (1993), which they attributed to substrate trapping by microbes.

In conclusion, the fermentation studies using data of gas and VFA production can give more insight into the processes occurring in *in vitro* forage evaluation systems. The results also indicate that caution is required in the interpretation of gas production profiles. For forage evaluation, it is important to distinguish between degradation and fermentation, as not all degraded CW material is necessarily fermentable.

## 8. GENERAL DISCUSSION

### 8.1 Composition and digestibility in relation to plant development

Several important conclusions can be drawn from the detailed analyses of the growth and ageing of individual plant organs in Chapters 2, 3 and 4. These are the following.

- The specific CW mass ( $s_{CW}$ ) of an organ remains unchanged after it has fully expanded. The increase in CWC during ageing is solely a result of the decline in the specific mass of cell contents ( $s_{CC}$ ).
- When assimilate supply is low for growing organs, for instance at high temperature,  $s_{CC}$  of plant organs is more reduced than  $s_{CW}$ , resulting in higher CWC.
- CWD of individual organs declines during ageing. The proportion of indigestible cell wall increases with a constant fractional rate per leaf appearance interval ( $\beta$ ), approaching an asymptote ( $\alpha_p$ ). The asymptote is lower for leaf blades than for leaf sheaths and stem internodes, but is not affected by insertion level, temperature or population.
- CWD decline of whole tillers is a function of tiller development stage, when expressed in leaf appearance intervals.
- Cutting results in a higher  $\alpha_p$  of only those growing leaves that are hit by cutting. These leaves have a minor contribution to total OM mass, so that crop CWD is only slightly affected in early stages of regrowth.

The constant  $s_{CW}$  after full plant organ expansion can be understood from the sequence of growth processes in the plant organs of grasses. The plant organs of grasses grow from a single intercalary meristem. The processes of cell division, cell elongation and cell wall synthesis take place in a ca. 6 cm long zone above the meristem (Nelson 1992). A leaf segment that has left the zones of cell division and cell elongation (2 cm in total) is displaced by ca. 0.85 mm h<sup>-1</sup> (Schnyder & Nelson 1987). Thus, within 2 days after cell division and elongation have ceased and full expansion is reached, the cell wall synthesis has ceased also. Consequently, the growth of the leaf has stopped and ageing has commenced already some time before the ligule appears (Begg & Wright 1962), in particular in later formed leaves, which have to grow through an increasingly longer sheath tube (Chapter 2). This results in higher CWC and lower CWD at the

moment of ligule appearance for consecutively formed leaves (Chapter 2, Table 3). The lower  $s_{CW}$  of leaves on tillers regrowing after cutting (Chapter 3, Table 1) indicates that the cell wall synthesis during the growth of plant organs can be reduced when assimilate supply is low. Cell wall accumulation terminated after full organ expansion, even when assimilate supply was abundant, as demonstrated for all plant organs of reproductive tillers after flag leaf appearance (Chapter 4, Fig 4).

The decline in 48 h *in vitro* CWD of plant organs to a constant level (CWD asymptote:  $1000 - \alpha_p$ ) is a general feature in grasses. This can be derived from the experiments with *Phleum pratense* (Davies 1969, as analysed by Hacker & Minson 1981), *Avena sativa* and *Lolium multiflorum* (Van Cruchten 1974; Wilman & Altimimi 1982), *Dactylis glomerata* (Davies 1976), *Panicum maximum* (Wilson 1976); *Hordeum vulgare* (Nordang *et al.* 1992), *Zea mays* (Cone & Engels 1993) and *Sorghum bicolor* (Wilson & Hatfield 1997). However, its time pattern has never been analysed and quantified in detail as in this thesis, because the measurements and modelling of changes in crop digestibility have focussed primarily on bulked leaf and stem plus sheath fractions or on whole plants, which show a linear decline of dry matter, organic matter and cell wall digestibility over a large time period (Terry & Tilley 1964; Chapter 4, Fig 6).

From the references listed above it can be concluded that the asymptotic CWD varies between species. Moreover, the asymptotic CWD of blades and sheaths tended to be lower at higher temperature (Chapter 4, Fig 5b). Similar values for CWD can be calculated from the observations by Van Cruchten (1974) in *Lolium multiflorum*. Moreover, from the field experiment of Wilman & Altimimi (1982) values of asymptotic CWD of stem internodes of *L. perenne* and *L. multiflorum* of 230 g kg<sup>-1</sup> can be derived, which are similar to those observed in Chapter 4.

The value of  $\beta$  is expected to be reasonably constant, as it is probably a reflection of the rate of chemical processes such as polymeric cross-linking in the cell walls, which are mainly affected by temperature (see Buxton & Fales 1994). In the experiments presented in Chapter 4, temperature had limited effects on asymptotic CWD, the CWD decline rate per leaf appearance interval and the distribution of whole tiller cell wall between plant organ fractions, so that the CWD decline of whole tillers could be modelled as a function of development stage, expressed in leaf appearance intervals.

## 8.2 Perspectives for improvement of cell wall digestibility

When considered as a single factor, the cell wall digestibility of grasses can be improved most effectively by increasing the asymptotic CWD of plant organs (Chapter 5), in particular when (re)growth periods are extended under low N fertilization regimes (Chapter 1). CWD is determined by cell wall characteristics of tissues and tissue proportions. Parenchyma cell walls are rapidly and mostly completely digestible in temperate grasses, whereas the primary cell walls and parts of the secondary cell walls in vascular and sclerenchyma bundles can become indigestible (Engels & Schuurmans 1992; Cone & Engels 1993; Wilson 1994), or digestion rate becomes so low that the incubation period or rumen retention time is too short for complete digestion. Thus, increasing the proportion of parenchyma cell wall and reducing the degree of polymeric cross-linking during ageing of vascular and sclerenchyma bundle cell walls can result in higher asymptotic CWD.

Since anatomical studies indicate that variation exists in the tissue proportions within leaves (Deinum *et al.* in prep), it might also be possible to increase the proportion of parenchyma cell wall. However, effects on other plant characteristics such as the proportion of cell contents that is used for synthesis of cell walls during leaf growth and other physiological parameters have to be considered in the evaluation, as already demonstrated in the sensitivity analysis of the simulation model (Chapter 5). Results of several experiments have suggested that improvements of CWD are possible (e.g., Lentz & Buxton 1991). Also the higher potential cell wall digestibility (determined after 360h *in sacco*), combined with higher intake and milk production from tetraploid cultivars of *L. perenne* compared to a diploid cultivar (Hageman *et al.* 1992, 1993), have indicated that prospects for improved digestibility and animal performance from already highly digestible *Lolium* cultivars exist (Lantinga & Groot 1996).

The sensitivity analysis of the model presented in Chapter 5 showed no significant effects on crop digestibility due to variation in morphological characteristics (leaf appearance rate, leaf blade length and width). Correlations between digestibility and morphological and anatomical characteristics reported in literature have never been strong (Sleper & Drolsom 1974; Wilson & Hattersley 1989; Masaoka *et al.* 1991; Buxton & Lentz 1993). This can probably be attributed to the fact that morphology, anatomy and physiology are not strictly coupled, allowing great variation between species and genotypes in construction and functioning, and in their response

to changes environmental conditions (Niklas 1992). Thus, screening on the basis of morphological characteristics and the use of morphology-based simulation models can be dismissed as useful and time- and cost saving means to reach improvement of herbage quality.

In this study, *Lolium* species were used as a model to reveal principles of composition and digestibility changes in grasses. These species was chosen for its popularity as a forage grass in the temperate areas of Western Europe, in particular The Netherlands. Similar investigations are required for tropical grasses, since large improvements in digestibility of these grasses can still be achieved. In extensive farming systems in the tropical regions management practices such as frequent cutting and fertilization can not always be employed the the most optimal manner, so that forage improvement through species and cultivar selection and breeding is even more important than in intensive farming systems in temperate regions (Wilson & Minson 1980; Hanna 1993).

### **8.3 Object-oriented modelling of plant growth and digestibility**

Considering the modelling results (Chapter 5), object-oriented models can be useful in the simulation of plant growth, as was also demonstrated for wheat (*Triticum aestivum*) by Bos (1999) and for the tree species *Pinus sylvestris* by Perttunen *et al.* (1996). An advantage of the object-oriented modelling approach is the reduction of mathematical and statistical abstraction (Sequeira *et al.* 1991). Moreover, in the ecological context it enables the calculation of the individual's contribution to the population (Sequeira *et al.* 1991). For the model presented in this thesis, this applies to the different organs that vary in position, size, mass, composition and digestibility. Also the gradual transition of 'double ridged' tillers to the 'reproductive' development stage could be modelled on an individuals basis. This approach is particularly suitable for modelling the behaviour of individual plants or plant modules in complex and varying environments, *e.g.*, white clover (*Trifolium repens*) plants in pastures. Only few adjustments are required to the model presented here to allow the modelling of diverse plant species, both monocotyledons and dicotyledons.

Since the 1970's, plant modelling has primarily focussed on plant physiology (process models). The importance of morphological and anatomical aspects is increasingly recognized as



they determine canopy structure and light interception, gas exchange, hydraulics and mechanical stability (Niklas 1992; Kurth 1994). The object-oriented approach supports the combined modelling of diverse plant aspects, as demonstrated for physiological and morphological plant characteristics in Chapter 5. When more quantitative analyses of plant anatomy are available, also anatomical characteristics can be incorporated into an integrated plant growth model (see Salminen *et al.* 1994). This will not only contribute to improved plant modelling, but could also enhance the understanding of the role of plant morphology and anatomy in the plant – animal interface. Apart from chemical characteristics such as molecular composition and polymeric binding, the digestibility of plant parts is largely determined by cell arrangement and cell wall thickness (Wilson & Mertens 1995). However, shape, size and anatomical structure of plants have significance for all phases of ingestion and digestion of roughages. For instance, the herbage selection by grazing animals not only depends on animal characteristics (mouth shape, sense organs, requirement), but can largely be explained from the canopy structure, as leaves of highest digestibility are present in the upper strata of the canopy, which are first reached by grazing animals (Hodgson 1981). The longitudinal venation of grass leaves makes biting and chewing inefficient, since cracks made by teeth are not easily propagated, and the resistance to comminution during ingestion and rumination is proportional to the cross-sectional area of fibres in the ingested material (Vincent 1990).

#### **8.4 The use of the cumulative gas production technique**

The advantage of the use of the cumulative gas production technique as opposed to the 48 h *in vitro* digestibility method (Goering & Van Soest 1970) is that it measures fermentation instead of degradation. Degraded cell wall is not completely fermented, as shown in Chapter 7. In a preliminary experiment gas production from CC of the top leaf, as used in Chapter 7, and the third and fourth leaf from the top were compared. The latter leaves that were ca. 30 and 40 days older than the top leaf, respectively. It was found that the gas production, and thus probably fermentability, of cell contents drastically declined during leaf ageing (Fig 1). When relationships between gas production and OM fermentation are determined for all feedstuff components, the cumulative gas production technique can potentially give a better indication of feeding quality

of roughages than the 48 h *in vitro* digestibility method.

To achieve this, more information is required about the contribution of cell contents and cell wall to gas production, and how these can be separated from the gas production profiles, using multi-phasic curve fitting as shown in Chapter 6. Then the cumulative gas production measurements can be used in elaborate studies as presented in Chapters 2, 3 & 4. For standard forage evaluation, untreated material should be incubated, avoiding pretreatment of the cell contents and cell wall fractions, as this can affect fermentation characteristics (Van Soest *et al.* 1991).

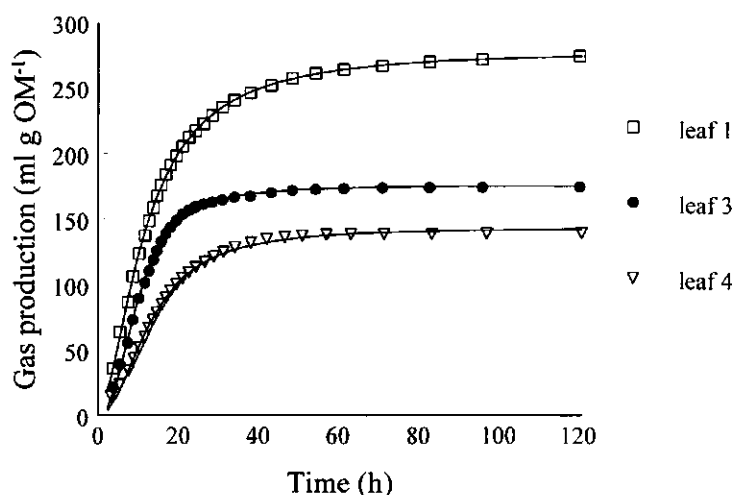


**Fig 1.** Measured gas production from cell contents of leaves 1 (top leaf), 3 and 4 of Italian ryegrass (*L. multiflorum*) tillers. The solid lines indicate the fitted monophasic curves. See Chapter 7 for a detailed description of the experimental procedure. Crude protein content: 258 (SE 18.2), 203 (SE 3.0), 226 (SE 1.2) g kg<sup>-1</sup> dry matter; ash content: 212 (SE 6.1), 305 (SE 2.6), 374 (SE 5.0) g kg<sup>-1</sup> DM, for leaves 1, 3 and 4, respectively.

Another challenge is to relate gas production kinetics of forages to other measures of feed quality, such as *in sacco* degradation and *in vivo* digestibility. Some studies concerning this topic have been published, *e.g.*, Blümmel & Ørskov (1993), Khazaal *et al.* (1993), Groot *et al.* 1994, Nsahlai & Umunna (1996) and Cone *et al.* (1998). A good correlation between long term (>100h) gas production and digestibility can be expected for the cell wall fraction of forages, as after 50h of incubation gas production relates closely to CWD (Chapter 7), and long term CWD (potential CWD, *in sacco*) relates closely to *in vivo* CWD (Tamminga & Van Vuuren 1996). On

the other hand, the gas production technique offers the possibility to estimate digestibility as a function of rumen retention time.

The methods for measurement of gas production profiles differ considerably, for instance in (e.g., Chapter 6 of this thesis, Menke *et al.* 1979, Steingass & Menke 1986, Theodorou *et al.* 1994, Cone *et al.* 1994, Stefanon *et al.* 1996):

- concentration of the substrate and the inoculum;
- duration of the incubation period;
- composition of the medium;
- frequency of measurements (and thus release of pressure from the headspace).

Clearly, for effective comparison of measurements between research groups a standardized method of gas production measurements needs to be adopted.

In conclusion, the cumulative gas production technique potentially can give better insight in the fermentation characteristics and feeding quality of feedstuffs, but many aspects require further study and standardization.

## REFERENCES

- Akin D E, Fales S L, Rigsby L L, Snook M E 1987 Temperature effects on leaf anatomy, phenolic acids and tissue digestibility in tall fescue. *Agron J* **79** 271-275.
- Anonymous 1998 Dutch recommended variety list for agricultural crops. [71<sup>e</sup> Beschrijvende rassenlijst voor landbouwgewassen] Wageningen. In Dutch.
- Begg J E, Wright M J 1962 Growth and development of leaves from intervalary meristems in *Phalaris arundinacea* L. *Nature* **194** 1097-1098.
- Beuvink J M W, Spoelstra S F 1992 Interactions between substrate, fermentation end-products, buffering systems and gas production upon fermentation of different carbohydrates by mixed rumen organisms *in vitro*. *Appl Microbiol Biotechnol*, **37** 505-509.
- Blümmel M, Ørskov E R 1993 Comparison of *in vitro* gas production and nylon bag degradability of roughages in predicting feed intake in cattle. *Anim Feed Sci Technol*, **40** 109-119.
- Bos H J 1999 *Plant morphology, environment, and leaf area growth in wheat and maize*. Doctoral thesis, Agricultural University, Wageningen.
- Bos H J, Neuteboom J H 1998 Growth of individual leaves of spring wheat (*Triticum aestivum* L.) as influenced by temperature and light intensity. *Ann Bot* **81** 141-149.
- Brereton A J, Carton O T 1988 Sward height, structure and herbage use. *Proceedings of the Research Meeting at the Welsh Agricultural College, Aberystwyth*, 13-15 Sept. 1988. British Grassland Society, Hurley.
- Burns I G 1992 Influence of plant nutrient concentration on growth rate: use of a nutrient interruption technique to determine critical concentrations of N, P and K in young plants. *Plant and Soil* **142** 221-233.
- Buxton D R, Fales S L 1994 Plant environment and quality. *Forage quality, evaluation and utilization*, ed Fahey G C. American Society of Agronomy, Madison, Wisconsin, USA, pp 155-199.
- Buxton D R, Lentz E M 1993 Performance of morphologically diverse orchardgrass clones in spaced and sward plantings. *Grass For Sci* **48** 336-346.
- Chapman D F, Lemaire J 1993 Morphogenetic and structural determinants of plant regrowth after defoliation. In: *Grasslands for Our World*, ed Baker M J. SIR Publishing, Wellington, pp 55-64.
- Chesson A 1993 Mechanistic models of forage cell-wall degradation. In: *Forage cell-wall structure and digestibility*, eds Jung H G et al. Madison: American Society of Agronomy, pp 347-376.
- Cone J W, Beuvink J M W, Rodrigues M 1994 Use and applications of an automated time related gas production test for the *in vitro* study of fermentation kinetics in the rumen. *Revista Portuguesa de Zootecnia* **1** 25-37.
- Cone J W, Engels F M 1993 The influence of ageing on cell wall composition and degradability of three maize genotypes. *Anim Feed Sci Technol* **40** 331-342.
- Cone J W, Van Gelder A H, Valk H 1998 Prediction of nylon bag degradation characteristics of grass samples with the gas production technique. *J Sci Food Agric* **77** 421-426.
- Cornu A, Besle J M, Mosoni P, Grenet E 1994 Lignin-carbohydrate complexes in forages: structure and consequences in the ruminal degradation of cell-wall carbohydrates. *Reprod Nutr Dev* **34** 385-398.
- DaSilva J H S, Johnson W L, Burns J C, Anderson C E 1987 Growth and environment effects on anatomy and quality of temperate and subtropical forage grasses. *Crop Sci* **27** 1266-1273.

- Davies A 1971 Growth rates and crop morphology in vernalized and non-vernalized swards of perennial ryegrass in spring. *J Agric Sci Camb* **77** 273-282.
- Davies I 1969 *The influence of management on tiller development and herbage growth*. Welsh Plant Breeding Station, Technical Bulletin No. 3.
- Davies I 1976 Developmental characteristics of grass varieties in relation to their herbage production. 1. An analysis of high-digestibility varieties of *Dactylis glomerata* at three stages of development. *J Agric Sci Camb* **87** 25-32.
- Deenen P J A G 1994 *Nitrogen efficiency in intensive grassland farming*. Doctoral thesis, Agricultural University, Wageningen.
- Deinum B 1976 Effect of age, leaf number and temperature on cell wall and digestibility of maize. In: *Carbohydrate Research in Plants and Animals*. Landbouwhogeschool, Wageningen, pp 29-41.
- Deinum B 1981 *The influence of physical factors on the nutrient content of forages*. Mededelingen Landbouwhogeschool Wageningen, The Netherlands.
- Deinum B, Groot J C J, Maassen A in prep Growth and development, histology and anatomy, and digestion of leaves from *Lolium perenne* (L.) and *L. multiflorum* (Lam.).
- Demeyer D I 1981 Rumen microbes and digestion of plant cell walls. *Agric Environm* **6** 295-337.
- Engels F M 1989 A cell wall layer limiting digestion in grasses. *Acta Bot Neerl* **38** 95-96.
- Engels F M, Brice R E 1985 A barrier covering lignified cell walls of barley straw that restricts access by rumen microorganisms. *Curr Microbiol* **12** 217-224.
- Engels F M, Schuurmans J L L 1992 Relationship between structural development of cell walls and degradation of tissues in the maize stem. *J Sci Food Agric* **59** 45-51.
- Ennik G C 1966 *The influence of clipping and soil fumigation on shoot and root production of perennial ryegrass and white clover*. Instituut voor Biologisch en Scheikundig Onderzoek van Landbouwgewassen, Wageningen.
- France J, Dhanoa M S, Theodorou M K, Lister S J, Davies D R, Isac D 1993 A model to interpret gas accumulation profiles associated with *in vitro* degradation of ruminant feeds. *J Theor Biol* **163** 99-111.
- Gaasstra P 1959 *Photosynthesis of crop plants as influenced by light, carbon dioxide and stomatal diffusion resistance*. Mededelingen Landbouwhogeschool Wageningen 59, pp 1-68.
- Garg M R, Gupta B N 1992 Effect of different supplements on the degradability of organic matter, cell wall constituents, *in vitro* gas production and organic matter digestibility of wheat straw. *Anim Feed Sci Technol* **38** 187-198.
- Genstat 5 Committee 1993 *Genstat 5 Release 3 Reference Manual*. Clarendon Press, Oxford.
- Goering H K, Van Soest P J 1970 Forage fiber analysis. *Agricultural Handbook* 379. United States Department of Agriculture.
- Goudriaan J, Monteith J L 1990 A mathematical function for crop growth based on light interception and leaf area expansion. *Ann Bot* **66** 695-701.
- Goudriaan J, Van Laar H H 1994 *Modelling potential crop growth processes*. Dordrecht: Kluwer Academic Publishers.
- Grabber J H, Jung G A 1991 In-vitro disappearance of carbohydrates, phenolic acids, and lignin from parenchyma and sclerenchyma cell walls isolated from cocksfoot. *J Sci Food Agric* **57** 315-323.
- Groot J C J, Deinum B, Lantinga E A, Neuteboom J H 1994 Digestibility of cell walls of ageing grass leaves as estimated from *in vitro* and gas production techniques. In: *Grassland and Society, Proceedings of the 15th General Meeting of the European Grassland*

- Federation, June 6-9, 1994*, eds 't Mannetje L, Frame J. Wageningen, The Netherlands, pp 152-157.
- Hacker J B, Minson D J 1981 The digestibility of plant parts. *Herbage Abstracts* **51** 459-482.
- Hageman I W, Lantinga E A, Schlepers H, Neuteboom J H 1992 *Intake, feeding quality, milk production and sward quality under grazing of diploid and tetraploid perennial ryegrass. Report of two years comparative research.* [Opname, voederwaarde, melkproductie en zodekwaliteit bij beweiding van diploid en tetraploid Engels raaigrass. Verslag van twee jaar vergelijkend onderzoek.] Department of Agronomy, Agricultural University, Wageningen, 68 p. In Dutch.
- Hageman I W, Lantinga E A, Schlepers H, Neuteboom J H 1993 Herbage intake, digestibility characteristics and milk production of a diploid and two tetraploid cultivars of perennial ryegrass. In: *Proceedings of the XVII International Grassland Congress*, Palmerston North, New Zealand, pp 459-460.
- Hanna W W 1993 Improving forage quality by breeding. In: *International crop science I*, eds Buxton D R, Paulsen G M, Wilson R F. Crop Science Society of America, Madison, Wisconsin, USA, pp. 671-675.
- Hespel R B 1979 Efficiency of growth by ruminal bacteria. *Federation Proceedings* **38**, 2707-2712.
- Hidayat, Hillman K, Newbold C J, Stewart C S 1993 The contributions of bacteria and protozoa to ruminal forage fermentation *in vitro*, as determined by microbial gas production. *Anim Feed Sci Technol* **42** 193-208.
- Hill M J, Pearson C J 1985 Primary growth and regrowth responses of temperate grasses to different temperatures and cutting regimes. *Aust J Agric Res* **36** 25-34.
- Hodgson J 1981 Influence of sward characteristics on diet selection and herbage intake by the grazing animal. In: *Nutritional limits to animal production*, ed Hacker J B. Commonwealth Agricultural Bureaux, Farnham Royal, UK, pp. 153-165.
- Hungate R E 1966 *The Rumen and Its Microbes*. Academic Press, New York.
- Illius A W 1985 A predictive model of seasonal changes in herbage digestibility. *J Agric Sci Camb* **105** 505-512.
- Jones M B, Leafe E L, Stiles W, Collett B 1978 Pattern of respiration of a perennial ryegrass crop in the field. *Ann Bot* **42** 693-703.
- Kerley M S, Fahey Jr G C, Gould J M, Iannotti E L 1988 Effects of lignification, cellulose crystallinity and enzyme accessible space on the digestibility of plant cell wall carbohydrates in the ruminant. *Food Microstr* **7** 59-65.
- Khazaal K, Ørskov E R 1994 The *in vitro* gas production technique: an investigation on its potential use with insoluble polyvinylpyrrolidone for the assessment of phenolics-related anti-nutritive factors in browse species. *Anim Feed Sci Technol* **47** 305-320.
- Kurth W 1994 Morphological models of plant growth: possibilities and ecological relevance. *Ecol Modelling* **75-76** 299-308.
- Lantinga E A, Groot J C J 1996 Optimization of grassland production and herbage feed quality in an ecological context. In: *Utilization of local feed resources in dairy cattle*, eds Groen A F and Van Bruchem J. EAAP Publication no. 84, Wageningen Press, Wageningen, pp 58-66.
- Leedle J A Z, Greening R C 1988 Postprandial changes in methanogenic and acidogenic bacteria in the rumens of steers fed high- or low-forage diets once daily. *Appl Environ Microbiol* **54** 502-506.
- Lentz E M, Buxton D R 1991 Morphological trait and maturity group relations with digestibility of orchardgrass. *Crop Sci* **31** 1555-1560.

- Lin K W, Patterson J A, Ladish M R 1985 Anaerobic fermentation: microbes from ruminants. *Enzym Microbiol Technol* **7** 98-107.
- MacAdam J W, Kerley M S, Piwonka E J, Sisson D W 1996 Tiller development influences seasonal change in cell wall digestibility of big bluestem (*Andropogon gerardii*). *J Sci Food Agric* **70** 79-88.
- Masaoka Y, Wilson J R, Hacker J B 1991 Selecting for nutritive value in *Digitaria milanijana*. 3. Relation of chemical composition and morphological and anatomical characteristics to the difference in digestibility of divergently selected fullsibs, and comparison with *D. eriantha* ssp. *pentzii* (pangalagrass). *Aust J Exp Agric* **31** 631-638.
- McAllister T A, Bae H D, Jones G A, Cheng K -J 1994 Microbial attachment and feed digestion in the rumen. *J Anim Sci* **72** 3004-3018.
- Menke K H, Raab L, Salewski A, Steingass H, Fritz D, Schneider W 1979 The estimation of the digestibility and metabolizable energy content of ruminant feedingstuffs from the gas production when they are incubated with rumen liquor *in vitro*. *J Agric Sci Camb* **93** 217-222.
- Miller T L 1995 Ecology of methane production and hydrogen sinks in the rumen. In: *Ruminant Physiology: Digestion, Metabolism, Growth and Reproduction*, eds Von Engelhardt E, Leonhard-Marek S, Breves G, Giesecke D. Ferdinand Enke Verlag, Stuttgart, pp 317-331.
- Motulsky H J, Ransnas L A 1987 Fitting profiles to data using nonlinear regression: a practical and nonmathematical review. *FASEB J* **1** 365-374.
- Nelson C J 1992 Physiology of leaf growth of grasses. In: *Proc 14th General Meeting of the European Grassland Federation*, eds Parsinnen *et al.* pp 175-179.
- Nelson C J, Asay K H, Sleper D A 1977 Mechanisms of canopy development of tall fescue genotypes. *Crop Sci* **17** 449-452.
- Nelson C J, Moser L E 1994 Plant factors affecting forage quality. *Forage quality, evaluation and utilization*, ed Fahey G C. American Society of Agronomy, Madison, Wisconsin, USA, pp 115-154.
- Neter J, Wasserman W 1974 *Applied linear statistical models*. Richard D. Irwin Inc, Homewood, Illinois, 842 p.
- Niklas K J 1992 *Plant biomechanics – an engineering approach to plant form and function*. The University of Chicago Press, Chicago, USA, 607 p.
- Nordang L, Lantinga E A, Neuteboom J H 1992 Development of digestibility of grass leaf blades. In: *Proc 14th General Meeting of the European Grassland Federation*, eds Parsinnen *et al.* pp 604-605.
- Nsahlai I V, Umunna N N 1996 Comparison between reconstituted sheep faeces and rumen fluid inocula and between *in vitro* and *in sacco* digestibility methods as predictors of intake and *in vivo* digestibility. *J Agric Sci Camb* **126** 235-248.
- Ørskov E R, McDonald I 1979 The estimation of protein degradability in the rumen from incubation measurements weighted according to the rate of passage. *J Agric Sci* **92** 499-503.
- Parsons A J, Robson M J 1980 Seasonal changes in the physiology of S24 perennial ryegrass (*Lolium perenne* L.). 1. Response of leaf extension to temperature during the transition from vegetative to reproductive growth. *Ann Bot* **46** 435-444.
- Parsons A J, Robson M J 1981a Seasonal changes in the physiology of S24 perennial ryegrass (*Lolium perenne* L.). 2. Potential leaf and canopy photosynthesis during the transition from vegetative to reproductive growth. *Ann Bot* **47** 249-258.

- Parsons A J, Robson M J 1981*b* Seasonal changes in the physiology of S24 perennial ryegrass (*Lolium perenne* L.). 3. Partition of assimilates between root and shoot during the transition from vegetative to reproductive growth. *Ann Bot* **48** 733-744.
- Parthier B 1989 Phytohormones and other stress modulators. In: *Heat shock and other stress response systems of plants*, eds Nover L, Neumann D, Scharf K -D. Springer Verlag, Berlin, pp 82-87.
- Peacock J M 1975 Temperature and leaf growth in *Lolium perenne*. III. Factors affecting seasonal differences. *J Appl Ecol* **12** 685-697.
- Pell A N, Schofield P 1993 Computerized monitoring of gas production to measure forage digestion *in vitro*. *J Dairy Sci* **76** 1063-1073.
- Perttunen J, Sievänen R, Nikinmaa E, Salminen H, Saarenmaa H, Väkevä J 1996 Lignum: a tree model based on simple structural units. *Ann Bot* **77** 87-98.
- Rahim M A & Fordham R 1991 Effect of shade on leaf and cell size and number of epidermal cells in garlic (*Allium sativum*). *Ann Bot* **67** 167-171.
- Richards J H 1993 Physiology of plants recovering from defoliation. In: *Grasslands for our World*, ed Baker M J. SIR Publishing, Wellington, pp 46-54.
- Robson M J, Deacon M J 1978 Nitrogen deficiency in small closed communities of S24 ryegrass. II. Changes in the weight and chemical composition of single leaves during their growth and death. *Ann Bot* **42** 1199-1213.
- Russell J B, Wallace R J 1988 Energy yielding and consuming reactions. In: *The Rumen Microbial Ecosystem*, ed Hobson P N. Elsevier, Essex, pp 185-215.
- Ryle G J A 1970 Distribution patterns of assimilated <sup>14</sup>C in vegetative and reproductive shoots of *Lolium perenne* and *L. temulentum*. *Ann Appl Biol* **66** 155-167.
- Salminen H, Saarenmaa H, Perttunen J, Sievänen R, Väkevä J, Nikinmaa E 1994 Modelling trees using an object-oriented scheme. *Mathl Comput Modelling* **20** 49-64.
- Sambo E Y 1983 Leaf extension rate in temperate pasture grasses in relation to assimilate pool in the extension zone. *J Exp Bot* **34** 1281-1290.
- Schnyder H, Nelson C J 1987 Growth rates and carbohydrate fluxes within the elongation zone of tall fescue leaf blades. *Plant Physiol* **85** 548-553.
- Schofield P, Pitt R E, Pell A N 1994 Kinetics of fiber digestion from *in vitro* gas production. *J Anim Sci* **72** 2980-2991.
- Sequeira R A, Sharpe P J H, Stone N D, El-Zik K M, Makela M E 1991 Object-oriented simulation: discrete organ to organ interactions. *Ecol Modelling* **58** 55-89.
- Sheehy J E, Mitchell P L, Durand J -L, Gastal F, Woodward F I 1995 Calculation of translocation coefficients from phloem anatomy for use in crop models. *Ann Bot* **76** 263-269.
- Sherrod 1995 *Nonlinear Regression Analysis Programm (NLREG)*. Nashville, TN, USA.
- Skinner R H, Nelson C J 1994 Epidermal cell division and the coordination of leaf and tiller development. *Ann Bot* **74** 9-15.
- Skinner R H, Nelson C J 1995 Elongation of the grass leaf and its relationship to the phyllochron. *Crop Sci* **35** 4-10.
- Sleper D A, Drolsom P N 1974 Analysis of several morphological traits and their associations with digestibility in *Bromus inermis* Leyss. *Crop Sci* **14** 34-36.
- Stapleton J, Jones M B 1987 Effects of vernalization on the subsequent rates of leaf extension and photosynthesis of perennial ryegrass (*Lolium perenne* L.). *Grass For Sci* **42** 27-31.
- Stefanon B, Pell A N, Schofield P 1996 Effect of maturity on digestion kinetics of water-soluble and water-insoluble fractions of alfalfa and brome hay. *J Anim Sci* **74** 1104-1115.
- Steiner A A 1984 The universal nutrient solution. *Proceedings of the VIth International Congress on Soilless Culture*, Lunteren, The Netherlands, pp 633-650.



- Steingass H 1983 *Bestimmung des energetischen Futterwertes von wirtschaftseigenen Futtermitteln aus der Gasbildung bei der Pansenfermentation in vitro*. Ph.D. Thesis, University of Hohenheim, Germany.
- Tamminga S, Van Vuuren A M 1996 Physiological limits of fibrous feed intake and conversion in dairy cows. In: *Utilization of local feed resources in dairy cattle*, eds Groen A F and Van Bruchem J. EAAP Publication no. 84, Wageningen Press, Wageningen, pp 19-33.
- Terry R A, Tilley J M 1964 The digestibility of the leaves and stems of perennial ryegrass, cocksfoot, timothy, tall fescue, lucerne and sainfoin, as measured by an *in vitro* procedure. *J Brit Grassl Soc* 19 363-372.
- Theodorou M K, Davies D R, Nielsen B B, Lawrence M I G, Trinci A P J 1995 Determination of growth of anaerobic fungi on soluble and cellulosic substrates using a pressure transducer. *Microbiol* 141 671-678.
- Theodorou M K, Williams B A, Dhanoa M S, McAllan A B, France J 1994 A new gas production method using a pressure transducer to determine the fermentation kinetics of ruminant feeds. *Anim Feed Sci Technol* 48 185-197.
- Thomas H, Stoddart J L 1984 Kinetics of leaf growth in *Lolium temulentum* at optimal and chilling temperatures. *Ann Bot* 53 341-347.
- Thornley J H M, Johnson I R 1991 *Plant and crop modelling: a mathematical approach to plant and crop physiology*. Oxford, Clarendon. 667 p.
- Van Cruchten C J M 1974 *Digestibility of consecutively formed leaves of two Gramineae from temperate regions grown at two temperature regimes* [Verteerbaarheid van opeenvolgend gevormde bladeren van twee gramineeën uit de gematigde gebieden geteeld bij twee temperatuurregimes]. Wageningen Agricultural University, 34 p. In Dutch.
- Van Houtert M F J 1993 The production and metabolism of volatile fatty acids by ruminants fed roughages: a review. *Anim Feed Sci Technol* 43 189-225.
- Van Loo E N 1993 *On the relation between tillering, leaf area dynamics and growth of perennial ryegrass (Lolium perenne L.)*, Doctoral thesis, Agricultural University, Wageningen.
- Van Milgen J, Berger L L, Murphy J 1993 An integrated, dynamic model of feed hydration and digestion, and subsequent bacterial mass accumulation in the rumen. *Br J Nutr* 70 471-483.
- Van Soest P J 1994 *Nutritional ecology of the ruminant*. 2nd Edition. Oregon (USA), O&B Books Inc., 476 p.
- Van Soest P J, Robertson J B, Lewis B A 1991 Methods for dietary fiber, neutral detergent fiber, and nonstarch polysaccharides in relation to animal nutrition. *J Dairy Sci* 74 3583-3597.
- Vincent J F V 1990 *Structural biomaterials*. Princeton University Press, Princeton, New Jersey, USA, 259 p.
- Waghorn G C, Stafford K J 1993 Gas production and nitrogen digestion by rumen microbes from deer and sheep. *New Zealand J Agric Res* 36 493-497.
- Wilman D, Altimimi M A K 1982 The digestibility and chemical composition of plant parts in Italian and perennial ryegrass during primary growth. *J Sci Food Agric* 33 595-602.
- Wilson J R 1976 Variation of leaf characteristics with level of insertion on a grass tiller. I. Development rate, chemical composition and dry matter digestibility. *Aust J Agric Res* 27 343-354.
- Wilson J R 1994 Cell wall characteristics in relation to forage digestion by ruminants. *J Agric Sci Camb* 122 173-182.

- Wilson JR, Deinum B, Engels FM 1991 Temperature effects on anatomy and digestibility of leaf and stem of tropical and temperate forage species. *Neth J Agric Sci* **39** 31-48.
- Wilson J R, Hatfield R D 1997 Structural and chemical changes of cell wall types during stem development: consequences for fibre degradation by rumen flora. *Aust J Agric Res* **48** 165-180.
- Wilson J R, Hattersley P W 1989 Anatomical characteristics and digestibility of leaves in *Panicum* and other grass genera with C<sub>3</sub> and different types of C<sub>4</sub> photosynthetic pathway. *Aust J Agric Res* **40** 125-136.
- Wilson J R, Mertens D R 1995 Cell wall accessibility and cell structure limitations to microbial digestion of forage. *Crop Sci* **35** 251-259.
- Wilson J R, Minson D J 1980 Prospects for improving the digestibility and intake of tropical grasses. *Trop Grassl* **14** 253-259.
- Wilson R E, Laidlaw A S 1985 The role of the sheath tube in the development of expanding leaves in perennial ryegrass. *Ann Appl Biol* **106** 385-391.
- Wolin M J 1975 Interactions between bacterial species in the rumen. In: *Digestion and Metabolism in the Ruminant*, eds McDonald I W, Warner A C. Armidale: The University of New England Publishing Unit.
- Wolin M J 1979 The rumen fermentation: a model for microbial interactions in anaerobic ecosystems. *Adv Microb Ecol* **3** 49-77.
- Zwietering M H, Jongenburger I, Rombouts F M, Van 't Riet K 1990 Modeling of the bacterial growth curve. *Appl Environ Microbiol* **56** 1875-1881.

## SUMMARY

In the current agricultural practice in the temperate regions highly digestible grass cultivars are used. Grassland is fertilized sufficiently, so that the grass can be grazed or cut in a young stage. The diet of ruminants is supplemented with a considerable amount of concentrates. Presently, efforts are being made to reduce the input of fertilizers and concentrates. Consequently, when harvested at the same yield, the grass will be more mature and less digestible, or when harvested at the same digestibility, the yield will be lower. Simultaneously, the required quality increases, as the proportion of concentrates in the animal ration is reduced and the desired animal performance remains unchanged. A thorough understanding and quantitative measures of the maturation processes is required to estimate the consequences of changes in grassland management and to explore potential possibilities for improvement of the utilization of grass.

In the first part of this thesis (Chapters 2 to 4) the changes in composition and digestibility of plant organs of grass (*Lolium perenne* and *L. multiflorum*) during growth and ageing after full expansion were quantified. This knowledge was incorporated into an object-oriented simulation model (Chapter 5), which calculates growth, development and digestibility of grass throughout the growing season. In the Chapters 6 and 7 the use of the cumulative gas production method was evaluated. This technique can potentially become an alternative for the standard *in vitro* digestibility measurements.

Organic matter digestibility (OMD,  $\text{g kg}^{-1}$ ) is determined by cell wall content (CWC,  $\text{g kg}^{-1}$ ) and cell wall digestibility (CWD,  $\text{g kg}^{-1}$ ), since the soluble cell contents fraction is assumed to be completely digestible. The quantities mentioned above are derived from the mass of the constituent fractions of plants and organs. For detailed study of the dynamics of the organic matter, cell wall and cell contents, the specific mass of these constituents was determined during growth and ageing of plant organs. The specific mass was expressed in  $\text{mg cm}^{-2}$  for leaf blades and  $\text{mg cm}^{-1}$  for leaf sheaths, stem internodes and inflorescences.

The most important findings concerning the time course of morphological development and CWC and CWD from Chapters 2 to 4 are summarized below.

- The specific cell wall mass of the plant organs remains unchanged after the organs has reached full expansion. The increase in CWC is only caused by a decline in the specific cell contents mass.

- If the assimilate supply to growing organs is low, for instance at high temperature, the specific cell contents mass is reduced stronger than the cell wall mass, resulting in higher CWC.
- The decline of CWD of individual plant organs declines during ageing. The increase in the proportion of indigestible cell wall can be described by a negative exponential saturation curve, with a constant fractional rate per leaf appearance interval, approaching an asymptote. This asymptote is lower for leaf blades than for leaf sheaths and stem internodes, but is unaffected by insertion level, temperature or populations.
- The CWD decline for whole tillers is a function of the development stage of the tiller, when expressed in leaf appearance intervals.
- Cutting results in a lower CWD asymptote of elongating leaves that are hit. Possibly, this is caused by interruption of cell wall synthesis by cutting. Newly formed leaves are smaller but have the same composition as leaves of undisturbed tillers. Because the hit leaves form a small contribution to the total tiller OM mass, the effect of cutting on OMD is marginal.

The use of these trends in an object-oriented simulation model resulted in acceptable estimations of growth, development and digestibility of grass under contrasting circumstances, as described in Chapter 5. The results of the simulations were compared with measurements from two field experiments, that were carried out at different latitudes: in Wageningen, The Netherlands at 52° N and in Bodø, Norway at 67° N. Three *Lolium perenne* cultivars differing in heading dates were used, with average heading dates in The Netherlands of 9 May for Barylou, 29 May for Exito and 16 June for Kerdion. Crops were grown undisturbed or were cut early and/or late. In the first weeks of regrowth, and more so where stem development had further progressed, deviations between measured and modelled CWC and CWD were observed. The simulated CWC and CWD were higher and lower than those measured, respectively. This was caused by an error in the measurements: after cutting too much stem material remained on the field. The model using object oriented principles offers large opportunities for simulation of collections of individual plants and plant organs in a complex and varying environment. An example is the modelling of spatially determined competition between species, as between grass and white clover.

The gasses  $\text{CO}_2$  and  $\text{CH}_4$  are products of the microbial fermentation of feedstuffs in the reticulo-rumen. The amount of gas produced in *in vitro* experiments can be used as a measure of the time course of fermentation. This method could result in a accurate measure of actual fermentability of a feedstuff, whereas in the standard *in vitro* determinations merely the disappearance of cell wall particles is measured. The dissolved parts are not necessarily completely fermentable.

In Chapter 6, a multiphasic equation with considerable flexibility was presented. This equation could be used to model the cumulative gas production curves that arise from fermentation of largely contrasting type and concentrations of substrates and inoculation media, inocula. Also two methods to achieve more reliable multiphasic curve fits in two steps were described. Using the residuals between the observed cumulative gas production curve and a monophasic curve fit or the second derivative of the gas production curve, the number of phases and initial values for multiphasic curve fitting can be derived.

Differences in the fermentation patterns between cell wall and cell contents fractions of grass leaf blades (*L. multiflorum*) were measured in Chapter 7. The higher gas production rate during the first hours of incubation for cell contents when compared to cell wall was related to differences in the volatile fatty acid (VFA) production. For the cell wall fraction the kinetics of measured gas production were equal to those calculated from VFA production, using stoichiometrical equations. The measured gas production from the cell contents fraction was always lower than calculated. Possibly, the stoichiometrical equations are not valid for rapidly fermenting substrates. The gas production from the cell wall was not linearly related to the cell wall degradation. The kinetics of gas production and cell wall degradation were the same after correction of a 'lost fraction', that probably was not fermentable.

For improvement of interpretation of gas production curves, attention should be given to:

- The relation between phases in gas production and substrate composition.
- The role of cell contents in fermentative gas production from complete substrates, comprising cell contents and cell wall fractions.
- The relation between gas production and other measures of feeding quality.
- Standardisation of the gas production method.

## SAMENVATTING

In de hedendaagse landbouwpraktijk in de gematigde gebieden worden goed verteerbare grascultivars gebruikt. Grasland wordt ruim voldoende bemest, zodat het gras in een jong stadium begraasd of gemaaid kan worden. Als aanvulling op het dieet van herkauwers wordt tevens een aanzienlijke hoeveelheid krachtvoeder verstrekt. Momenteel wordt gestreefd naar reductie van het gebruik van kunstmeststoffen en krachtvoerders. Daardoor zal bij een gelijke opbrengst het gras in een later stadium en met lagere verteerbaarheid worden geoogst, terwijl bij oogsten van gras met gelijke verteerbaarheid de opbrengst lager zal zijn. Tegelijkertijd stijgt de gewenste kwaliteit, doordat het aandeel van krachtvoeder in het rantsoen daalt en de eisen aan dierlijke produktie gelijk blijven. Een goed begrip van en kwantitatief inzicht in de verouderingsprocessen is vereist om de consequenties van veranderingen in graslandgebruik in te schatten en om potentiële mogelijkheden voor verbetering van de benutting van gras te onderzoeken.

In het eerste deel van dit proefschrift (hoofdstukken 2 t/m 4) zijn de veranderingen in samenstelling en verteerbaarheid gekwantificeerd voor individuele plantenorganen van gras (*Lolium perenne* en *L. multiflorum*) gedurende hun groei, maar in het bijzonder na volgroeien en tijdens veroudering. Deze kennis is geïntegreerd in een object-georiënteerd simulatiemodel (hoofdstuk 5), dat de groei, ontwikkeling en verteerbaarheid van gras gedurende het groeiseizoen berekent. In de hoofdstukken 6 en 7 wordt het gebruik van de cumulatieve gas produktie methode geëvalueerd. Deze methode kan mogelijk als alternatief voor de standaard *in vitro* verteerbaarheidsbepaling worden gebruikt.

De verteerbaarheid van de organische stof (organic matter digestibility, OMD, g kg<sup>-1</sup>) wordt bepaald door het celwandgehalte (cell wall contents, CWC, g kg<sup>-1</sup>) en de verteerbaarheid van de celwanden (cell wall digestibility, CWD, g kg<sup>-1</sup>), omdat wordt aangenomen dat de celinhoud volledig verteerbaar is. De bovengenoemde grootheden worden afgeleid uit de massa van de planten en de organen. Voor gedetailleerde bestudering van de dynamiek van de massa aan organische stof, celwand en celinhoud werd de specifieke massa van deze componenten gevolgd, uitgedrukt in mg cm<sup>-2</sup> voor bladschijven en mg cm<sup>-1</sup> voor bladscheden, stengelinternodia en bloeiwijzen.

De belangrijkste bevindingen over het verloop van de morfologische ontwikkeling en de CWC en CWD uit de hoofdstukken 2 t/m 4 worden hieronder opgesomd.

- De specifieke celwand massa van plantenorganen verandert niet meer als het orgaan volgroeid is. De toename in de CWC wordt alleen veroorzaakt door een afname van de specifieke celinhoud massa.
- Als de assimilatievoorziening van groeiende organen laag is, bijvoorbeeld bij hoge temperatuur, wordt de specifieke celinhoud massa sterker gereduceerd dan de specifieke celwand massa, zodat de CWC stijgt.
- De CWD van individuele plantenorganen daalt gedurende veroudering. Het aandeel onverteerbare celwanden stijgt volgens een negatieve exponentiële verzadigingscurve, met constante fractionele snelheid per bladverschijningsinterval. De asymptoot die wordt benaderd is lager voor bladschijven dan voor bladscheden en stengelinternodia, maar wordt niet beïnvloed door insertie nivo, temperatuur of populatieverschillen.
- De afname van CWD voor hele spruiten is een functie van het ontwikkelingsstadium van de spruit, wanneer dit wordt uitgedrukt in bladverschijningsintervallen.
- Knippen leidt tot een lagere CWD asymptoot van groeiende bladeren, die door het knippen zijn geraakt. Mogelijk wordt dit veroorzaakt door het onderbreken van de celwandsynthese door het knippen. Nieuw gevormde bladschijven zijn kleiner, maar hebben dezelfde samenstelling en verteerbaarheid als bladschijven aan ongeraakte spruiten. Geraakte bladeren leveren slechts kleine bijdrage aan de organische stof opbrengst in volgende oogsten, zodat het effect op de gewasverteerbaarheid beperkt is.

Het gebruik van deze trends in een object-georiënteerd simulatiemodel resulteerde in goede voorspellingen van de groei, ontwikkeling en verteerbaarheid van gras gedurende het groeiseizoen onder uiteenlopende omstandigheden, zoals beschreven in hoofdstuk 5. De simulatieresultaten werden vergeleken met metingen uit twee veldproeven, die werden uitgevoerd op verschillende breedte-graden (Wageningen, Nederland: 52°N en Bodø, Noorwegen: 67°N) met drie Engels raaigras cultivars verschillend in gemiddelde schietdatum in Nederland (Barylou: 9 mei, Exito: 29 mei en Kerdion: 16 juni). Simulatie en metingen betroffen ongestoorde groei en de hergroei na een vroege en/of een late snede. Voor de eerste weken van de hergroei en naarmate de stengelontwikkeling verder was gevorderd bestonden afwijkingen tussen gemeten en gesimuleerde waarden (hogere CWC en lagere CWD gemeten dan gesimuleerd). Dit werd veroorzaakt door een afwijking in de metingen: na maaien bleef teveel stengelmateriaal achter op het veld. Het gebruikte model volgens object-georiënteerde

principes biedt grote mogelijkheden voor simulatie van verzamelingen van individuele planten(organen) in een complexe en variërende omgeving, bijvoorbeeld voor doorrekenen van concurrentieverhoudingen die ruimtelijk bepaald worden, zoals tussen gras en klaver.

De gasen  $\text{CO}_2$  en  $\text{CH}_4$  ontstaan als bijproduct van de fermentatie van voedermiddelen door micro-organismen in de pensnetmaag van herkauwers. De hoeveelheid gas die bij *in vitro* proeven wordt geproduceerd kan gebruikt worden als maat voor de fermenteerbaarheid van het voedermiddel in de tijd. Dit kan een nauwkeuriger schatting van de voederwaarde opleveren, omdat bij standaard 48 uur *in vitro* verteerbaarheid metingen de verdwijning van celwanddeeltjes wordt bepaald, die niet altijd volledig worden gefermenteerd door micro-organismen.

In hoofdstuk 6 werd een multi-fase vergelijking voorgesteld, dat door grote flexibiliteit de kinetiek kan beschrijven van cumulatieve gasproductiecurven, die ontstaan bij uiteenlopende soorten en concentraties van substraten, media en inocula. Tevens werden methoden beschreven om in twee stappen betrouwbaarder te fitten, door eerst uit een een-fase fit of de tweede afgeleide van de gascurve de initiële waarden voor de opeenvolgende fasen te schatten en daarna een multi-fase fit uit te voeren.

Verschillen in de fermentatiepatronen van celwanden en celinhoud fracties van bladschijven van gras (*L. multiflorum*) werden bepaald in hoofdstuk 7. De snellere gasproductie in het begin van de incubatie van celinhoud dan bij celwand was gerelateerd aan verschillende patronen van vluchtige vetzuurproductie (volatile fatty acids, VFA). Voor de celwand fractie was de gemeten kinetiek en het volume van de gasproductie gelijk aan dat berekend uit de VFA, met stoichiometrische vergelijkingen. Daarentegen was de gemeten gasproductie van celinhoud altijd lager dan berekend. Mogelijk zijn de stoichiometrische vergelijking niet geldig voor snel fermenteerbare substraten. De gasproductie van de celwand fractie was niet linear gerelateerd aan de celwandafbraak. De kinetiek voor gasproductie en afbraak was echter gelijk na correctie voor een verdwenen fractie, die waarschijnlijk niet fermenteerbaar was.

Aandachtspunten voor het verbeteren van de interpreteerbaarheid van de gasproductiecurven zijn als volgt.

- De relatie tussen fasen in de gasproductiecurven en substraatsamenstelling.



- De rol van celinhoud in de fermentatieve gasproductie van complete substraten, bestaande uit celinhoud en celwand fracties.
- De relatie tussen gasproductie en andere metingen van voederkwaliteit.
- Standaardisatie van de methode.

## ***CURRICULUM VITAE***

Jeroen Caspar Jan Groot werd op 2 augustus 1968 geboren in Alkmaar. Na het behalen van het diploma VWO-B aan het Petrus Canisius College in Alkmaar in 1986 studeerde hij Landbouwplantenteelt aan de Landbouwwuniversiteit Wageningen. In augustus 1992 studeerde hij af met als specialisatie Graslandkunde. Van 1992 tot 1996 werkte hij als Assistent in Opleiding bij de vakgroep Agronomie van de Landbouwwuniversiteit. Bij deze vakgroep werd het onderzoek voor dit proefschrift uitgevoerd in nauwe samenwerking met de vakgroep Theoretische Productie Ecologie van dezelfde universiteit. Vervolgens was hij als systeem-analist/programmeur in dienst van het Intern Software Huis van de ING-Bank. Sinds 1997 werkt hij in dezelfde functie voor het informatieseringsbedrijf Panfox in Rosmalen.